Synthetic Routes to
Asymmetrical Alkylenediimidosulfites
and Novel Heteroarene-linked
Bis-diimidosulfinates and Bis-triimidosulfonates

Dissertation zur Erlangung des
naturwissenschaftlichen Doktorgrades
der Bayerischen Julius-Maximilians-Universität Würzburg

vorgelegt von
Carola Selinka
aus Schweinfurt

Würzburg 2002

Eingereicht am:..

bei der Fakultät für Chemie und Pharmazie

1. Gutachter:..

2. Gutachter:..

der Dissertation

1. Prüfer:...

2. Prüfer:...

3. Prüfer:...

des öffentlichen Promotionskolloquiums

Tag des öffentlichen Promotionskolloquiums:..

Doktorurkunde ausgehändigt am:..

Die Natur liebt es, sich zu verbergen.

Heraklit

Contents

Abbreviations

2D	two dimensional
AcAc	acetylacetonate
adp	anisotropic displacement parameter
av.	average
*n*BuLi	*neo*-butyllithium
calc.	calculated
CCD	charge coupled device
COSY	correlated spectroscopy
CVD	chemical vapour deposition
Cy	cyclohexyl
d	day
dec.	decomposition
DEPT	distortionless enhancement by polarisation transfer
E	organic residue
e.g.	*exempli gratia*/ for example
esd	estimated standard deviation
Et	ethyl
Et$_2$O	diethyl ether
eq.	equation
eqv.	equivalent
exp.	experiment
ext.	extern
Fig.	figure
FT	fourier transformation
GooF	goodness-of-fit
h	hour
*i*Pr	*iso*-propyl
m	month
Me	methyl
MeLi	methyllithium
min	minute

MO	molecular orbital
Mp.	melting point
*n*Bu	*neo*-butyl
NMR	nuclear magnetic resonance
no.	number
Ph	phenyl
R	residue
Py	2-pyridyl
refl.	reflection
RT	room temperature
sat.	saturated
sec.Bu	*secondary*-butyl
*t*Bu	*tertiary*-butyl
tmeda	tetramethylethylendiamine
thf	tetrahydrofuran
sof	site occupation factor
vs.	*versus*
X	halogen or halide

List of Compounds

Compound	Number	Structure Code
$C_6H_{11}NSN^tBu$	1	–
$[thf_6Li_6\{\mu_6S\}\{(NSiMe_3)_3S\}_2]$	2	S2
$[(thf)Li\{H_3CS(NSiMe_3)_2\}]_2$	3	Dienstag
$[(Et_2O)Li\{H_3CS(NSiMe_3)(NC_6H_{11})\}]_2$	4	Sieben
$[Cu\{H_3CS(N^tBu)_2\}]_2$	5	Mai
$[(Et_2O)Li_2\{H_2CS(NSiMe_3)(N^tBu)\}]_2$	6	Montag
$[(thf)Li_2\{H_8C_4S(N^tBu)_2\}]_2$	7	August
$[(thf)Li_2\{(H_3CNC_4H_3)S(N^tBu)_2\}_2]$	8	Nochmal
$[(tmeda)Li\{(SC_8H_5)S(N^tBu)_2\}]$	9	Norwegen
$[Fe\{(SC_8H_5)S(N^tBu)_2\}_2]$	10	Was
$[Cu\{(SC_8H_5)S(N^tBu)_2\}]_2$	11	Cupfer
$[(tmeda)_2Li_2\{(^tBuN)_2S(SC_4H_2)S(N^tBu)_2\}]$	12	Neujahr
$[(tmeda)_2Li_2\{(Me_3SiN)_2S(SC_4H_2)S(NSiMe_3)_2\}]$	13	Selen
$[(tmeda)_2Li_2\{(^tBuN)_2S(SeC_4H_2)S(N^tBu)_2\}]$	14	September
$[(tmeda)_2Li_2\{(^tBuN)_2S(SC_4H_2)_2S(N^tBu)_2\}]$	15	Dryes
$[(thf)Li_2\{(SC_4H_2)S(N^tBu)_2\}]_2$	16	Sams
$[(thf)_2Li\{(H_3CNC_4H_3)S(N^tBu)_3\}]$	17	Sommer
$[(tmeda)Li\{(SC_4H_3)S(N^tBu)_3\}]$	18	Koppel 1
$[(tmeda)Li\{(SeC_4H_3)S(N^tBu)_3\}]$	19	Herbst
$[Cu\{OS(N^tBu)_3\}]_2$	20	Eisen
$[(tmeda)_2Li_2\{(^tBuN)_3S(SC_4H_2)S(N^tBu)_3\}]$	21a	Tritri
$[(thf)_2Li_2\{(^tBuN)_3S(SC_4H_2)S(N^tBu)_3\}]$	21b	Schweden

Lewis Diagrams of Compounds 2-21b

2

S

Me₃SiN　NSiMe₃　NSiMe₃

Li　Li　Li

S

Li　Li　Li

Me₃SiN　Me₃SiN　NSiMe₃

S

3

Me

Me₃Si—N　S　N—SiMe₃

thf---Li　Li---thf

Me₃Si—N　S　N—SiMe₃

Me

4

Me

Me₃Si—N　S　N—C₆H₁₁

Et₂O---Li　Li---OEt₂

H₁₁C₆—N　S　N—SiMe₃

Me

5

Me

^{t}Bu—N　S　N—^{t}Bu

Cu　Cu

^{t}Bu—N　S　N—^{t}Bu

Me

6

Me₃Si—N　Li　N—^{t}Bu

S

H₂C　Li—OEt₂

Et₂O—Li　CH₂

S

^{t}Bu—N　Li　N—SiMe₃

7

^{t}Bu—N　Li　N—^{t}Bu

S

(H₇C₃)HC　Li—thf

thf—Li　CH(C₃H₇)

S

^{t}Bu—N　Li　N—^{t}Bu

8

9

10

11

12

13

14

15

16

17

18
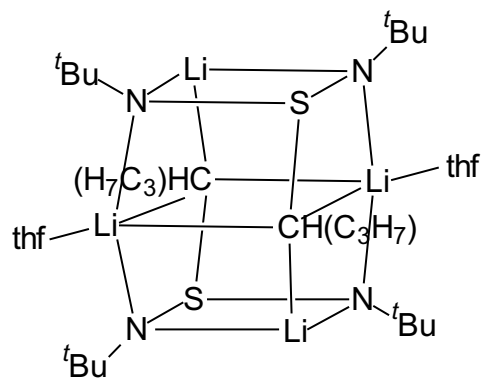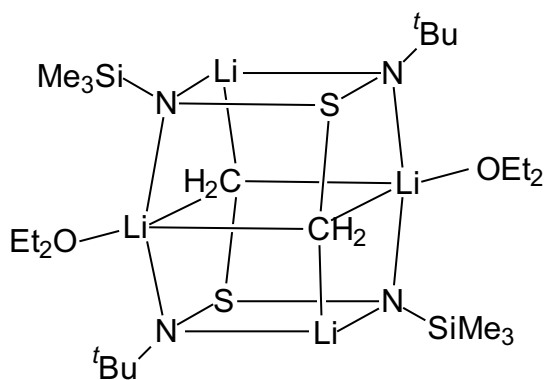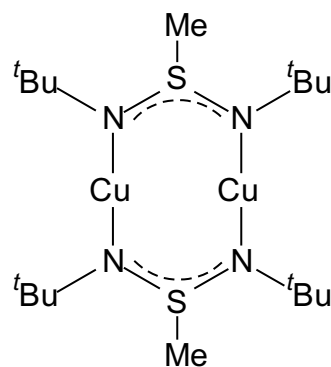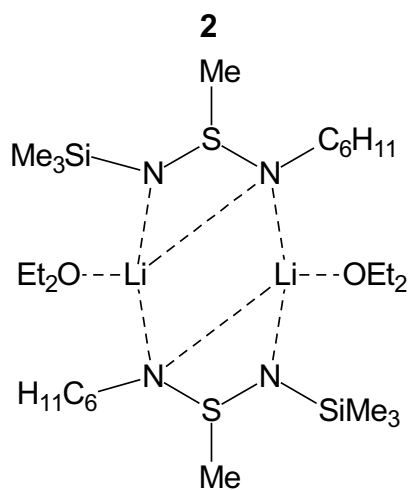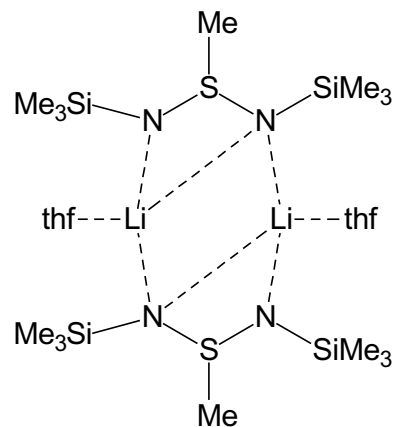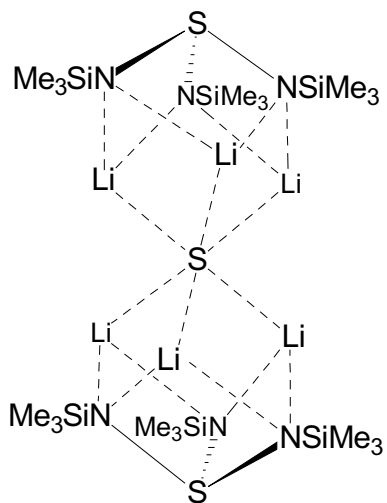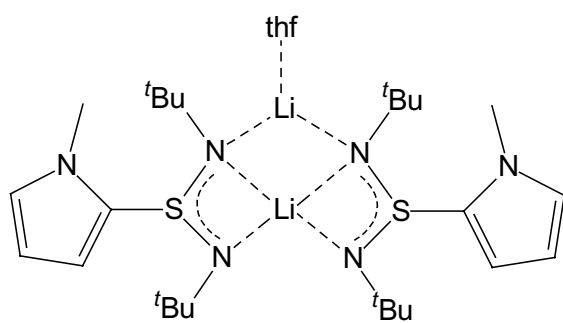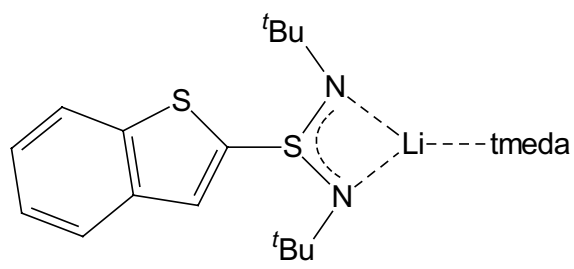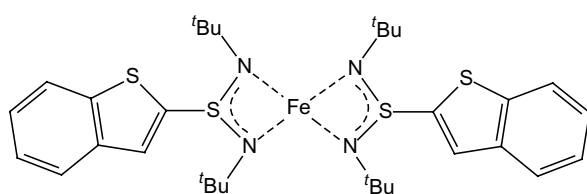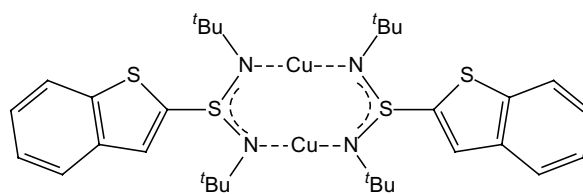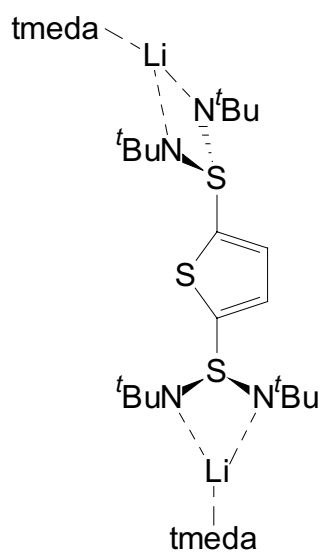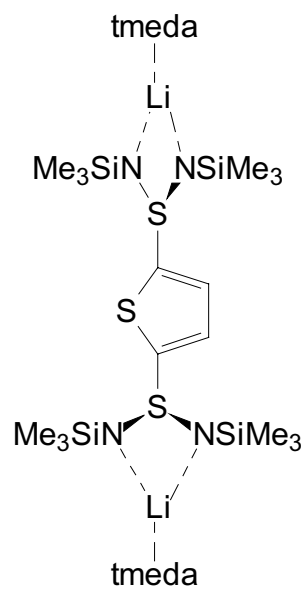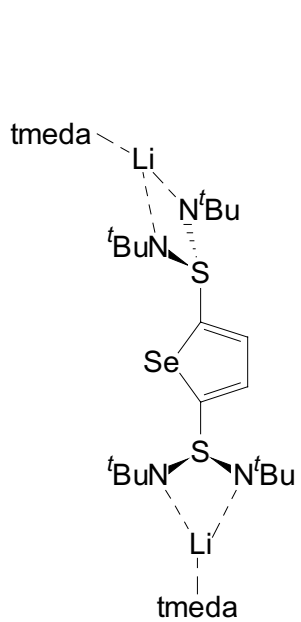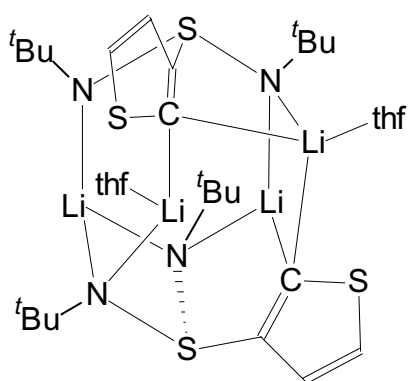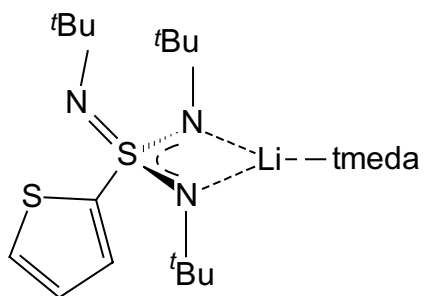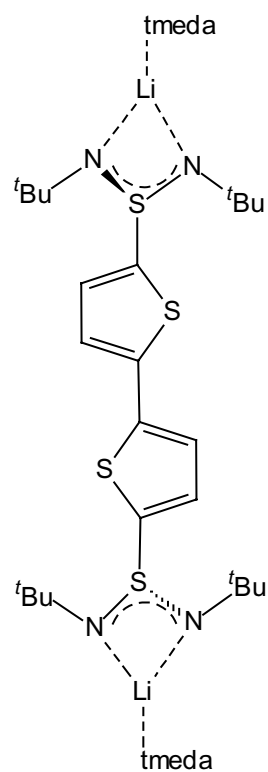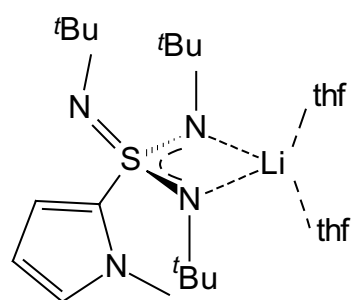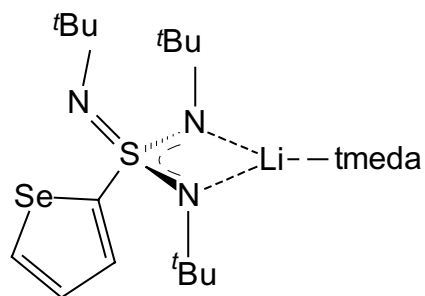
19
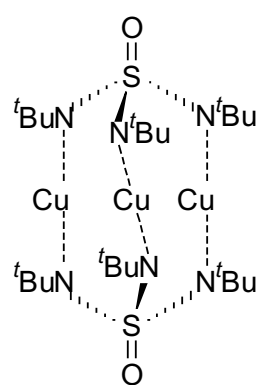
20
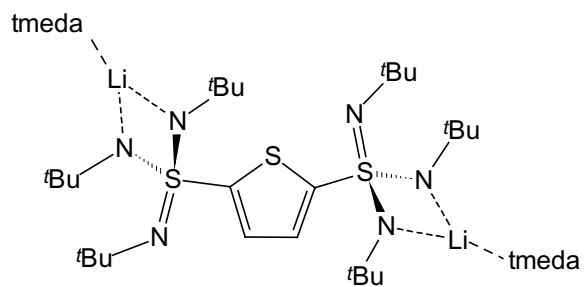
21a
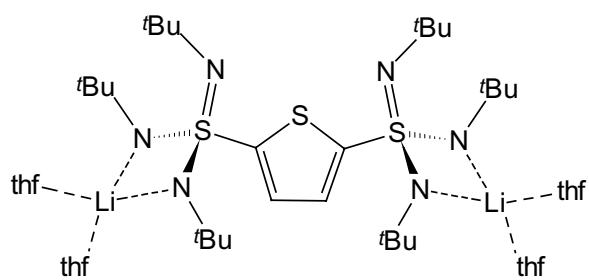
21b

1 Introduction

Oxoanions of sulfur, e.g. SO_2, SO_3^{2-}, SO_3 and SO_4^{2-}, are commonly encountered species in everyday life as well as in the laboratory. Acid rain, certainly the most discussed pollution of the environment during the eighties, is mainly caused by sulfuric acid.

For the solid state chemist and the crystal engineer, the various coordination modes of the tetrahedral SO_4^{2-} dianion are fascinating.[1]
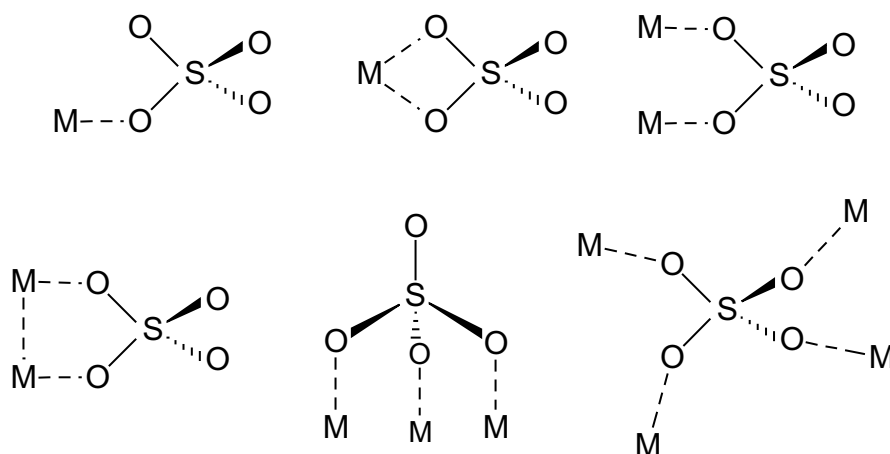
Figure 1: Coordination modes of SO_4^{2-}.

In addition, the isoelectronic principle, first espoused by *Langmuir*,[2] is a simple and useful concept, especially in inorganic chemistry. For the synthetic chemist the first preparation of an unknown compound has often been prompted by the existence of an isoelectronic analogue. Furthermore, many isoelectronic species undergo analogous reactions.

The replacement of the oxygen centres in sulfur-oxygen species by isoelectronic imido groups (=NR) is currently a flourishing area of an enormous scope.[3]

Table 1: Imido analogues of p-block oxoanions.

$[B(NR)_3]^{3-[4a]}$	$[C(NR)_3]^{2-[4b]}$		
	$[Si(NR)_3]^{2-[4c]}$	$[P(NR)_3]^{3-[4e]}$	$[S(NR)_3]^{2-[4j]}$
	$[Si(NR)_4]^{4-[4d]}$	$[P(NR)_4]^{3-[4f]}$	$[S(NR)_4]^{2-[4k]}$
		$[As(NR)_3]^{3-[4g,h]}$	$[Se(NR)_3]^{2-[4l]}$
		$[Sb(NR)_3]^{3-[4i]}$	$[Te(NR)_3]^{2-[4m]}$

Our research interest is focused on sulfur nitrogen compounds like $S(NR)_2$, $[S(NR)_3]^{2-}$, $S(NR)_3$ and $[S(NR)_4]^{2-}$.[5] More recently, the oxygen centres can also be replaced by the isoelectronic alkylene groups ($=CR_2$), leading to alkylene-diimidosulfites $[(R_2C)S(NR)_2]^{2-[6]}$ and alkylenetriimidosulfates $[(R_2C)S(NR)_3]^{2-}$.[7]

During the last 50 years sulfur nitrogen chemistry attracted remarkable research interest. A highlight certainly was the discovery of the superconductive properties[8] of polymeric $(SN)_x$, already synthesised in 1910.[9] In the nineteen-seventies binary sulfur nitrogen cycles like S_4N_4 came up and gave a new impetus to sulfur nitrogen chemistry. Already in 1956 *Goehring* and *Weis* succeeded in the landmark synthesis of the first sulfurdiimide $S(NR)_2$,[10] which is isoelectronic to SO_2. The potential of sulfurdiimides is tremendous. They gained synthetic significance in organic synthesis as intermediates[11] and in coordination chemistry as ligands.[12] Due to their manifold reactivity, they have been employed in different reactions in various fields of chemistry e.g. cycloaddition and en reaction,[13] asymmetric amination[14] and dehydration.[15]
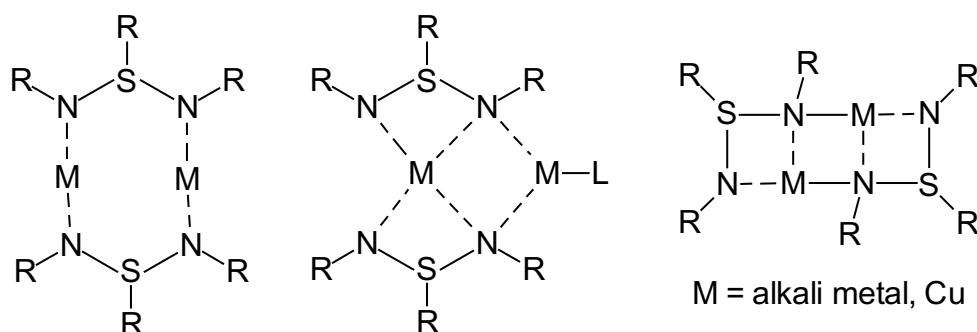
M = alkali metal, Cu

Figure 2: Coordination motifs of alkyldiimidosulfinates.

Our research group began initially to work with $S(NR)_2$ with the intention to create diimidosulfinates as monoanionic ligands by nucleophilic addition of alkali metal alkyls or aryls to the formal S=N double bond.[5]

To expand this initial work, metal amides instead of metal alkyls were used in the addition reaction, yielding, after deprotonation of the remaining hydrogen atom, a tripodal dianionic $S(NR)_3^{2-}$ ligand.[4i] Prior to this work there were only two examples of triimidosulfite dianions as ligands in the literature, $S(NSO_2(C_6H_4)Me)_3^{2-}$ and $S(NSO_2C_6H_5)_3^{2-}$.[16,17] Although immediately fascinating, the use of these dianions as ligands in coordination chemistry was hampered by their confusing redox properties. Even traces of an oxidant, like oxygen, led to a deep blue colour of the compound, indicating the presence of radical species. The structure of the radical could be determined *via* ESR spectroscopy.[18] Two cap shaped triimidosulfite ligands face each other with their concave side and accommodate only three lithium cations. Interaction of the unpaired electron with three nitrogen and three lithium atoms gives rise to a septet of decets in the ESR spectrum. Recent work of *Chivers et al.* show subsequently the same result for the heavier congeners $Se(NR)_3^{2-}$ and $Te(NR)_3^{2-}$.[19]

Complete oxidation of the triimidosulfite dianion with halogens led to the sulfurtriimide $S(N^tBu)_3$.[4m] Until recently, only two reactions were known in which the sulfurtriimide is formed. These syntheses starting from NSF_3[20] or OSF_4[21] are quite hazardous and give poor yields. In comparison the new synthesis *via* triimidosulfite is relatively simple and gives high yields. Syntheses of mixed substituted sulfurtriimides are known, but in most cases product mixtures are received and the yields are low.[22] The reactivity of the sulfurtriimide, similar to that of the sulfurdiimide, is dominated by the electropositive character of the sulfur atom. Nucleophilic addition of a lithium alkyl to the S=N bond gives alkyltriimidosulfonates.[23] In 1968 several alkyltriimidosulfonic acids were prepared by the reaction of thioles with chloroamine and alkylamine.[24]

Sulfate compounds with one ore more oxygen atoms isoelectronically replaced by a NR group are known since 1968, whereas the tetraimidosulfate **b** was only synthesised in 1997[4m] and the tetraalkylenesulfate **c** is still unknown.
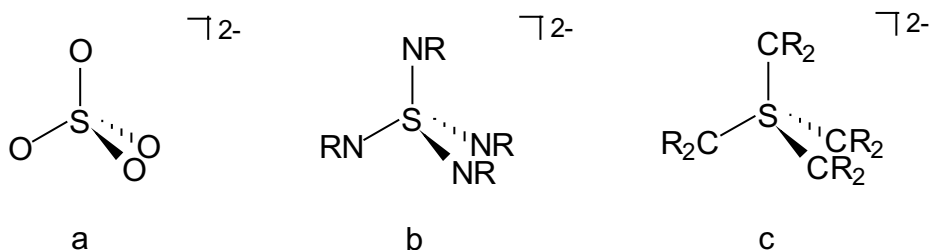
Figure 3: Isoelectronic replacement of oxygen by NR- or CR$_2$-groups, respectively.

Appel and *Ross* reported[25] about the synthesis of [K$_3$(NH)$_3$SN·NH$_3$] from the reaction of S,S-dimethylsulfurdiimine with KNH$_2$ in liquid ammonia. Although analytical evidence is vague and no structural information is available rewriting their original formula to [K$_2$(HN)$_4$S·KNH$_2$] would give rise to the first example of a tetraimidosulfate [S(NR)$_4$]$^{2-}$ (figure 3 b; R = H).

Table 2: Isoelectronic S-O$_x$/S-(NR)$_x$/S-(NR)$_x$(CR$_2$)$_y$ compounds (Highlighted compounds have not been reported previously!).

SO$_2$	S(NR)$_2$	S(CR$_2$)(NR)	S(CR$_2$)$_2$
SO$_3{}^{2-}$	S(NR)$_3{}^{2-}$	S(CR$_2$)(NR)$_2{}^{2-}$	S(CR$_2$)$_2$(NR)$^{2-}$
SO$_3$	S(NR)$_3$	S(CR$_2$)(NR)$_2$	S(CR$_2$)$_2$(NR)
SO$_4{}^{2-}$	S(NR)$_4{}^{2-}$	S(CR$_2$)(NR)$_3{}^{2-}$	S(CR$_2$)$_2$(NR)$_2{}^{2-}$
R(SO$_2$)$_2{}^{4-}$	NR[S(NR)$_2$]$_2{}^{4-}$	E[S(NR)$_2$]$_2{}^{4-}$	E[S(CR$_2$)(NR)]$_2{}^{4-}$
R(SO$_3$)$_2{}^{4-}$	NR[S(NR)$_3$]$_2{}^{4-}$	E[S(NR)$_3$]$_2{}^{4-}$	E[S(CR$_2$)(NR)$_2$]$_2{}^{4-}$

R = alkyl, aryl;

Different to their oxygen analogues, the polyimido sulfur anions are soluble, even in nonpolar organic solvents. In contrast to the simple oxoanions, they form molecular contact ion pairs in cage complexes surrounded by a lipophilic layer rather than infinite solid state lattices by multiple oxygen/cation contacts.
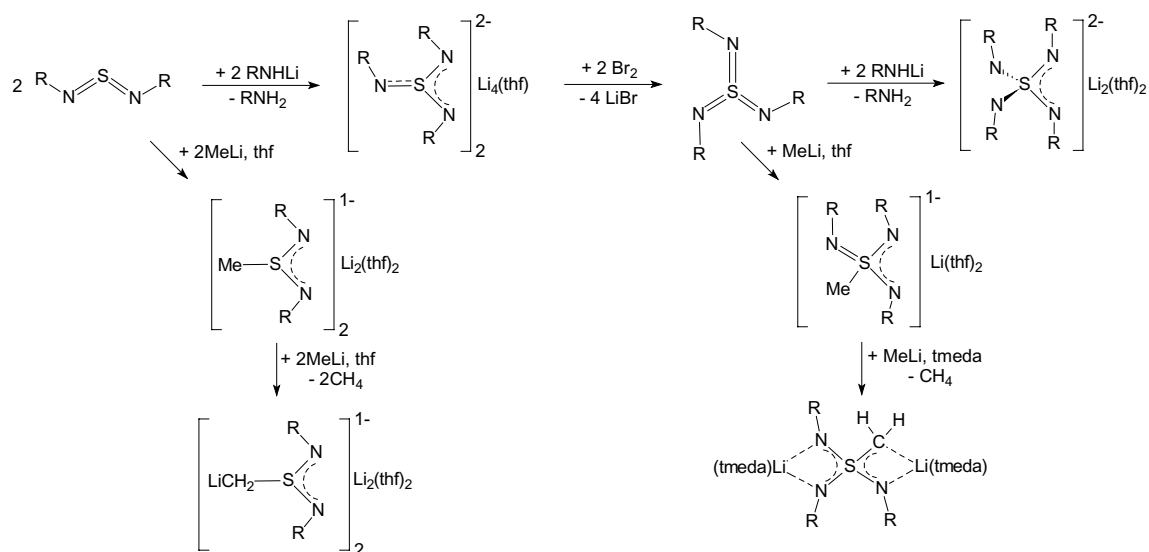
Scheme 1: Synthetic pathways to the imido sulfur compounds established by Pauer, Fleischer, Walfort and Ilge in our group.

The addition of a lithium alkyl to sulfurdiimide led to diimidosulfinates [RS(N^{t}Bu)$_2$]$^-$ (R = Me, sec.Bu).[7a] In a second step the α-carbon atom in R was metalated with one equivalent of methyllithium to give the S-ylides. This class of compounds can be rationalised as sulfite analogues, where two oxygen atoms are isoelectronically replaced by a N^{t}Bu group each and the remaining oxygen atom is replaced by a CR$_2$ group. Similar to Corey's S-ylides (R$_2$(O)S$^+$–$^-$CR$_2$) and Wittig's phosphonium ylides (R$_3$P$^+$–$^-$CR$_2$) these molecules contain a positively charged sulfur atom next to a carbanionic centre. Therefore nucleophilic addition reactions of the carbon atom are feasible.

Walfort[7a] carried out the same experiment with sulfurtriimide instead of sulfurdiimide and resulted in the synthesis of methylenetriimidosulfate [(tmeda)$_2$Li$_2${H$_2$CS(N^{t}Bu)$_3$}] (scheme 1, bottom right).

The reaction of sulfurdiimide with the anionic carbon centre in [H$_2$CS(N^{t}Bu)$_2$]$^{2-}$ gave the intermediate alkyl-bis-(diimidosulfinate) [(^{t}BuN)$_2$SCH$_2$S(N^{t}Bu)$_2$]$^{2-}$ (scheme 1, left), the first molecule in which two sulfurdiimide units are connected via an organic bridge. The acidity of the hydrogen atoms at the bridging CH$_2$ group is high enough to give, upon deprotonation, the [(^{t}BuN)$_2$SCHS(N^{t}Bu)$_2$]$^{3-}$ trianion.
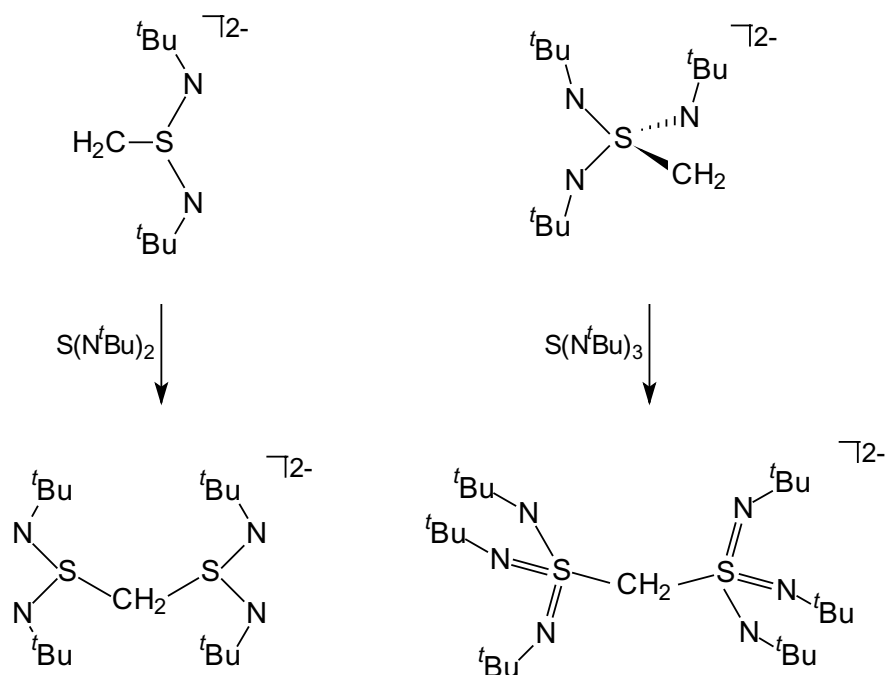
Scheme 2: The known addition reactions of alkylenediimidosulfite and alkylenetriimidosulfate.

Alkylenetriimidosulfate [Li$_2${(CH$_2$)S(N^{t}Bu)$_3$}], the carba/imido analogue of SO$_4{}^{2-}$, can readily be synthesised by deprotonation of lithium S-methyl-tri(*tert.*-butyl)triimidosulfonate H$_3$CS(N^{t}Bu)$_3{}^-$ with methyllithium. Addition of one equivalent of sulfurtriimide S(N^{t}Bu)$_3$ to the sulfur(VI)-ylide gave [(thf)$_2$Li$_2${(N^{t}Bu)$_3$S}$_2$CH$_2$].[6a]
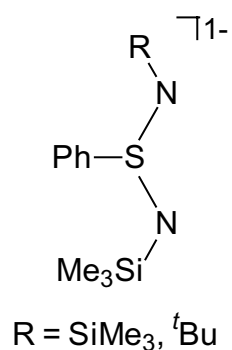
Figure 4: Known aryldiimidosulfinates.

Pauer[5] investigated the influence of different substituents at sulfur and nitrogen on the coordination mode of diimidosulfinates. He succeeded in the syntheses of the first aryldiimidosulfinates, which are monoanionic dipodal ligands. *Walfort*

introduced an acetylene bridge between the phenyl group and the sulfur atom and got [(thf)$_2$Li{(N^{t}Bu)$_3$SCCPh}] (figure 4, right).[26]

No aryltriimidosulfonates are known until now, due to steric reasons.

In analogy to the sulfur nitrogen compounds, a series of compounds with the higher homologues of sulfur (selenium and tellurium) are known.[27] 1976 *Derkach*, *Barashenko* and coworkers reported on the syntheses of seleniumdiimides (Se(NR)$_2$, R = acyl, sulfonyl).[28] *Herberhold* and *Jellen* succeeded in 1986 in the isolation of the first aliphatically substituted seleniumdiimide (Se(N^{t}Bu)$_2$).[29] Seleniumdiimides are highly reactive precursors in organic synthesis.[30,31] More frequently they are used *in situ*.[13] *Chivers* and coworkers reported 16 years ago the syntheses and structures of the Se(N^{t}Bu)$_3{}^{2-}$anion,[32] as well as the tellurium compounds Te(N^{t}Bu)$_2$[33] and [{Li$_2$Te(N^{t}Bu)$_3$}$_2$].[34] Although less stable, the selenium and telluriumdiimides provide a similar reactivity. Moreover, they are promising precursors in the synthesis of new group 2/12 complexes required in the CVD or sol-gel processes, to obtain II/VI semiconducting materials. Recently *Valkonen et al.*[35] reported on the synthesis of (Me$_3$SiNSN)$_2$Se, a synthon for sulfur selenium nitrides.

For the structural investigation of sulfur nitrogen compounds, single crystal X-ray structure analysis is vital. The standard ^{1}H and ^{13}C NMR techniques are not suitable because of the small shift range in these compounds. ^{15}N is the only nucleus with an appropriate shift range in these compounds, but due to the low natural abundance ^{15}N NMR spectroscopy cannot be regarded a standard method for characterisation. ^{7}Li NMR is sometimes suitable to identify the different types of lithium environments, especially when the experiment is carried out at low temperature.

<u>Scope of the thesis:</u>

Pauer, *Fleischer*, *Ilge* and *Walfort* in our group already investigated several aspects of sulfurtriimides, triimidosulfites, tetraimidosulfates and S-methyl-triimidosulfonates, but still many questions remained open.

The first aim was the synthesis of a triimidosulfite with three different NR-substituents, a so called asymmetrical triimidosulfite. Subsequent oxidation with bromine should lead to the respective sulfurtriimide. These molecules, converted to metal ligands in catalytically active species, would open a wide avenue to enantioselective catalysts, which could be used in organic syntheses. The reactivity of these catalysts should be tuneable by variation of the residues at the nitrogen atoms.

Second task of this work was the synthesis of sulfur(IV)-ylides with chiral centres. These systems should be able to react like *Wittig's* phosphonium ylides. Initial experiments of *Walfort* suggested that they might be powerful synthetic tools in C=C and C=N bond formation reactions. With chiral systems it should be possible to obtain stereoselective reaction pathways.

The third and most emphasised field of this thesis should open the application of the S-N species to material science. Two SET active S-N moieties should be connected *via* a conjugated linker facilitating electronic communication between them. Heteroaromatic linker like thiophene, methylpyrrole and selenophene would additionally provide Lewis-basic centres to coordinate various metal cations. Metal doped $[S(NR)_n]_m$ oligo- or polymers should result, possibly showing the same colour changes upon single electron oxidation as observed earlier in $[Li_2\{(N^tBu)_3S\}]_2$.

2   S(IV)-Compounds

2.1   The   attempted   asymmetrically   substituted triimidosulfites

In 1975 *Gieren* and *Narayana* reported on the synthesis and solid state structure of the first triimidosulfite $S(NR)_3^{2-}$ (R = $SO_2(C_6H_4)Me$).[17] *Roesky* and coworkers reported about a similar compound (R = $SO_2C_6H_5$).[16] In 1992 *Pauer*, from our research group, succeeded in the synthesis of an alkyl substituted triimidosulfite (R = ^tBu).[4j] In analogy to the addition of alkali metal alkyls to sulfurdiimides, triimidosulfites can be obtained by the addition of alkali metal amides to a formal S=N double bond of sulfurdiimides.
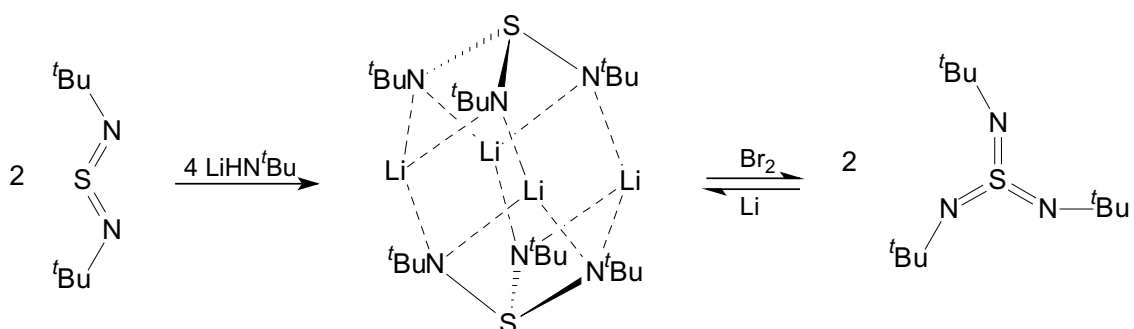
Scheme 3: Preparation of triimidosulfite and sulfurtriimide.

Nitrogen containing ligands are being used more and more in asymmetric catalysis.[36] They turned out to be suitable for any type of catalysis, especially for heterogeneous catalysis, which is one of their main advantages over phosphanes. More and more interest is even faced towards mixed, nitrogen and phosphorus containing ligands. The expected advantage is the synergetic effect of the different coordinating atoms.[37]

In this context a triimidosulfite with three different organic residues, instead of three ^tBu-groups, should be a promising tripodal dianionic ligand system for asymmetric induction in catalysis. The sulfur atom in this type of molecule represents a centre of chirality.

S(NSiMe$_3$)$_3$ and S(N^{t}Bu)$_3$ are the only sulfurtriimides, which are useful in preparative chemistry, but their yields are poor and the reaction conditions are hazardous. *Fleischer* achieved a much easier access to tri(*tert.*-butyl)sulfurtriimide in the oxidation of [Li$_2${(N^{t}Bu)$_3$S}]$_2$ with an excess of bromine (scheme 3, right).

2.1.1   N-*tert.*-butyl-N'-cyclohexylsulfurdiimide (1)

Hitherto innumerable sulfurdiimides with various NR groups are known.[38] They are used as intermediates and have interesting semiconducting and photoconducting properties.

In the approach to asymmetrically substituted sulfurtriimides it turned out that it is essential to avoid trimethylsilyl substituents as silyl group migration, well established in Si-N chemistry, always yielded the [thf$_6$Li$_6${µ$_6$S}{(NSiMe$_3$)$_3$S}$_2$] (**2**), which apparently is the thermodynamically sink.

The obvious conclusion was to prepare new sulfurdiimides without silyl groups, e. g. N-*tert.*-butyl-N'-cyclohexylsulfurdiimide (**1**).

$$Cy\diagdown_N\diagup^S\diagdown_O \quad + \quad Li-N\diagup^{^tBu}_{SiMe_3} \quad \xrightarrow{\text{Hexane}} \quad Cy\diagdown_N\diagup^S\diagdown_N\diagup^{^tBu} \quad + \quad Li\diagup^O\diagdown_{SiMe_3} \quad (1)$$
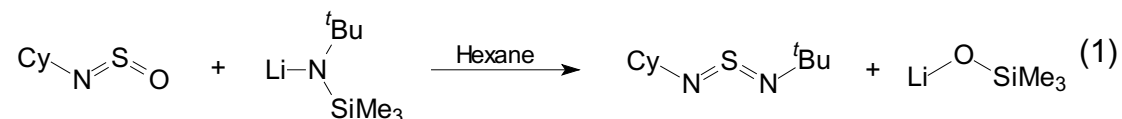
The reaction of cyclohexylthionylamine with lithium-*tert.*-butyltrimethylsilylamide yielded lithium trimethylsilanolate and the expected N-*tert.*-butyl-N'-cyclohexylsulfurdiimide. The reaction of ^{t}BuNSO with LiNCy(SiMe$_3$) is practicable as well, but results in lower yields.

2.1.2   [thf$_6$Li$_6${µ$_6$S}{(NSiMe$_3$)$_3$S}$_2$] (2)

2.1.2.1 Several ways to [thf$_6$Li$_6${µ$_6$S}{(NSiMe$_3$)$_3$S}$_2$] (**2**)

Fleischer reported the synthesis of [thf$_6$Li$_6${µ$_6$S}{(N^{t}Bu)$_3$S}$_2$] in the reduction reaction of S(N^{t}Bu)$_2$ and lithium metal in thf.[39]

$$3\ S(N^tBu)_2\ +\ 6\ M \xrightarrow{\text{thf}}$$
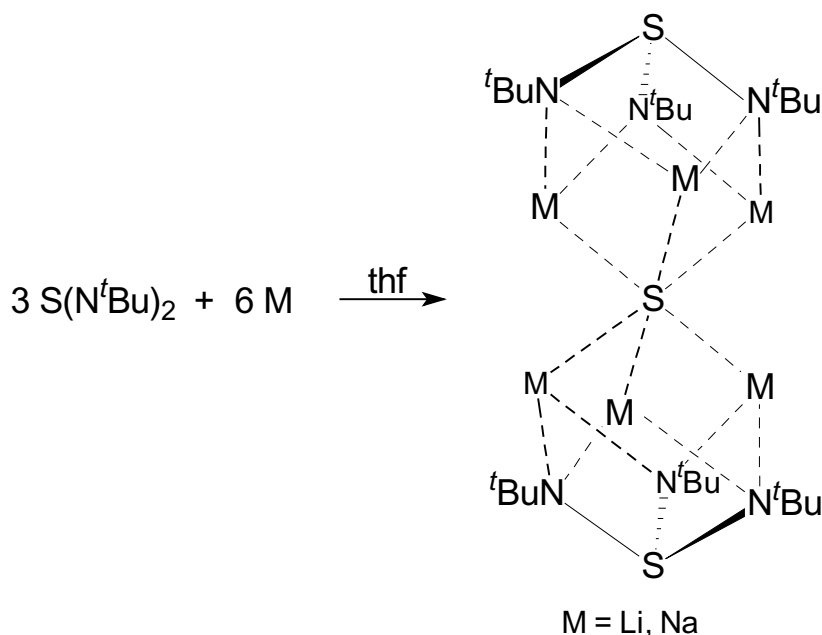
M = Li, Na

Scheme 4: Preparation and structural motive of the sulfide adducts [thf₆M₆{μ₆S}{(N^tBu)₃S}₂] (M = Li, Na) (coordinating thf omitted for clarity).

Formally [thf$_6$Li$_6${μ$_6$S}{(N^{t}Bu)$_3$S}$_2$] is a Li$_2$S adduct of [Li$_2${(N^{t}Bu)$_3$S}]$_2$. In one equivalent of the starting material the imido groups are both transferred to the sulfur atoms of the other two, while the sulfur centre of the first is reduced from S(IV) to the S^{2-} centre in [thf$_6$Li$_6${μ$_6$S}{(N^{t}Bu)$_3$S}$_2$]. A mechanistic explanation can be found in the PhD thesis of *R. Fleischer*.[39] As initiation step for the radical reaction, a single electron transfer from the metal to the sulfurdiimide is discussed. The following reaction sequence, including radical species and redox reactions, leads to the dilithium sulfide adduct.

This is not the only way to get the dilithium sulfide adduct. Unintended redox reactions which lead to the dilithium sulfide adduct were observed in numerous other reactions, e. g. in the reaction of [(Et)(Me)CS(N^{t}Bu)$_2$]$^{2-}$ with sulfur-diimide.[6a]

Similar reactions, with sodium and potassium metal, were performed by *Ilge*[40] in our group. In the reaction of S(N^{t}Bu)$_2$ with elemental sodium she gained [thf$_6$Na$_6${μ$_6$S}{(N^{t}Bu)$_3$S}$_2$], the isotype complex to [thf$_6$Li$_6${μ$_6$S}{(N^{t}Bu)$_3$S}$_2$]. The higher alkaline metal potassium gave the radical [thf$_3$K$_3${(N^{t}Bu)$_3$S}$_2$]. However, all reactions yielded products containing the S(N^{t}Bu)$_3{}^{2-}$ moiety.

To synthesise the asymmetrically substituted triimidosulfites various parameters in a multitude of experiments were varied. In most cases, however, the dilithium sulfide adduct, either the known ^{t}Bu substituted or the new trimethylsilyl substituted dilithium sulfide adduct (**2**) was isolated.

The findings are summarised in scheme 5 and scheme 6.

$$3\ S(N^tBu)_2 \qquad 2\ CyNSN^tBu \qquad 2\ CyNSN^tBu$$
$$+ \qquad\qquad + \qquad\qquad +$$
$$6\ Li \qquad\qquad 4\ LiHN^tBu \qquad 4\ LiHNCy$$

thf   hexane / Δ
                    thf   thf
                    Δ   hexane

$$[thf_6Li_6(\mu_6S)\{(N^tBu)_3S\}_2]$$

12-crown-   thf   thf
4-ether   2m

$$2\ S(N^tBu)_2 \qquad 3\ S(N^tBu)_3 \qquad 6\ Me_3SiNSN^tBu$$
$$+ \qquad\qquad + \qquad\qquad +$$
$$4\ LiHN^tBu \qquad 6\ Li \qquad 6\ Li$$

Scheme 5: Reactions to [thf$_6$Li$_6$(µ$_6$S){(N^{t}Bu)$_3$S}$_2$].

$$6\ CyNSNSiMe_3 \qquad 3\ S(NSiMe_3)_2 \qquad 6\ CyNSNSiMe_3\ +\ 6\ LiHN\text{—}$$

thf   thf   thf/Hexane

$$[thf_6Li_6(\mu_6S)\{(NSiMe_3)_3S\}_2]$$

Scheme 6: Reactions to [thf$_6$Li$_6$(µ$_6$S){(NSiMe$_3$)$_3$S}$_2$].

It is striking, that even if asymmetric sulfurdiimides are used in the reactions, only identically substituted lithium sulfide adducts are obtained.

The sequence, showing the decreasing stabilisation effect of the substituents, is the following:

$$^tBu > SiMe_3 > Cy.$$

As long as there is at least one ^tBu group in the sulfurdiimide, $[thf_6Li_6(\mu_6S)\{(N^tBu)_3S\}_2]$ is the only identifiable product. If there are no ^tBu groups in the sulfurdiimide and at least one $SiMe_3$ groups, $[thf_6Li_6(\mu_6S)\{(NSiMe_3)_3S\}_2$ (**2**) is obtained. (This sequence of stability is known from reactivity investigations.)

But the question still remained: Why did all these reactions led to the dilithium sulfide adduct?

An explanation might be provided by the following experiment:

$$3\ [(thf)Li_4\{S(N^tBu)_3\}_2] \xrightarrow[S_8]{thf} 2\ [(thf)_6Li_6(\mu_6S)\{(N^tBu)_3S\}_2] \qquad (2)$$
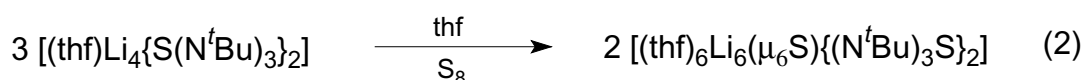
Triimidosulfite and elemental sulfur reacts to give the related lithium sulfide adduct. Sulfur is always present in the reactions of the employed sulfurdiimides, because it is not possible to eliminate the sulfur totally in the purification process.

2.1.2.2 Structure of [thf$_6$Li$_6$$\{\mu_6S\}\{$(NSiMe$_3$)$_3S\}_2$] (**2**)

*Figure 5: Solid state structure of [thf$_6$Li$_6$$\{\mu_6S\}\{$(NSiMe$_3$)$_3S\}_2$] (**2**) (coordinating thf omitted for clarity).*
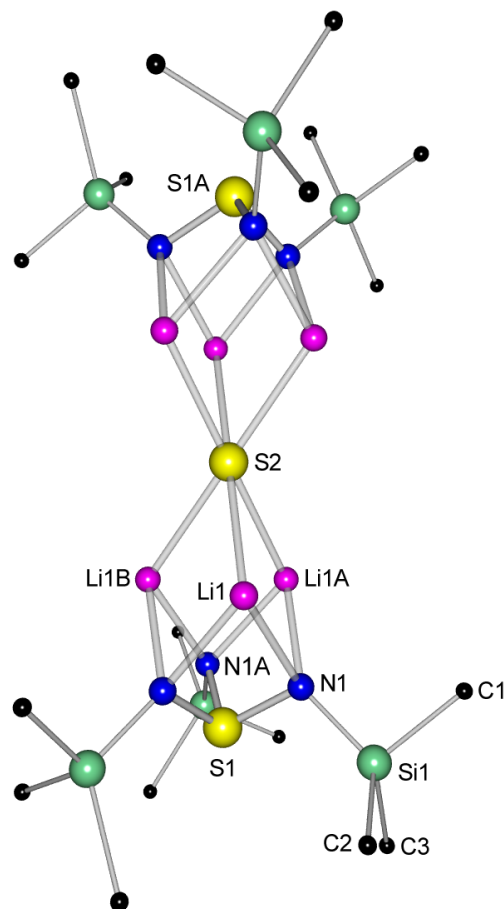
*Table 3: Selected bond lengths [pm] and angles [°] of **2**.*

S1 – N1	163.6(3)	N1 – S1 – N1A	102.17(12)
N1 – Li1	213.7(6)	S1 – N1 – Si1	119.63(16)
N1 – Li1A	207.8(6)	N1 – Si1 – C1	108.19(17)
Li1 – S2	243.9(5)	N1 – Si1 – C2	113.82(17)
		N1 – Si1 – C3	113.93(17)

The view along the threefold axis of the molecule reveals that the lithium atoms of the Li$_3$(N^{t}Bu)$_3$S moiety are not located at the SN$_2$ bisector, but shifted closer towards one nitrogen atom causing alternating shorter (207.8(6) pm) and longer (213.7(6) pm) Li–N bonds (scheme 7). The silicon atom of the silyl group is slightly removed from the S–N axis and bent towards the loosely coordinated

lithium atom. The nitrogen atom can be regarded as sp^2 hybridised. The shorter Li–N bonds are caused by coordinating the metal with a sp^2 AO which contains the negative charge. The longer Li···N bonds result from the weaker metal interaction with the non-hybridised p-orbital of the nitrogen atom. This effect has been ascertained earlier.[41] The asymmetric Li–N coordination in **2** is not as pronounced as in [thf$_6$Li$_6${μ$_6$S}{(N^{t}Bu)$_3$S}$_2$], due to the lower steric strain of silyl groups.

Li—N: 207.8(6) pm
Li····N: 213.7(6) pm
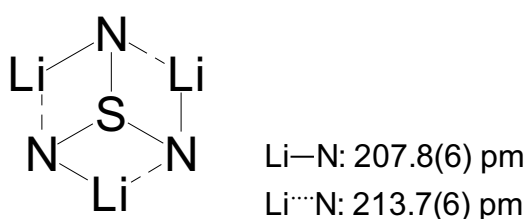
Scheme 7: View along the threefold axis revealing alternating short Li–N and long Li···N bonds.

The central sulfide anion (S2 in figure 5) is coordinated to six lithium cations and the Li–S distances (Li–S: (243.9(5) pm) are shorter than those in solid lithium sulfide Li$_2$S (247 pm).[42]

N1-Si1-C1: 108.19(17)°
N1-Si1-C2: 113.82(17)°
N1-Si1-C3: 113.93(17)°
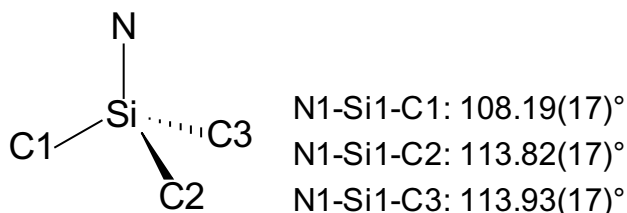
Scheme 8: N-Si-C angles in the silyl group of [thf$_6$Li$_6${μ$_6$S}{(NSiMe$_3$)$_3$S}$_2$].

There is a remarkable difference in the angles at the silicon atoms. N1-Si1-C2 and N1-Si1-C3 have both values of averaged 113.9(17)°. N1-Si1-C1 however has an angle which is about 5.6° smaller (108.19(17)°). C1 approaches closer to the surface Li1A-Li1-N1. Furthermore C1 is almost in plane with the N1-Si1-S1 plane (8.7° deviation).

2.1.2.3 The intermediate [(thf)Li$_2${(N^{t}Bu)$_2$(NSiMe$_3$)S}]$_2$

Although most reactions of sulfurdiimides with different lithium amides led to molecules of the [thf$_6$Li$_6${μ$_6$S}{(NR)$_3$S}$_2$] type (figure 5), in one case an

intermediate could be isolated as [(thf)Li$_2${(N^{t}Bu)$_2$(NSiMe$_3$)S}]$_2$. In the addition reaction of di(trimethylsilyl)sulfurdiimide with two equivalents of *tert.*-butyl lithium amide di(*tert.*-butyl)-trimethylsilyl-triimidosulfite was isolated. As the data of the single crystal X-ray analysis were not satisfactory, it is not possible to discuss the structure in any detail. However, the composition of [(thf)Li$_2${(N^{t}Bu)$_2$(NSiMe$_3$)S}]$_2$ was determined unambiguously and allows insides in the reaction sequence to give finally the dilithium sulfide adduct.

$$2S(NSiMe_3)_2 \ + \ 4LiHN^tBu \ \xrightarrow{\text{thf}} \ [(thf)Li_2\{(N^tBu)_2(NSiMe_3)S\}]_2 \qquad (3)$$
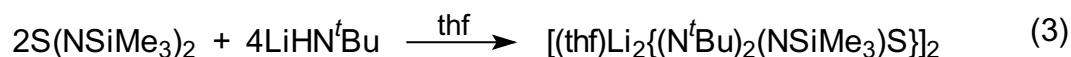
As can be seen in equation (3), one NSiMe$_3$ group is already removed from the resulting sulfite unit. In this reaction as well the different stabilisation effects of the nitrogen substituents is evident, as has been shown in scheme 5 (N^{t}Bu > NSiMe$_3$). The final formation of the dilithium sulfide adduct [thf$_6$Li$_6$(μ_6S)-{(N^{t}Bu)$_3$S}$_2$] in this reaction sequence can be rationalised in the same way as for the dilithium sulfide adducts mentioned in chapter 2.1.2.1. Purified S(NSiMe$_3$)$_2$ contains small amounts of sulfur and causes the formation of the dilithium sulfide adduct. The formation of hexamethyldisilazane and trimethylsilylamine as by-products is obvious.

The structure of [(thf)Li$_2${(N^{t}Bu)$_2$(NSiMe$_3$)S}]$_2$ extents the already known coordination polyhedra of the dilithium triimidosulfites.

The donor-free lithium salt [Li$_2${(N^{t}Bu)$_3$S}]$_2$ exhibits a dimeric structure, comprising two cap shaped dianions, facing each other with their concave sites in a staggered conformation (scheme 9, **a**). In the presence of the donor molecule thf one lithium atom leaves the area between the caps to the periphery and is coordinated only by two nitrogen atoms (scheme 9, **b**). [(thf)Li$_2${(N^{t}Bu)$_2$(NSiMe$_3$)S}]$_2$, (scheme 9, **c**) shows a dimeric structure with two lithium cations coordinated η^2 by two nitrogen atoms of one ligand. These lithium atoms have left the central lithium plane of the molecule and are additionally coordinated by thf. The other two lithium cations are bridging both ligands via μ_4 coordination of two nitrogen atoms of each ligand.
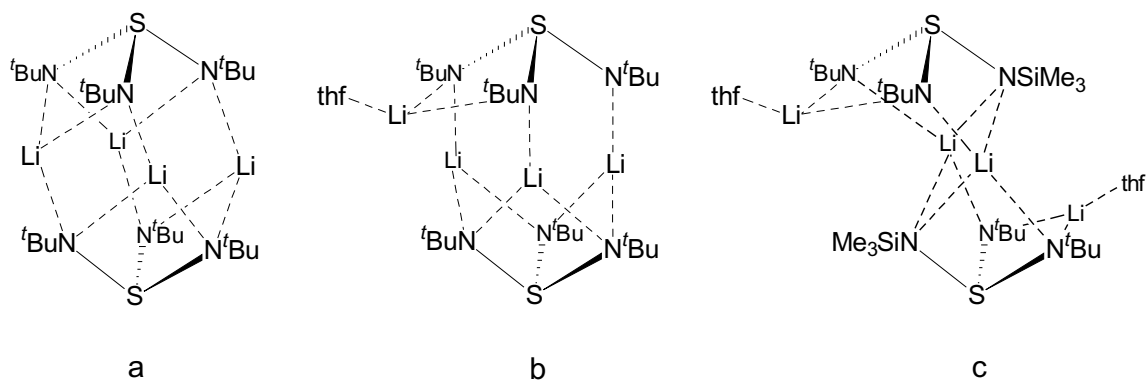
*Scheme 9: Structure of [Li$_2${(N^{t}Bu)$_3$S}]$_2$ (**a**), its thf adduct (**b**) and [Li$_2${(N^{t}Bu)$_2$(NSiMe$_3$)S}]$_2$ (**c**).*

2.1.3   Approach to other asymmetrically substituted triimidosulfites

It was a challenging aim to follow the isoelectronic principle, first established by *Langmuir*,[2] to replace the NR group by its higher homologue PR.
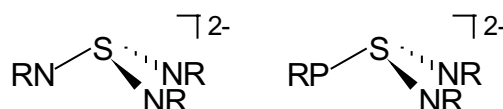
Scheme 10: Triimidosulfite and diimidomonophosphidosulfite.

Furthermore the bond energies of P=S and N=S (see Table 4) reveal, that the P=S bond is as stable as the N=S bond, whereas the P–P bonds in P$_4$-rings are less stable. This should enable the exchange of -NR against -PR in triimidosulfites.

Table 4: Different energies of phosphorus and sulfur bonds.

	Calc.	Exp.
N=S	334.94 +/- 23 kJ/mol[43]	-
P=S	297.26 - 443.80 kJ/mol[44]	335[45]/394 kJ/mol)[46]
P–P(P$_4$-ring)	-	201 kJ/mol[45]

In the first step of the envisaged synthesis the *prim.* cyclohexylphosphane is lithiated with one equivalent of *n*BuLi. The resulting lithiumphosphanide should react with sulfurdiimide to diimidomonophosphidosulfite. But the phosphide reacts completely to a coupling product: 1,2,3,4-tetracyclohexyl-1,2,3,4-

tetraphosphetane. Phosphorous is endeavoured to build chains or rings, especially four- or five-membered P rings are often obtained in reactions as by-products.[47]

$$4CyPHLi \ + \ 2S(N^tBu)_2 \ \longrightarrow \ \begin{array}{c} Cy \quad \quad Cy \\ \diagdown P{-}P \diagup \\ | \quad \ | \\ P{-}P \\ \diagup \quad \ \diagdown \\ Cy \quad \quad Cy \end{array} \ + \ ?$$
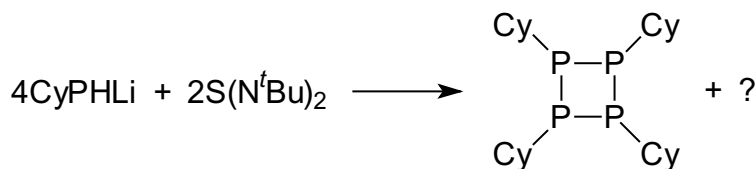
Scheme 11: 1,2,3,4-tetracyclohexyl-1,2,3,4-tetraphosphetane.

2.2   Alkylenediimidosulfites

2.2.1   Introduction

The reactivity of lithium organyl diimidosulfinates was first studied in 1976.[48] The reactions of sulfurdiimides with alkali metal aryls and alkyls led to diimidosulfinates. The structures of diimidosulfinates were first studied systematically by *Pauer*. The lithium species can undergo metal exchange reactions, and therefore the diimidosulfinates gained interest in the transition metal chemistry and in lanthanide- and actinide-chemistry as dipodal ligands. *Pauer* examined the influence of the variation of the following parameters on the structure:

-    metal atom

-    substituents at the nitrogen atoms

-    substituent at the sulfur atom

-    additional donor molecules

He could identify six different structure types:

A1

Me₃Si—N—S(Ph)—N—SiMe₃ ... (structure)

A2

B

- M = Li,[5c] Na, K, Rb, Cs;[5a] L = thf
- M = K; L = DME[5d]

- R = SiMe₃,[5a] Cy[5d]

-M = Li; R = SiMe₃, tBu,[5c] Cy;[5d] L = OEt₂
- M = Na; R = SiMe₃; L = DME[5d]

C1

C2

D

- M = Ca, Sr, Ba[50]
- M = Mg only one thf[5d]

[5b]

- M = Li; R1 = tBu; R2 = tBu[5a]
- M = Cu; R1 = Ph; R2 = SiMe₃[5d]
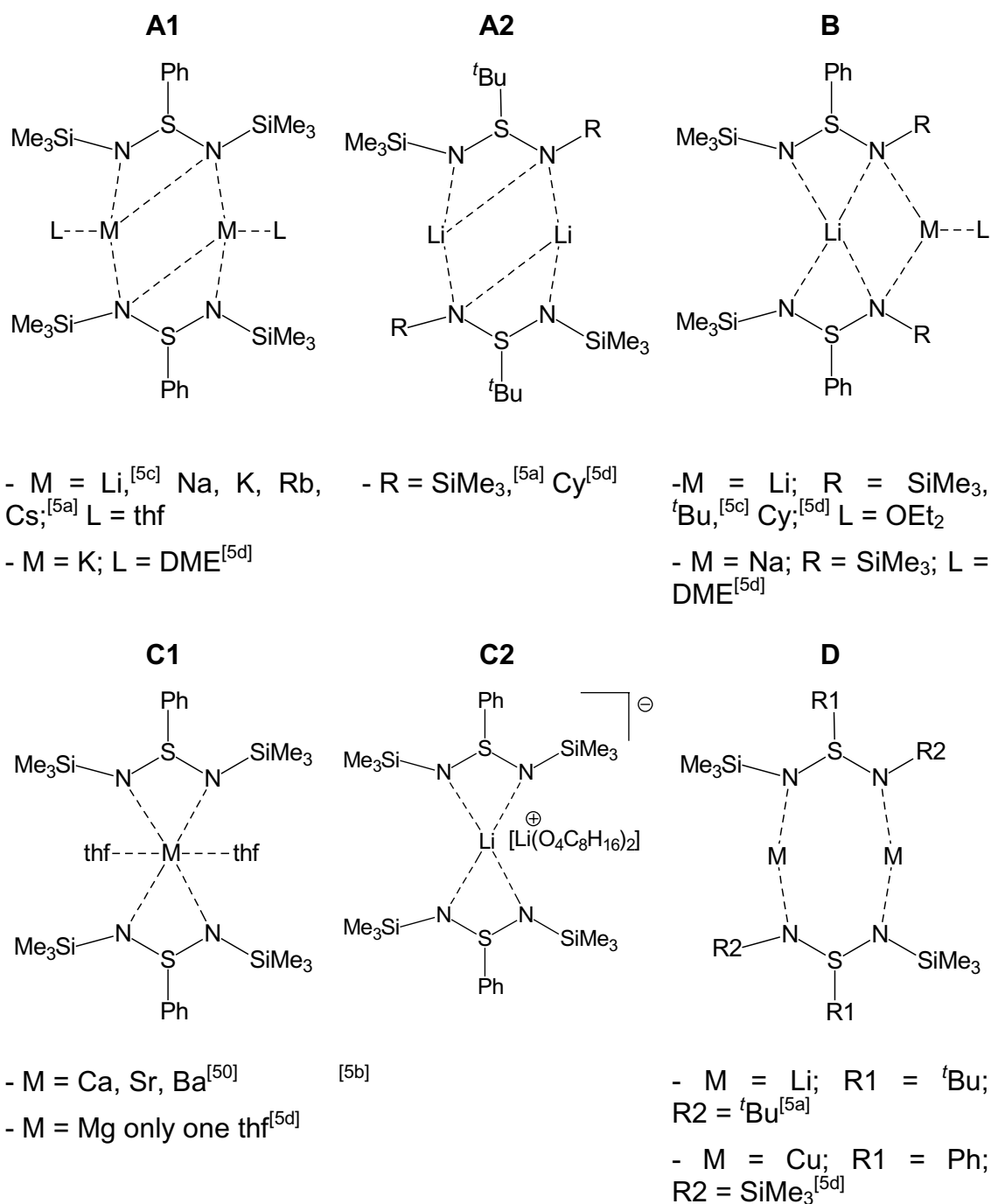
Figure 6: Different structure types of diimidosulfinates.

As the previously synthesised diimidosulfinates did not have CH-acidic S-bound substituents they were unsuitable to give alkylenediimidosulfites upon deprotonation. Hence those investigations were first extended to the S-methyl substituted species.

2.2.2   Alkyldiimdosulfinates

2.2.2.1 Preparation of [(thf)Li{H$_3$CS(NSiMe$_3$)$_2$}]$_2$ (**3**) and
[(Et$_2$O)Li{H$_3$CS(NSiMe$_3$)(NC$_6$H$_{11}$)}]$_2$ (**4**)

Methyllithium easily adds to the double bond of S(NSiMe$_3$)$_2$ to give the methyldiimidosulfinate [(thf)Li{H$_3$CS(NSiMe$_3$)$_2$}]$_2$ (**3**). An additional equivalent of MeLi deprotonates the S-bonded methyl group and [(Et$_2$O)Li$_2${H$_2$CS(NSiMe$_3$)$_2$}]$_2$ is formed, a sulfurylide, synthesised at the same time in our group and from *Hänssgen* and coworkers.[6] The analogue addition reaction of Me$_3$SiNSNCy and one equivalent MeLi was successful, whereas the analogous reaction with CyNSN*^{t}*Bu failed.

$$2S(NSiMe_3)R + 2MeLi \xrightarrow{\quad donor \quad} [(donor)Li\{H_3CS(NSiMe_3)R\}]_2 \qquad (4)$$

3: R = NSiMe$_3$; donor = thf
4: R = NCy; donor = Et$_2$O
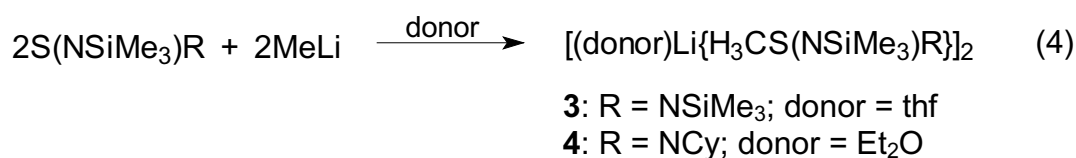
To obtain sodium or potassium derivatives of methyldiimidosulfinates, methyldiimidosulfinic acid (figure 7) was reacted with the respective alkaline metal hydrides, but no deprotonation occurred.
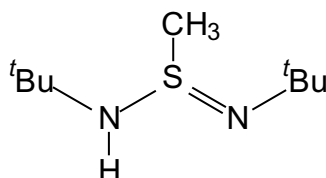
Figure 7: Methyldiimidosulfinic acid.

2.2.2.2 Crystal structure of [(thf)Li{H$_3$CS(NSiMe$_3$)$_2$}]$_2$ (**3**) and
[(Et$_2$O)Li{H$_3$CS(NSiMe$_3$)(NC$_6$H$_{11}$)}]$_2$ (**4**)

Compounds **3** and **4** are dimers in the solid state. They are isostructural and therefore discussed together. The structures reveal a stair shaped tricycle, known from *Pauers* diimidosulfinates[5] and belong to structure type **A1** (figure 6). The SN$_2$Li rings are situated on opposite sites of the central Li$_2$N$_2$ ring and together they built up a stair like framework. Each of the lithium atoms is

chelated by both nitrogen atoms of a diimidosulfinate ligand while an additional Li-N bond provides the dimeric link.
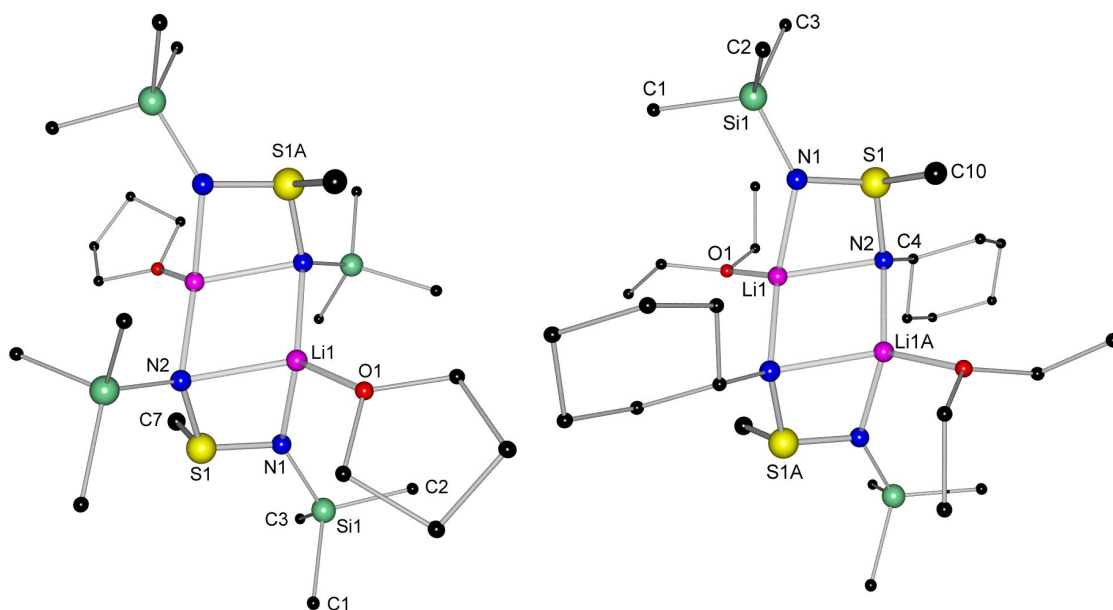
Figure   8:   Solid   state   structure   [(thf)Li{H₃CS(NSiMe₃)₂}]₂   (3)   (left)   and [(Et₂O)Li{H₃CS(NSiMe₃)(NC₆H₁₁)}]₂ (4) (right).

An inversion centre is located in the middle of each Li_2N_2 ring. Each lithium atom is coordinated by three nitrogen atoms and one additional thf or diethyl ether molecule, respectively. The Li1–N1 distance is in both structures the shortest of the Li–N bonds, because N1 is only coordinated to one lithium atom. As two lithium atoms compete for the negative charge at N2 those Li-N bonds are longer. The Li1–N2 bonds are the longest Li–N bonds among those in the dimers with 218.8(3) pm for **3** and 220.8(3) pm for **4**, respectively. This implies that the latter is closer to the eight membered ring depicted as **D** in figure 6.

In **4** this bond elongation is more pronounced, possibly as a consequence of the higher steric strain of diethyl ether compared to thf in **3**. The mean value of the Li–N distances in **3** is 210.73(3) pm and 211.4(3) pm in **4** and is therefore significantly above the expected value of 199 pm (sum of covalent radius of nitrogen and the radius of the lithium atom in LiH).[49]

*Table 5: Selected bond lengths [pm] and angles [°] of **3** and **4**.*

	3	4
S1 – N1	160.42(15)	159.77(13)
S1 – N2	162.10(14)	163.21(12)
S1 – C7/C10	180.2(2)	180.26(18)
N1 – Si1	170.79(15)	170.30(13)
N1 – Li1	203.8(3)	204.3(3)
N2 – Li1	218.8(3)	220.8(3)
Li1 – N2A	209.6(3)	209.2(3)
N2 – Si2/C4	173.36(15)	148.39(18)
N1 – S1 – N2	104.00(8)	104.06(6)
N1 – S1 – C7/C10	103.68(9)	103.78(8)
N2 – S1 – C7/C10	102.76(9)	103.32(8)
S1 – N2 – Li1A	123.30(12)	125.17(10)
N1 – Li1 – N2A	123.24(16)	123.97(13)

Like the S-phenyldiimidosulfinates ($PhS(NR)_2^-$), the $MeS(NR)_2^-$ anions act as dipodal chelating ligands with the negative charge delocalised over the SN_2 moieties. The S–N distances in **3** (av. S–N: 161.26(15) pm) and **4** (av. S–N: 161.49(13) pm) resemble those of $R'S(NR)_2^-$ (av. S–N: 160 pm)[5] and $[S(Me_3SiN)_2LiN(SiMe_3)_2SN(Me_3Si)_2]$ (av. S–N: 159 pm).[50] Although the two S–N bond lengths in **3** and **4** differ only marginally (1.5 pm in **3** and 3.4 pm in **4**) the shorter S–N bond length correlates to the greater S-N-C bond angle indicating predominantly sp^2-character of the more closely bond nitrogen atoms.

The N-S-N angles in **3** (104.00(8)°) and **4** (104.06(6)°) are almost identical and in comparison to $[(thf)Li\{H_5C_6S(NSiMe_3)_2\}]_2$, with a N-S-N angle of 105.9°, slightly smaller. Even the sum of angles in **3** and **4** at S1 is 4.2° (310.44°) and 3.4° pm (311.16°), smaller than in $[(thf)Li\{H_5C_6S(NSiMe_3)_2\}]_2$ (314.6°).[5c] This demonstrates the more electron-releasing property of the methyl group compared to the phenyl group. It results in a more emphasised stereochemically active lone-pair at the sulfur atom and hence in closer proximity of the three S-bound substituents.

Another important parameter is the stair angle, the angle between the plane N1-S1-N2-Li1 and the plane Li1-N2-Li1A-N2A.
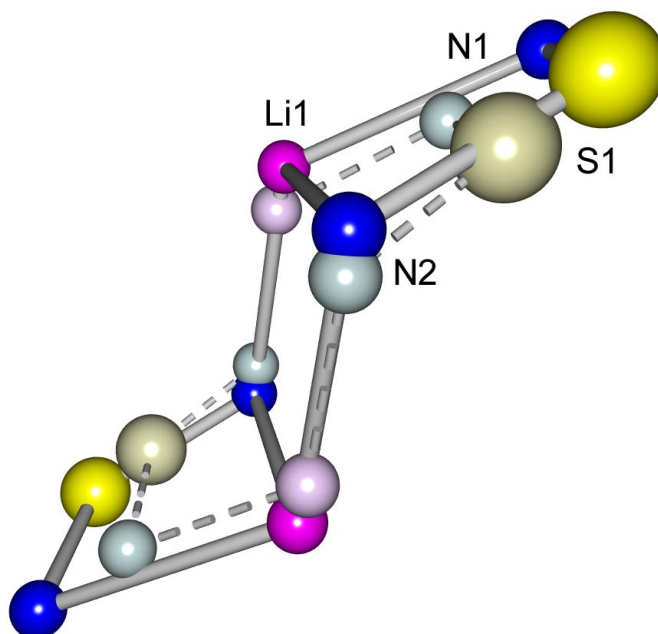
*Figure 9: Comparison of **3** (intensive colours) with [(thf)Li{H$_5$C$_6$S(NSiMe$_3$)$_2$}]$_2$ (pastel colours) (SiMe$_3$-groups and solvent molecules omitted for clarity).*

In [(thf)Li{H$_5$C$_6$S(NSiMe$_3$)$_2$}]$_2$ this angle is 144.0°, in **3** it is 122.5° and in **4** it is 123.6°, respectively. Therefore the angles are 21.5° and 20.4° smaller, respectively. This means that the dimers **3** and **4** are not as flat as [(thf)Li{H$_5$C$_6$S(NSiMe$_3$)$_2$}]$_2$. This is a direct consequence of the more pyramidal environment of the sulfur atoms.

Pauer used two different substituents at the sulfur atom (phenyl and *tert*.-butyl groups), different metals and varied other parameters, but the S–C bond lengths remained within smallest deviations in the standard range of 180 pm.[9] The methyl residue at sulfur joins in and has no significant influence on the S–C bond length.

2.2.2.3 [Cu{H$_3$CS(N^{t}Bu)$_2$}]$_2$ (**5**)

Fleischer of our group reported several transmetalation reactions for the tripodal triimidosulfite. Amides of alkaline earth metals (Mg, Ca, Ba) and tin,[51] predominantly used in deprotonation reactions, were applied. In the obtained

compounds the dimeric structure of two cap shaped ligands facing each other with their concave sides was retained (scheme 9).

Other often used transmetalation reagents are metal halides. *Walfort*[52] reacted lithium triimidosulfite with different coinage metal halides and got molecules of the following type:
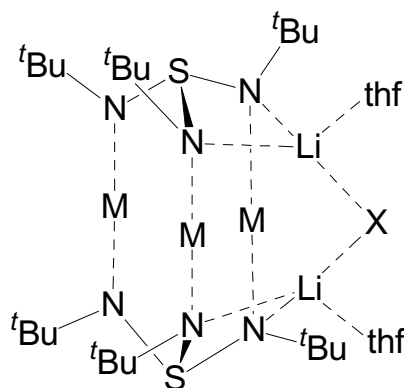
Figure 10: Structure of [(thf)$_2$M$_3$Li$_2$X{(N^{t}Bu)$_3$S}$_2$] (M = Cu, X = I;M = Ag, X = Br, I).

In this type of molecule the alkyl groups at the nitrogen atoms are arranged in an eclipsed conformation, because of the preferred linear twofold coordination of coinage metals.

Pauer reacted in a one pot reaction S(NSiMe$_3$)$_2$, MeLi and waterfree CuCl and resulted in the synthesis of [Cu{H$_5$C$_6$S(SiMe$_3$)$_2$}]$_2$.[5d] The analogue reaction of S(N^{t}Bu)$_2$ with MeLi led to [Cu{H$_3$CS(N^{t}Bu)$_2$}]$_2$ (**5**).
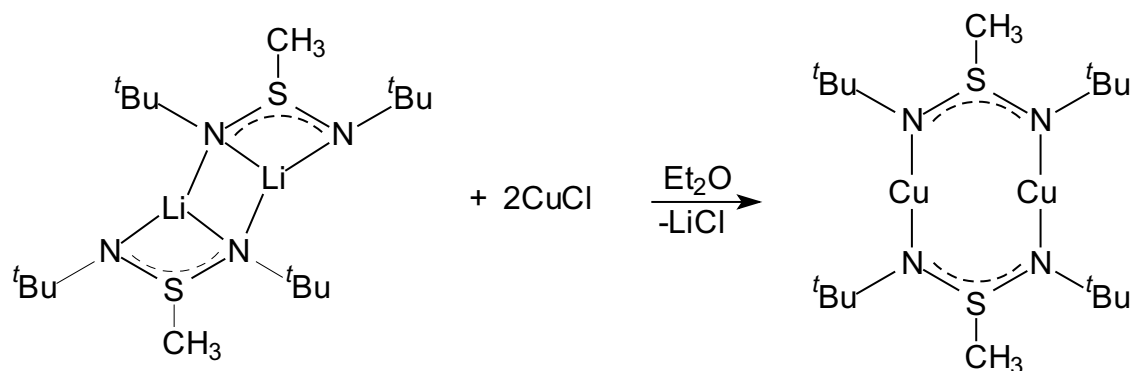
*Scheme 12: Preparation of [Cu{H$_3$CS(N^{t}Bu)$_2$}]$_2$ (**5**).*

Crystal structure

Even though there was Et_2O in the reaction mixture, no Et_2O could be detected in the solid state structure of $[Cu\{H_3CS(N^tBu)_2\}]_2$ (**5**).
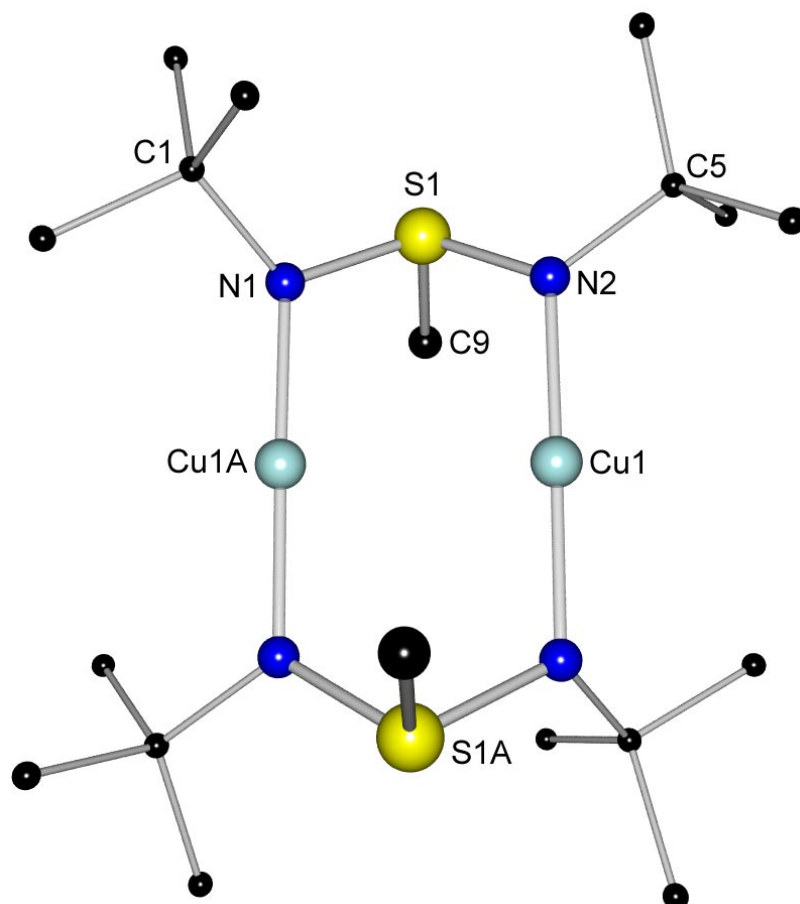
*Figure 11: Solid state structure of $[Cu\{H_3CS(N^tBu)_2\}]_2$ (**5**).*

*Table 6: Selected bond lengths [pm] and angles [°] of **5**.*

S1 – N1	162.76(18)	Cu1 ··· Cu1A	269.40(6)	N1 – S1 – N2	109.79(9)
S1 – N2	163.36(18)	Cu1 – N1A	188.32(17)	N1 – S1 – C9	97.65(11)
S1 – C9	179.0(2)	Cu1 – N2	187.32(17)	N2 – S1 – C9	104.00(11)
N1 – C1	149.7(3)			N2 – Cu1 – N1A	178.91(8)
N2 – C5	148.6(3)				

The compound is isostructural to copper-phenyl-N,N'-bis(trimethylsilyl)sulfinate prepared by *Pauer*.[5d] The ladder type structure of the lithium starting material is transformed into a plane structure, which consists of an eight membered

metallacycle (figure 6, **D**). The two NSN units are connected by an inversion centre.

The copper atoms of [Cu{H$_3$CS(N^{t}Bu)$_2$}]$_2$ (**5**) are located half-way between the two nitrogen atoms, the Cu–N-distances are 187.32(17) pm and 188.32(17) pm, respectively, and thus almost exactly as long as in [Cu{H$_5$C$_6$S(SiMe$_3$)$_2$}]$_2$.[5d] Compared to a biological system like plastocyanine, with Cu–N-bond lengths of 204 pm and 210 pm in the reduced Cu(I) state, they are very short.[53] This short and stable Cu–N bonds are responsible for the different properties, in comparison to the lithium derivatives. In opposite to the hydrolytic instability of the lithium species, compound **5** has a high hydrolytic stability.

The transannular Cu⋯Cu distance in **5** (269.40(6) pm) is longer than in the isotypic copper benzamidinate (242.5(2) pm),[54] due to the greater cone angle of the N-S-N system. It is too long to be considered a metal–metal interaction, like the one in the three-centre two-electron bond in [Li(thf)$_4$][Cu$_5$Cl$_4${Si(SiMe$_3$)$_3$}$_2$] with a Cu⋯Cu bond length of 240.3(2) pm.[55] Moreover, the dislocation of the copper atoms from the N⋯N vector to the outside (N-Cu-N 178.91°) indicates electrostatic repulsion rather than attraction. This was observed previously in [(thf)$_2$Cu$_3$Li$_2${(N^{t}Bu)$_3$S}$_2$] with a N-Cu-N angle of 177.8(2)°.[52]

The averaged S–N bond length in [Cu{H$_3$CS(N^{t}Bu)$_2$}]$_2$ (**5**) of 163.06(18) pm is about 2 pm longer than in [(thf)Li{H$_3$CS(NSiMe$_3$)$_2$}]$_2$ (**3**) and [(Et$_2$O)Li-{H$_3$CS(NSiMe$_3$) (NC$_6$H$_{11}$)}]$_2$ (**4**) (no crystallographic data are available for [Li[H$_3$CS(N^{t}Bu)$_2$]$_2$]). In [Cu{H$_5$C$_6$S(SiMe$_3$)$_2$}]$_2$ the S–N bonds are even shorter (av. 161.9 pm).[5d]

S1 is located 59.66 pm above the best plane defined by N1-N1A-Cu1-Cu1A This is almost the same value as in [Cu{H$_5$C$_6$S(SiMe$_3$)$_2$}]$_2$. Consequently, the dimer **5** is not plane. The sulfur atoms are located above and below the N1-N1A-Cu1-Cu1A plane, respectively. In contrast to **5** the copper diimidodiphenyl phosphinate [Cu{Ph$_2$P(NSiMe$_3$)$_2$}]$_2$ is twisted[56] and the copper carbamate [Cu{C(NC$_6$H$_4$-p-CH$_3$)$_2$}]$_2$ is flat.[54]

Finally it has to be concluded, that there is no obvious influence of different substituents at nitrogen or sulfur on the geometric features of the copper sulfinates.

2.2.3   Alkylenediimidosulfites

Hitherto our group was interested in the synthesis of nitrogen analogues of sulfinates, sulfites, sulfonates and sulfates, but our current aim is to generate analogues through replacement of oxygen by CR_2 groups. The chemistry of the nitrogen species was well investigated by *Pauer* and *Fleischer*, but only little was known about the carbon analogues. *Walfort* was the first to uncover a synthetic route to this compounds and made $[(thf)Li_2\{H_2CS(N^tBu)_2\}]_2$.[6a]
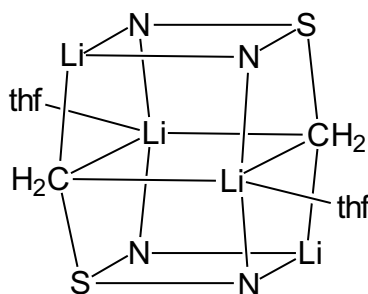
Figure 12: Structure of the first alkylenediimidosulfite (^{t}Bu at nitrogen omitted for clarity).

The direct chemical replacement of an oxygen atom or an imido group by a CR_2 group is not practicable. A route to such compounds is the following synthetic pathway. In a first step addition of a lithium alkyl to sulfurdiimide leads to the alkyldiimidosulfinate $[RS(N^tBu)(R')]^-$, like $[(thf)Li\{H_3CS(NSiMe_3)_2\}]_2$ (**3**) and $[(Et_2O)Li\{H_3CS(NSiMe_3)(NC_6H_{11})\}]_2$ (**4**). In the second step the α-carbon atom in R is metalated with one equivalent of lithium alkyl and the dianionic S-ylide is obtained. This class of compounds can be rationalised as sulfite analogues where two oxygen atoms are isoelectronically replaced by NR groups and the remaining oxygen atom is replaced by a CR_2 group. Similar to *Corey's* S-ylides $(R_2(O)S^+-^-CR_2)$ and *Wittig's* phosphonium ylides $(R_3P^+-^-CR_2)$ these molecules contain a positively charged sulfur atom next to a carbanionic centre.

It was of mayor interest to introduce stereo-information in this sulfur ylides as they might serve as chiral auxiliaries in asymmetric catalysis or as

enantioselective alkylene- or imide-tranfer reagents in organic synthesis. The asymmetrical substituted sulfurdiimide Me$_3$SiNSN^{t}Bu was employed in the synthesis.

2.2.3.1 Preparation of [(Et$_2$O)Li$_2${H$_2$CS(NSiMe$_3$)(N^{t}Bu)}]$_2$ (6) and [(thf)Li$_2${H$_8$C$_4$S(N^{t}Bu)$_2$}]$_2$ (7)

6 can be synthesised in a one-pot reaction. Two equivalents of S(NSiMe$_3$)(N^{t}Bu) react with four equivalents. of methyllithium to give the S-ylide 6.

$$2S(NSiMe_3)(N^tBu) + 4MeLi \xrightarrow[-2CH_4]{Et_2O} [(Et_2O)Li_2\{H_2CS(NSiMe_3)(N^tBu)\}]_2 \quad (5)$$

$$\mathbf{6}$$
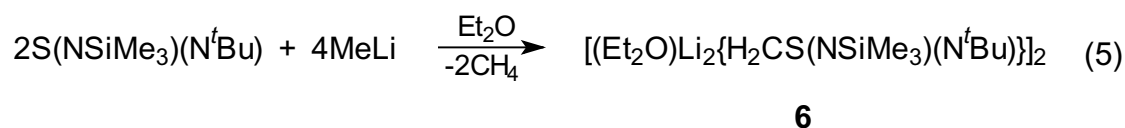
The alkylation and deprotonation of bis(*tert*.-butyl)sulfurdiimide worked with two eqv. of *n*BuLi.

$$2S(N^tBu)_2 + 4nBuLi \xrightarrow[-2C_4H_{10}]{thf} [(thf)Li_2\{H_8C_4S(N^tBu)_2\}]_2 \quad (6)$$

$$\mathbf{7}$$
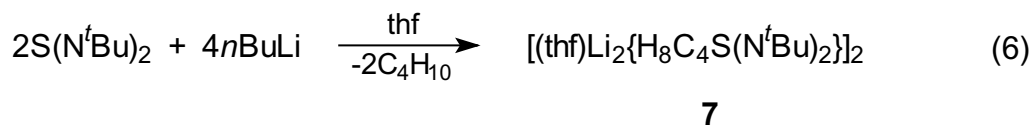
Attempts to deprotonate [(Et$_2$O)Li{H$_3$CS(NSiMe$_3$)(NC$_6$H$_{11}$)}]$_2$ (4) with MeLi failed under various conditions.

2.2.3.2 Crystal structures of [(Et$_2$O)Li$_2${H$_2$CS(NSiMe$_3$)(N^{t}Bu)}]$_2$ (6) and [(thf)Li$_2${H$_8$C$_4$S(N^{t}Bu)$_2$}]$_2$ (7)

The crystal structure of [(Et$_2$O)Li$_2${H$_2$CS(NSiMe$_3$)(N^{t}Bu)}]$_2$ (6) consists of two distorted SN$_2$C$_2$Li$_3$ cubes with a common C$_2$Li$_2$ face. The different environment of the NSN backbone, compared to the *tert*.-butyl species, has only slight effects on the geometric properties. The S–N bond lengths (av. 164.5(3) pm) are in the same range as in [(thf)Li$_2${H$_2$CS(N^{t}Bu)$_2$}]$_2$ (av. 165.8 pm) and [(thf)Li$_2${(Et)(Me)CS(N^{t}Bu)$_2$}]$_2$ (av. 165.1 pm).[6a]
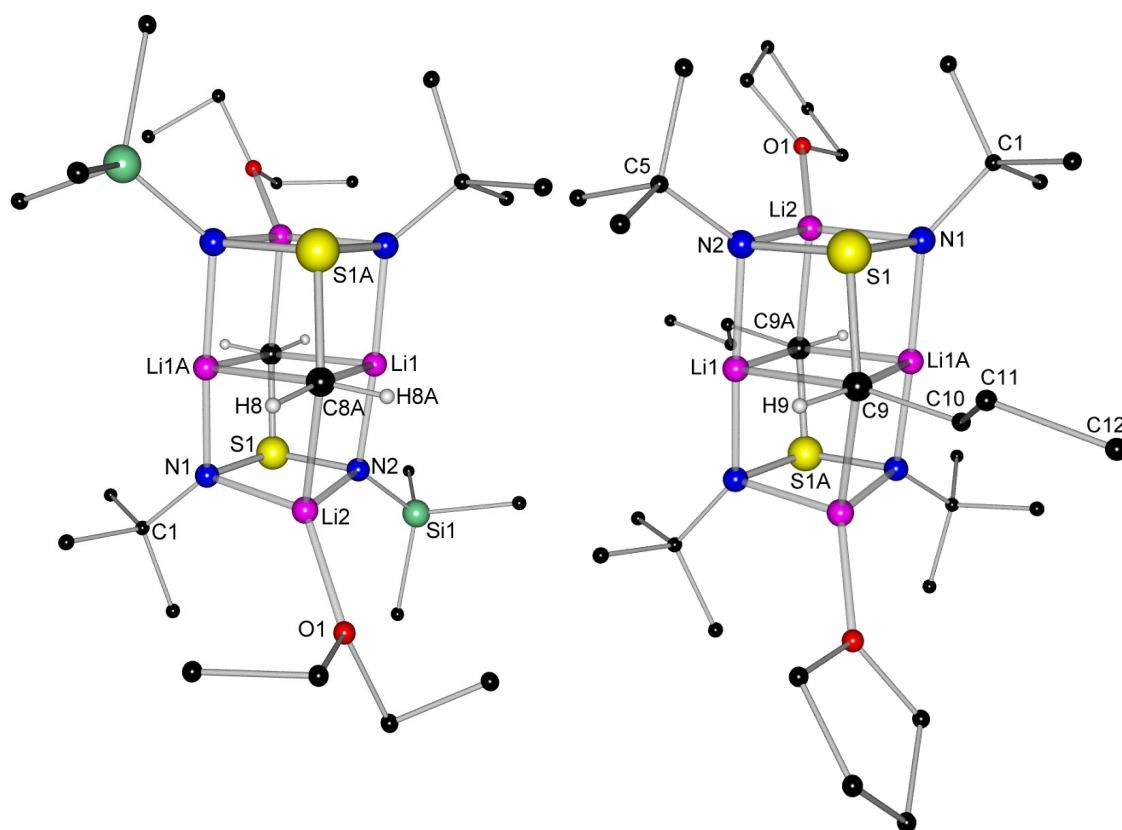
Figure 13: Solid state structure of [(Et₂O)Li₂{H₂CS(NSiMe₃)(N^{t}Bu)}]₂ (6) (left) and [(thf)Li₂{H₈C₄S(N^{t}Bu)₂}]₂ (7) (right).

The S–C bond length of 177.7(3) pm in **6** is as long as the S–C single bond found in alkyldiimidosulfinates (about 181 pm)[5] or alkyltriimidosulfonates (about 179 pm).[23] No bond shortening, anticipated from a charge delocalisation, is ascertained. This findings confirm the assumption, that the molecule has an ylidic type resonance formula.
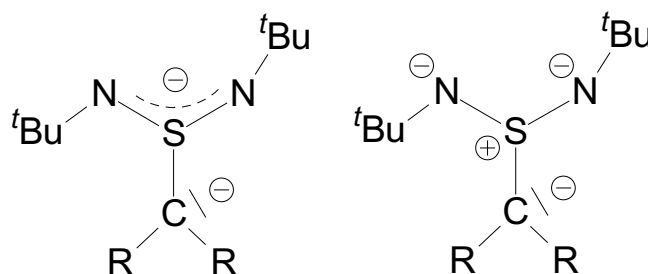
Scheme 13: Ylidic structures of alkylenediimidosulfites.

The S–N and S–C bond lengths indicate that one negative charge is delocalised over the SN_2 backbone, while the second negative charge is localised at the carbon atom.

*Table 7: Selected bond lengths [pm] and angles [°] of **6** and **7**.*

	6	**7**
S1 – N1	163.9(3)	165.41(19)
S1 – N2	165.0(3)	166.28(19)
S1 – C8/9	177.7(3)	179.9(2)
N1 – Li1A	198.2(6)	198.1(4)
N1 – Li2	208.2(6)	209.9(5)
N2 – Li1	200.0(6)	198.9(4)
N2 – Li2	208.5(7)	205.4(4)
C8/9 – Li1	238.0(7)	244.2(5)
C8/9 – Li1A	240.4(7)	236.0(4)
C8/9 – Li2A	229.3(6)	230.2(5)
N1 – S1 – N2	104.45(14)	104.55(10)
N1 – S1 – C8/9	100.16(16)	98.99(10)
N2 – S1 – C8/9	100.04(15)	99.88(10)
N2 – Li1 – N1A	176.4(4)	177.6(2)
S1 – C8/9 – Li2A	144.0(2)	142.82(16)
S1 – N1 – Li2	89.4(2)	87.89(14)
S1 – N2 – Li2	89.0(2)	89.20(14)
Li1 – C8/9 – Li1A	69.3(2)	68.34(17)
C8/9 – Li1 – C8A/9A	110.6(3)	111.66(17)

Since a centre of inversion is located in the middle of the C_2Li_2 four membered ring **6** is racemic. In the solid state structure the $SiMe_3$ group and the ^tBu group are disordered.

The structure of $[(thf)Li_2\{H_8C_4S(N^tBu)_2\}]_2$ (**7**) is isomorphous, but not isostructural to $[(Et_2O)Li_2\{H_2CS(NSiMe_3)(N^tBu)\}]_2$ (**6**). The main structural features of both are the same. The averaged S–N bond length of 165.85(19) pm is almost identical to that found in **6** (164.5(3) pm). The replacement of the

methylene group in [(thf)Li$_2${H$_2$CS(N^{t}Bu)$_2$}]$_2$ by the bulkier butylene group in **7** has only little effects on the S–C bond length (178.6(3) pm in [(thf)Li$_2${H$_2$CS(N^{t}Bu)$_2$}]$_2$[20a]; 179.9(2) pm in **7**).

The conversion of a hexagonal prismatic structure in [Li$_2${N^{t}Bu)$_3$S}]$_2$ into two distorted SN$_2$C$_2$Li$_3$cubes with a common C$_2$Li$_2$ face has been discussed by *Walfort*[57] in detail.
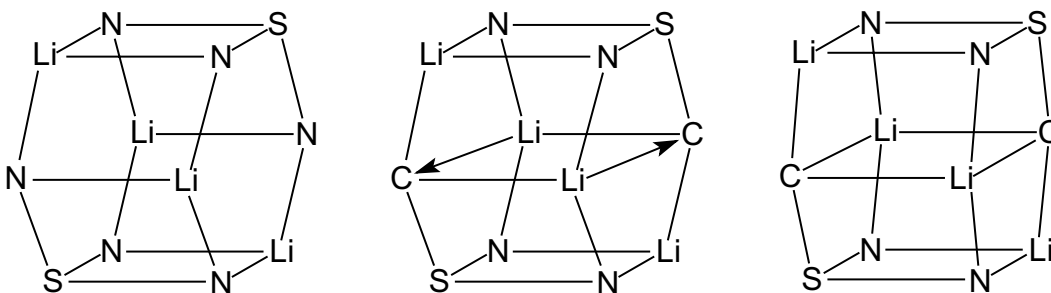
Figure 14: Conversion of a hexagonal prismatic structure into two distorted SN$_2$C$_2$Li$_3$-cubes with a common C$_2$Li$_2$ face.

Compound [(thf)Li$_2${H$_8$C$_4$S(N^{t}Bu)$_2$}]$_2$ (**7**) is an intermediate case. The C9–Li1 bond length (244.2(5) pm) is very long, indicating that **7** is on the way to a hexagonal prismatic structure. A database search for C–Li bonds[58] resulted in the following diagram 1, which shows that the C9–Li1 bond length, and the C8–Li1 bond length as well, are among the longest C–Li bonds reported.
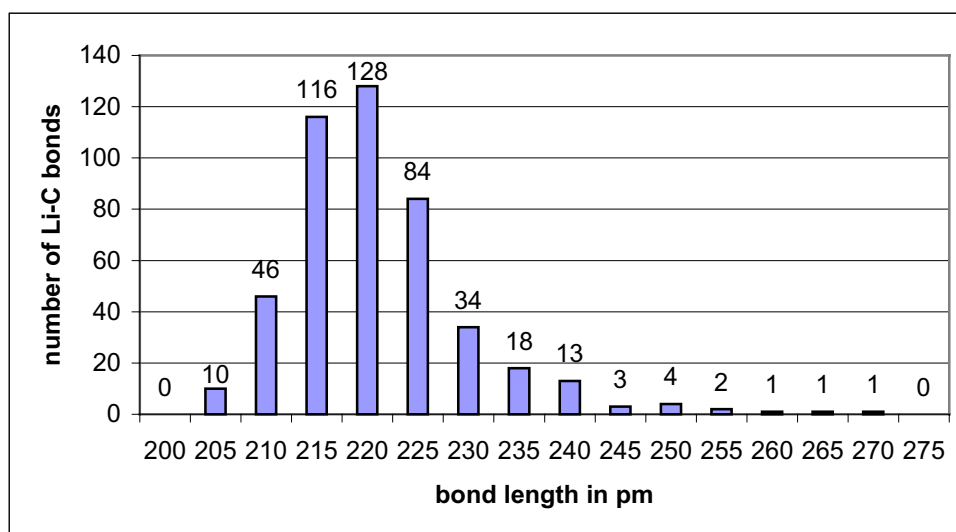
Diagram 1: C–Li bond lengths from CCDC (LiC$_4$).

2.2.3.3 NMR-Data of S-ylides

Walfort reported the synthesis of [(thf)Li$_2$[H$_2$CS(N^{t}Bu)$_2$]]$_2$.[6a] He obtained standard NMR-Data (^{1}H, ^{7}Li, ^{13}C) and was able to assign all peaks. But in the ^{13}C-NMR one peak was missing: the ylidic CH$_2$ carbon atom. A CH-COSY spectrum was recorded, which is presented infigure 15. In the ^{1}H-NMR spectrum the CH$_2$-protons could be detected as well. The ylidic carbon atom could be identified by its CH coupling peak at a chemical shift of δ = 40.58 ppm with $^1J_{C-H}$ = 110 Hz.
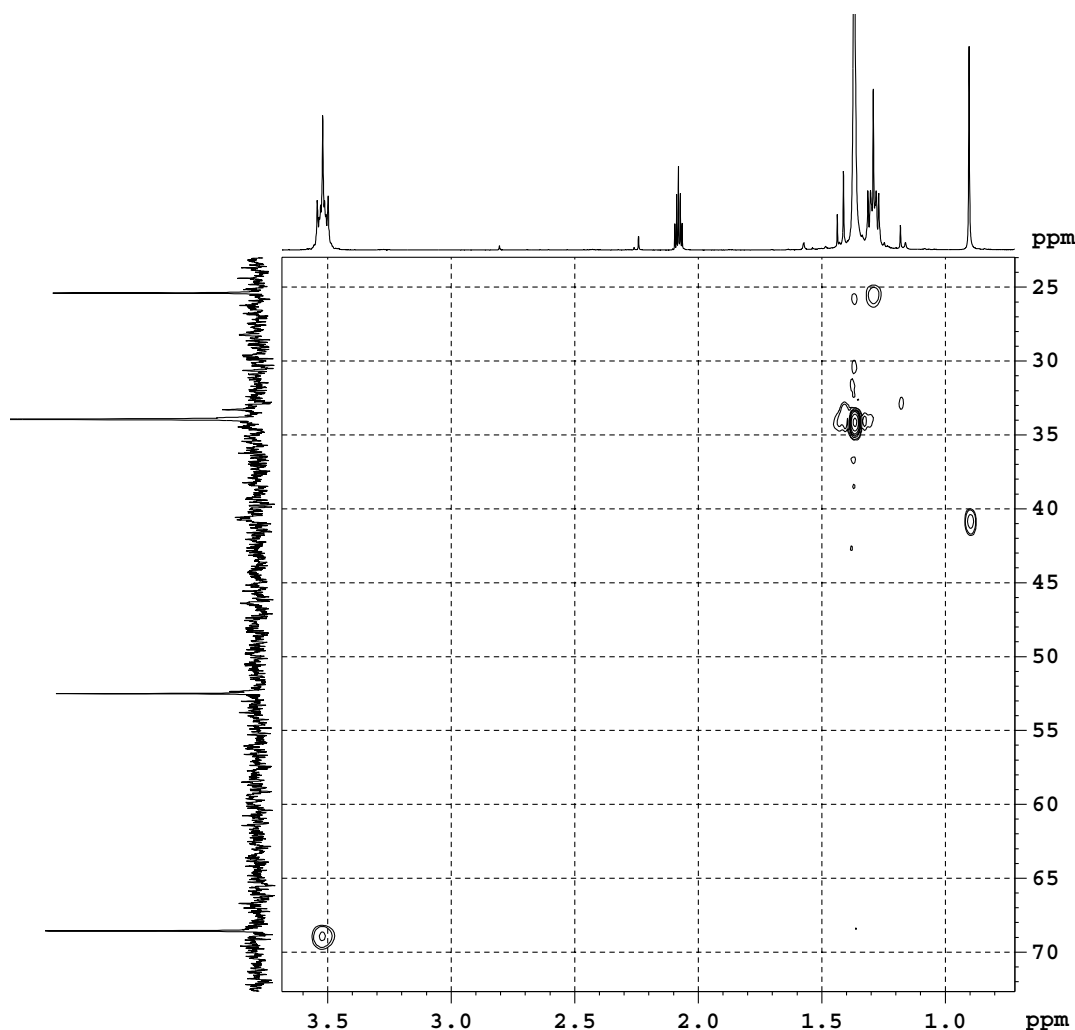
Figure 15: CH-COSY Spectrum of [(thf)Li$_2$[H$_2$CS(N^{t}Bu)$_2$]]$_2$.

For [(Et$_2$O)Li$_2$[H$_2$CS(NSiMe$_3$)(N^{t}Bu)]]$_2$ (**6**) it was less difficult. A DEPT experiment was performed and the ylidic carbon atom could be identified at a shift of 42.94 ppm.
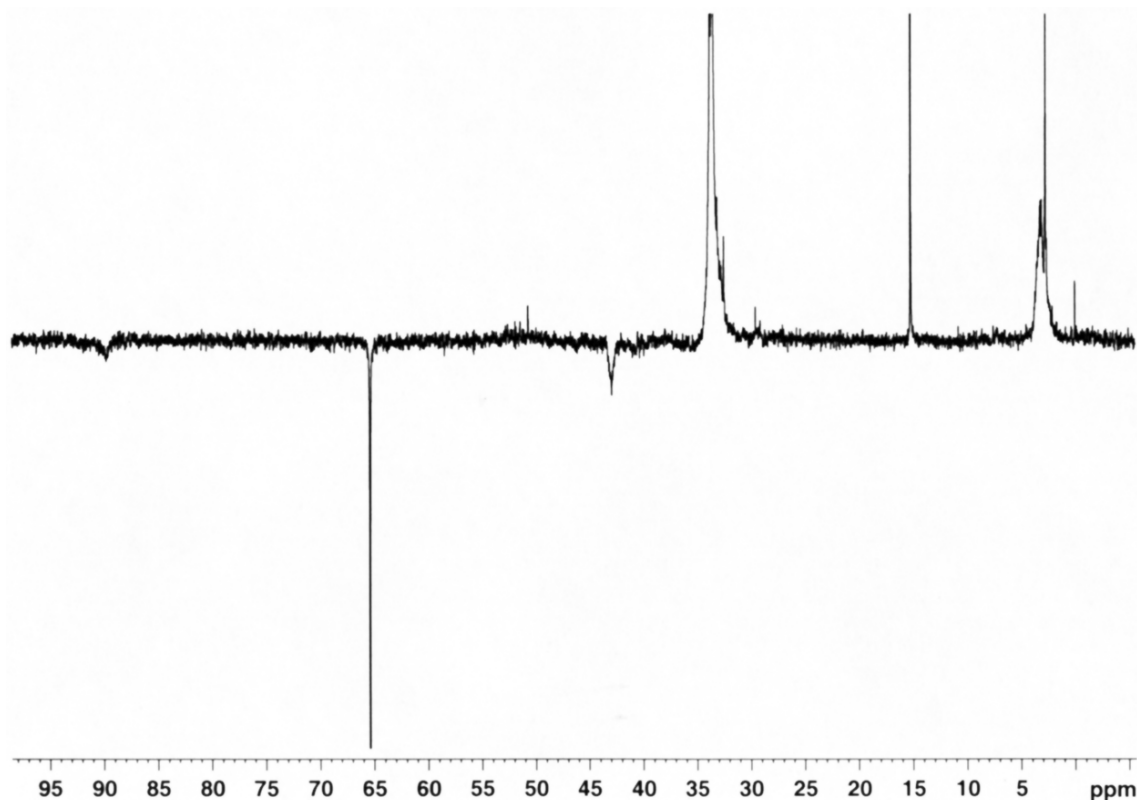
*Figure 16: DEPT spectrum of [(Et₂O)Li₂{H₂CS(NSiMe₃)(N^tBu)}]₂ (**6**).*

A ^{7}Li NMR experiment for [(Et$_2$O)Li$_2${H$_2$CS(NSiMe$_3$)(N^{t}Bu)}]$_2$ (**6**) at room temperature showed just one singlet at δ = 3.00 ppm. According to the structure two signals are expected, but the coalescence temperature seemed to be exceeded. No low temperature experiments have been performed until now.

2.3   Aryldiimidosulfinates

The addition of alkali metal organyls R^{1}M to sulfurdiimides S(NR)$_2$ is a handy method to get alkali metal alkyldiimidosulfinates. The latter are good starting materials for transmetalation reactions, using their high tendency to form alkali metal halides.

Until now, only phenyldiimidosulfinates are known in the area of aromatic systems. Their structural properties under different conditions were examined by *Pauer*.[5] In this thesis the research interest is extended to heteroaromatic systems like furan, methylpyrrole, benzotiophene, thiophene and benzothiazol. One could expect, that besides the nitrogen coordination of the metal, additional

coordination of the ring heteroatom could occur. Models for this coordination mode are the ligand systems prepared by *Strähle*,[59] coordinating a metal ion *via* two or three nitrogen atoms and one sulfur atom.
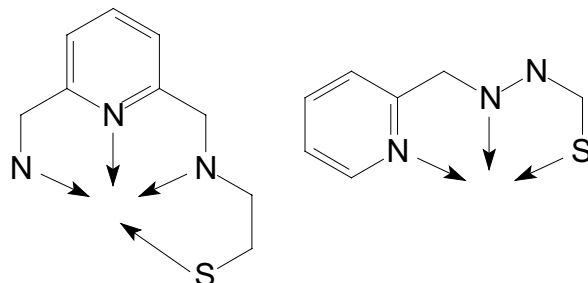
Figure 17: Ligand systems prepared by Strähle.

2.3.1 Aryldiimidosulfinates

2.3.1.1 Preparation of [(thf)Li$_2${(H$_3$CNC$_4$H$_3$)S(N^{t}Bu)$_2$}$_2$] (**8**) and [(tmeda)Li{(SC$_8$H$_5$)S(N^{t}Bu)$_2$}] (**9**)
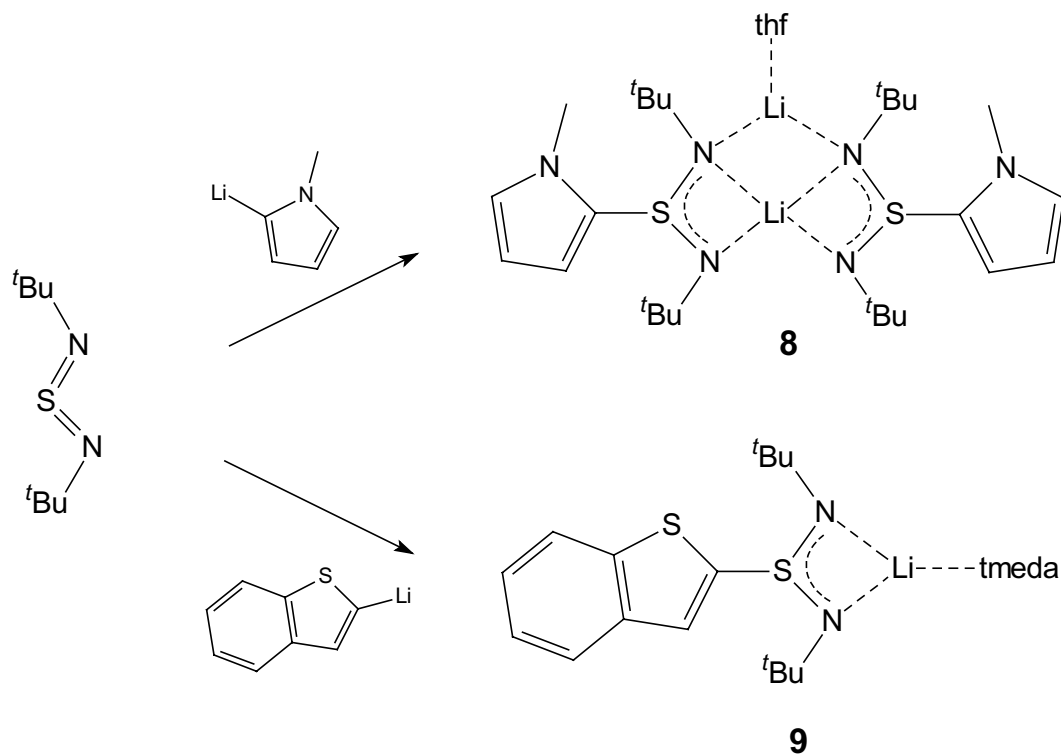
*Scheme 14: Preparation of **8** and **9**.*

The first step of both preparations is the monolithiation of the heteroaromatic system in the 2-position.[60] The exact monolithiation of heteroaromatic systems is not trivial, the conditions have to be selected with care, otherwise dilithiation occurs.[61]

Subsequent addition of an equimolar amount of $S(N^{t}Bu)_2$ led to the compounds $[(thf)Li_2\{(H_3CNC_4H_3)S(N^{t}Bu)_2\}_2]$ (**8**) and $[(tmeda)Li\{(SC_8H_5)S(N^{t}Bu)_2\}]$ (**9**).

2.3.1.2 Crystal structure $[(thf)Li_2\{(H_3CNC_4H_3)S(N^{t}Bu)_2\}_2]$ (**8**)
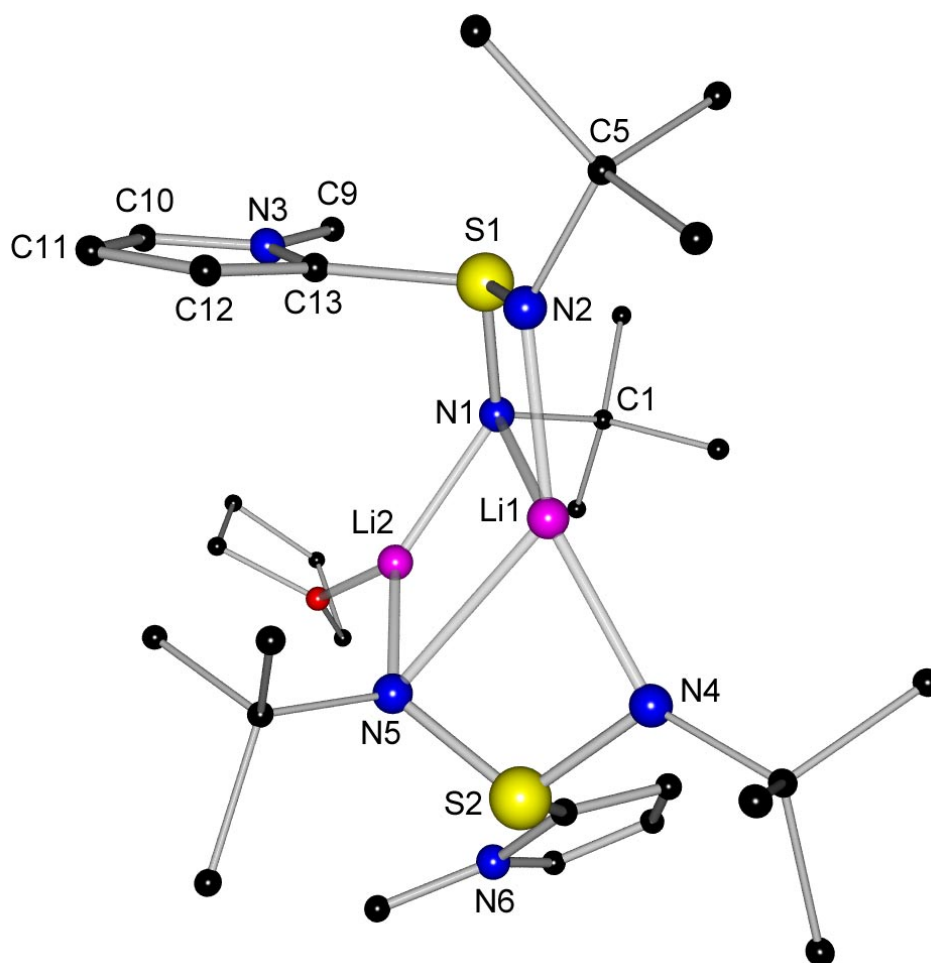
*Figure 18: Structure of $[(thf)Li_2(H_3CNC_4H_3)S(N^{t}Bu)_2)_2]$ (**8**) in the solid state.*

Two independent molecules crystallise in the asymmetric unit of compound $[(thf)Li_2\{(H_3CNC_4H_3)S(N^{t}Bu)_2\}_2]$ (**8**). The bond parameters are not significantly different, therefore only one molecule will be discussed.

Table 8: Selected bond lengths [pm] and angles [°] of 8.

S1 – N1	162.7(3)	N1 – Li1	246.8(6)	N1 – S1 – N2	106.82(14)
S1 – N2	160.4(3)	N1 – Li2	201.2(7)	N4 – S2 – N5	107.09(14)
S1 – C13	177.3(4)	N2 – Li1	196.2(6)	C13 – S1 – N1	98.6(17)
S2 – N4	159.1(3)	N4 – Li1	198.3(6)	C13 – S1 – N2	105.02(17)
S2 – N5	162.0(3)	N5 – Li1	236.7(7)	C26 – S2 – N4	102.57(16)
S2 – C26	178.8(3)	N5 – Li2	200.5(6)	C26 – S2 – N5	100.17(14)
C12 – C13	137.3(5)				

Like all diimidosulfinates synthesised so far, $[(thf)Li_2\{(H_3CNC_4H_3)S(N^tBu)_2\}_2]$ (**8**) is forming a dimeric structure in the solid state. **8** can be assigned to the structural type **C** in figure 6, the twist tricyclic structure.[5c] The heteroatom of the pyrrole ring is not involved in the metal coordination.

All four nitrogen atoms of the two diimidosulfinate molecules are coordinated to the same lithium cation (Li1). The second lithium cation (Li2) is only twofold coordinated by N1 and N5. This extra coordination of N1 and N5 induces an elongation of averaged 2.6 pm of the corresponding S–N-bond lengths. While Li2 is coordinated trigonal planar, Li1 is coordinated in an unusual manner. It is strongly coordinated by N2 and N4 (N–Li av. 198.7 pm) and slightly coordinated by N1 and N5 (N–Li av. 241.8 pm). Thus Li1 is coordinated trigonal pyramidal. N2, N4 and N5 are in the basal position of the pyramid, shared by Li1, and N1 is located in the apical position. The N1–Li1 bond length (246.8(6) pm) is one of the longest found for fourfold coordinated lithium (see diagram 3). The S1–C13 bond length with 177.3(3) pm is in the lower range for typical S–C$_{aromatic}$ single bonds. The pyrrole ring is rotated in the S1–C9 bond in such a manner, that the shorter S–N bond is exactly in plane with the pyrrole ring. A bond elongation of 2 pm of the ring C=C double bond arranged closer to the diimidosulfinate subunit is observed. All these facts are pointing to an interaction of the π-systems in the pyrrole substituent and the SN$_2$-subunit. However, in comparison to electron diffraction data of *N*-methylpyrrole,[62] no significant bond length variations could be detected.

2.3.1.3 Crystal structure of [(tmeda)Li{(SC$_8$H$_5$)S(N^{t}Bu)$_2$}] (**9**)
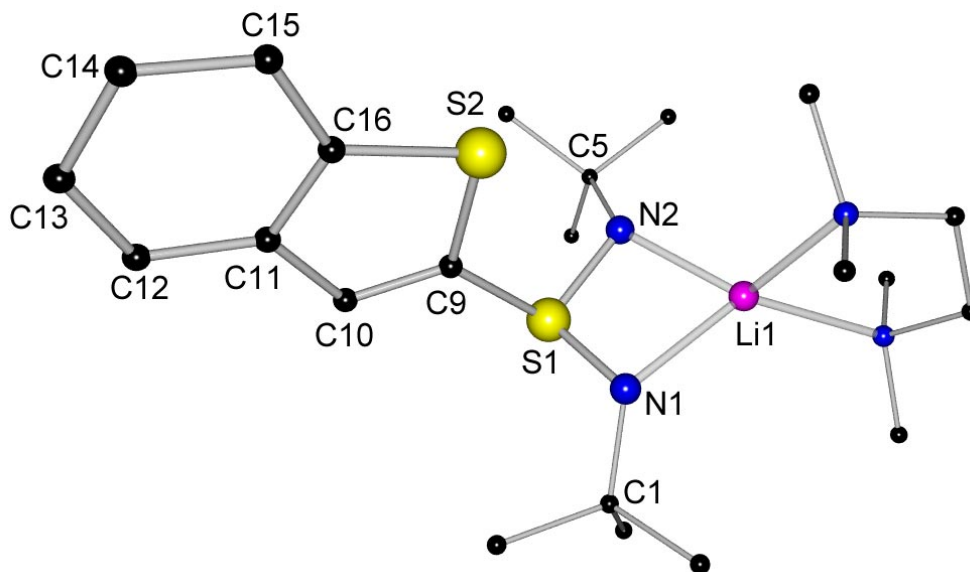
*Figure 19: Solid state structure of [(tmeda)Li{(SC$_8$H$_5$)S(N^{t}Bu)$_2$}] (**9**).*

*Table 9: Selected bond lengths [pm] and angles [°] of **9**.*

S1 – N1	161.9(3)	N1 – Li1	202.2(7)	N1 – S1 – N2	99.63(15)
S1 – N2	161.9(3)	N2 – Li1	201.8(6)	N1 – S1 – C9	103.32(15)
S1 – C9	181.4(3)	N5 – Li1	221.2(7)	N2 – S1 – C9	104.93(15)
C9 – C10	135.3(6)	N6 – Li1	206.8(7)	S1 – C9 – C10	126.0(3)
C9 – S2	174.5(3)			S1 – C9 – S2	120.74(19)

Two independent molecules crystallise in the asymmetric unit of [(tmeda)Li{(SC$_8$H$_5$)S(N^{t}Bu)$_2$}] (**9**). The bond parameters are not significantly different, therefore only one molecule will be discussed.

In contrast to all other diimidosulfinates synthesised so far, compound **9** is forming a monomer in the solid state. The lithium atom is coordinated distorted tetragonal by both nitrogen atoms of the diimidosulfinate unit and one tmeda molecule. The negative charge is delocalised through both S–N bonds with S–N bond lengths (av. 161.9(3) pm) between SN single and double bonds. The S1–C9 bond length with 181.4(3) pm is in the upper range for S–C$_{aromatic}$ single bonds. The benzothiophene substituent is rotated 21.1° about the S–C bond with S2 pointing towards N2. This is not an effect of better conjugation of the

C9=C10 double bond and the SN$_2$-subunit, it is caused by steric interactions of the benzothiophene group with two neighboured tmeda molecules in the crystal lattice.

2.3.2   Comparison   of   [(thf)Li$_2${(H$_3$CNC$_4$H$_3$)S(N^{t}Bu)$_2$}$_2$]   (8)   with [(tmeda)Li{(SC$_8$H$_5$)S(N^{t}Bu)$_2$}] (9)

[(thf)Li$_2${(H$_3$CNC$_4$H$_3$)S(N^{t}Bu)$_2$}$_2$] (**8**) and [(tmeda)Li{(SC$_8$H$_5$)S(N^{t}Bu)$_2$}] (**9**) both are monoanionic systems, with the negative charge delocalised over a chelating N-S-N unit. One difference is obvious, **8** is a dimer and **9** is a monomer in the solid state. This can be explained by the different coordinating solvents. Tmeda, a chelating solvent, allows no further coordination, thus the resulting molecules are monomeres. The S–C$_{aromatic}$ bond in **8** is on average 3.4 pm shorter than in **9**, correlated to the interaction of the π-system in the pyrrole substituent with the SN$_2$ subunit.

In (thf)Li$_2${(H$_3$CNC$_4$H$_3$)S(N^{t}Bu)$_2$}$_2$] (**8**) the SN$_2$ ligand has a wider 'bite' (N$\cdots$N distance av. 259.1 pm) than in [(tmeda)Li{(SC$_8$H$_5$)S(N^{t}Bu)$_2$}] (**9**) (247.75 pm), thus a difference of 11.35 pm. The steric strain caused by the dimeric structure of **9** might be the answer.

2.4   Reactions of Aryldiimidosulfinates

The reactivity of the aryldiimidosulfinates was investigated. Reactions like hydrolyses with ^{t}BuNH$_3$Cl and oxidation failed. Transmetalation reactions with metal halides, like the one which led to [Cu{H$_3$CS(N^{t}Bu)$_2$}]$_2$ (**5**), seemed promising.

The vast catalytic abilities of iron and the stability of the aryldiimidosulfinates were the motivation to synthesise an iron(II)aryldiimidosulfinate complex. A combination of both properties might yield a novel class of oxidation catalysts. Particularly the active sites in metallaproteins like nitrogenases[63] and Rieske-proteins[64] witness the synergistic effect between sulfur and iron. *Walfort* in our group previously reported the reaction of dilithium triimidosulfite with Fe(AcAc)$_2$. But not the expected iron triimidosulfite was the isolated product, [Fe$_2$(μ-N^{t}Bu)$_2${(N^{t}Bu)$_2$S}$_2$] resulted instead.[57]
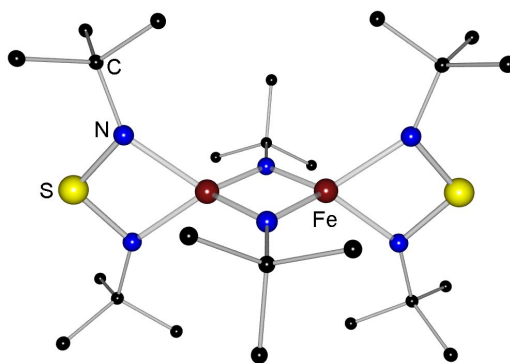
Figure 20: Solid state structure of [Fe$_2$(μ-N^{t}Bu)$_2${(N^{t}Bu)$_2$S}$_2$].

^{t}BuN^{2-} abstraction from the triimidosulfite occurred to give sulfurdiimide. The sulfurdiimide and ^{t}BuN^{2-} combined with Fe^{2+} to the new iron complex.

The reason for using [(tmeda)Li{(SC$_8$H$_5$)S(N^{t}Bu)$_2$}] (**9**) in the transmetalation reactions was the expected participation of the heteroaromatic sulfur atom in metal coordination. Sulfur iron clusters are the active sites in iron nitrogenases.[65]

2.4.1 Preparation of [Fe{(SC$_8$H$_5$)S(N^{t}Bu)$_2$}$_2$] (10) and [Cu{(SC$_8$H$_5$)S(N^{t}Bu)$_2$}]$_2$ (11)
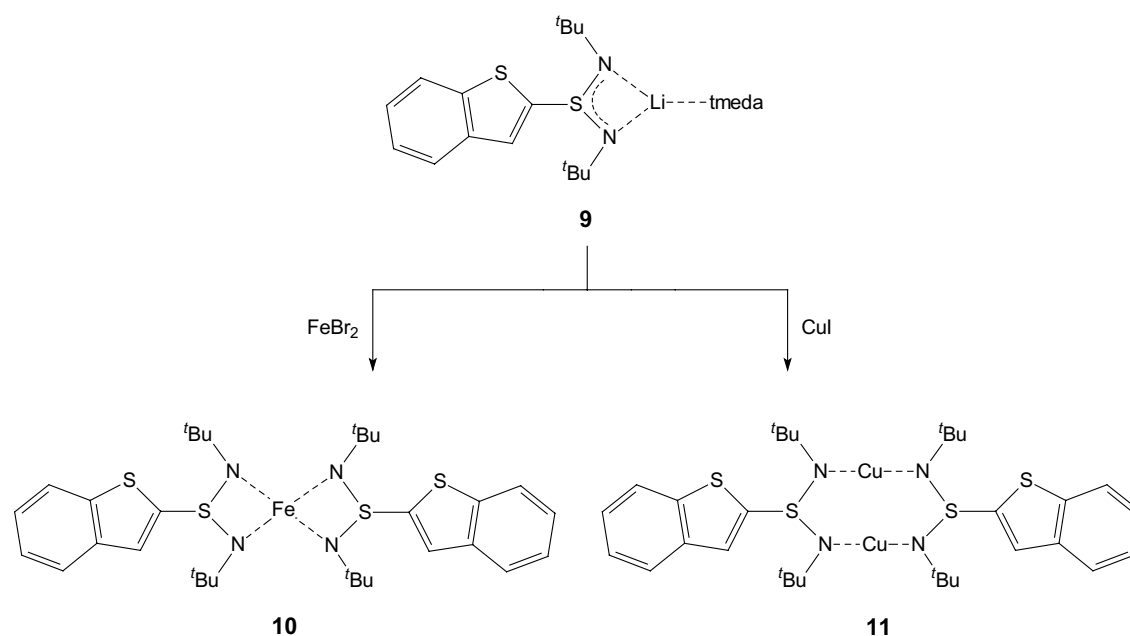
*Scheme 15: Preparation of [Fe{(SC$_8$H$_5$)S(N^{t}Bu)$_2$}$_2$] (**10**) and [Cu{(SC$_8$H$_5$)S(N^{t}Bu)$_2$}]$_2$ (**11**).*

Compound **10** is obtained in the transmetalation reaction of [(tmeda)Li-{$(SC_8H_5)S(N^tBu)_2$}] (**9**) with an equimolar amount of $FeBr_2$ in a hexane/tmeda solution.

The transmetalation reaction of **9** with CuI and CuBr, respectively, in hexane in the presence of tmeda gives **11**.

2.4.2   Crystal structure of [Fe{$(SC_8H_5)S(N^tBu)_2$}$_2$] (10)
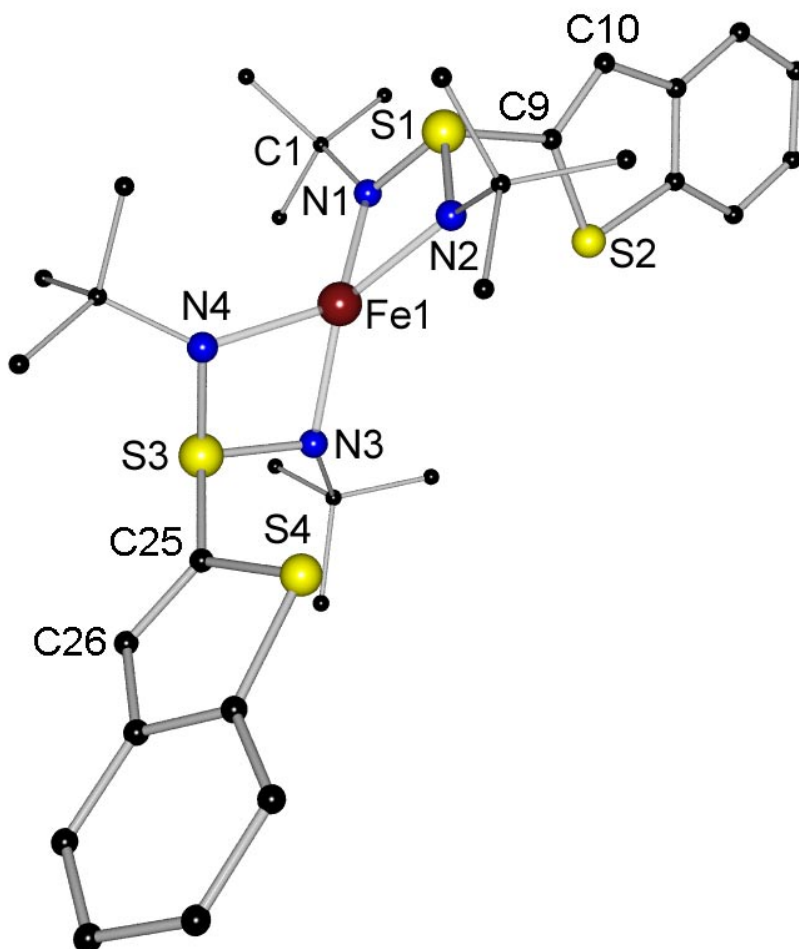
*Figure 21: Solid state structure of [Fe{$(SC_8H_5)S(N^tBu)_2$}$_2$] (**10**).*

Transmetalation of **9** with $FeBr_2$ led to the dimeric iron complex [Fe{$(SC_8H_5)S(N^tBu)_2$}$_2$] (**10**). No further donor solvent is coordinated to the central iron atom. One half noncoordinating tmeda molecule could be detected in the asymmetric unit. The structural motive is deduced from **C1** in figure 6 by splitting the solvent from the metal.

*Table 10: Selected bond lengths [pm] and angles [°] of **10**.*

S1 – N1	163.07(12)	S3 – N3	163.43(12)	N1 – S1 – N2	94.67(6)
S1 – N2	162.75(12)	S3 – N4	163.30(13)	N1 – S1 – C9	105.16(6)
S1 – C9	178.04(14)	S3 – C25	178.16(15)	N2 – S1 – C9	107.09(6)
C9 – C10	135.3(2)	C25 – C26	135.5(2)	N3 – S3 – N4	94.73(6)
C9 – S2	174.45(14)	C25 – S4	174.70(15)	N1 – Fe1 – N2	71.83(5)
Fe1 – N1	205.03(12)	Fe1 – N3	203.57(12)	N1 – Fe1 – N3	127.80(5)
Fe1 – N2	203.40(12)	Fe1 – N4	204.06(12)	N1 – Fe1 – N4	129.53(5)
				N2 – Fe1 – N3	140.43(5)
				N2 – Fe1 – N4	125.45(5)
				N3 – Fe1 – N4	72.27(5)

The ferrous iron is coordinated distorted tetrahedral by both nitrogen atoms of each diimidosulfinate unit, whereas the most tetra coordinated ferrous compounds are planar, e. g. in tetrapyrroles. The distortion can be seen by the four different N–Fe1–N angles (72.27(5)°, 125.45(5)°, 129.53(5)°, 140.43(5)°) and from the fact that the planes of N1-S1-N2 and N3-S2-N4 intersect at an angle of 84.1°. The negative charge is delocalised through both equal S–N bonds, with S–N bond lengths (av. 163.14(13) pm) between the values for a S–N single and double bond. The S–C bond length of averaged 178.10(15) pm is in the typical range for S–C$_{aromatic}$ single bonds. The benzothiophene substituent is rotated only by 3.6° about the S–C bond with respect to the N-S-N bisector. Therefore no electronic interaction of the benzothiophene substituent and the diimidosulfinate unit is given.

The Fe–N bond length in **10** is on average 3.4 pm longer than the Fe–N(sulfurdiimide) bond length in [Fe$_2$(μ-N^{t}Bu)$_2${(N^{t}Bu)$_2$S}$_2$][57] and is in the range of long Fe–N bonds. In the iron carbamate complex [Fe{(^{t}BuC(NC$_6$H$_{11}$)$_2$}$_2$] however, the Fe–N bond length is on average 5.89 pm longer than in **10**.[66]

It seems worth mentioning that non of the two heteroaromatic sulfur atoms is employed in iron coordination. With 419.17(4) and 417.92(4) pm both distances are far too long to be regarded a bond (sum of covalent radius of sulfur and the radius of iron: 220.5 pm).[49]

2.4.3 Crystal structure of [Cu{(SC$_8$H$_5$)S(N^{t}Bu)$_2$}]$_2$ (11)
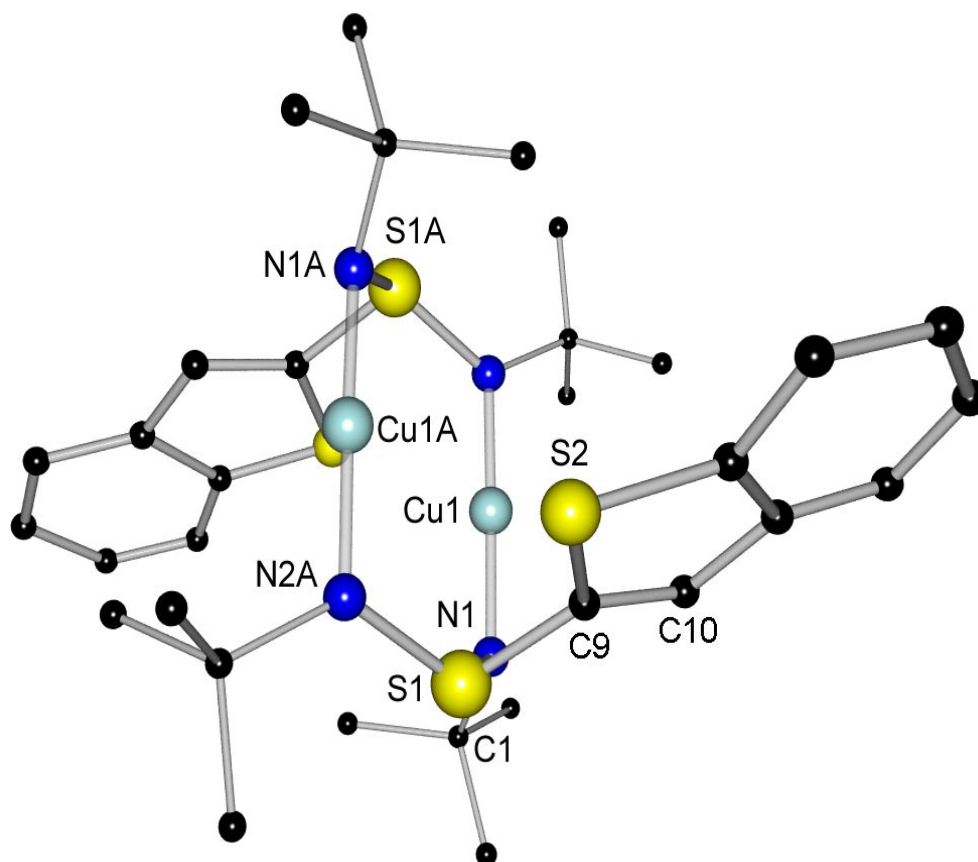
*Figure 22: Structure of [Cu{(SC$_8$H$_5$)S(N^{t}Bu)$_2$}]$_2$ (**11**) in the solid state.*

*Table 11: Selected bond lengths [pm] and angles [°] of **11**.*

S1 – N1	162.3(2)	Cu1 ··· Cu1A	278.52(6)	N1 – S1 – N2A	115.35(11)
S1 – N2A	161.0(2)	Cu1 – N1	188.4(2)	N1 – S1 – C9	95.65(16)
S1 – C9	177(2)	Cu1 – N2	187.9(2)	N2A – S1 – C9	100.6(14)
C9 – S2	179(4)	C9 – C10	131(2)	N1 – Cu1 – N2	178.37(9)

Two independent molecules crystallise in the asymmetric unit of compound **11**. The bond parameters are not significantly different, therefore only one molecule will be discussed. The benzothiophene rings of the second molecule are disordered on four positions.

In the dimeric product the two copper cations are each coordinated by one nitrogen atom of each diimidosulfinate unit in a linear fashion. The copper-copper distance of 278.52(6) pm shows no bonding interaction. The negative

charge is delocalised across both S–N bonds (av. 161.7(2) pm). The N-S-N plane intersects the plane defined by Cu1A-Cu1-N2A-N1 at an angle of 39.6°, almost the same value as in $[Cu\{H_5C_6S(NSiMe_3)_2\}]_2$ with 40.4°.[5] The benzothiophene substituents are arranged in an unusual manner. The N-S-N bisector is arranged almost perpendicular to the heteroarene plane. This rotation of the aryl ring, in contrast to the corresponding lithium species $[(tmeda)Li\{(SC_8H_5)S(N^tBu)_2\}]$ (**9**), was ascertained for $[Cu\{H_5C_6S(NSiMe_3)_2\}]_2$ as well.[5]

A discernible approach of the heteroaromatic ring to the copper-copper line could be detected in $[Cu\{(SC_8H_5)S(N^tBu)_2\}]_2$ (**11**), what can be realised by the equal distances S2···Cu1A and C10···Cu1 with 330.2 pm. In $[Cu\{H_5C_6S(NSiMe_3)_2\}]_2$ comparable C···Cu distances are 344.5 pm and 339.3 pm. In crystal structures bonding interactions are discussed up to a Cu···S distance of 323.7 pm.[67] A reason which further favours an interaction, is the widened NSN angle of 115.35°. Furthermore the wider 'bite' of the NSN ligand in **11** (N···N: 273.2 pm) is remarkable in comparison to the N···N distance of 247.75 pm in $[(tmeda)Li\{(SC_8H_5)S(N^tBu)_2\}]$ (**9**).

2.4.4   Comparison of different copper structures

Table 12: Different parameters of Cu-structures (bond lengths in [pm] and angles in [°]).

	$[Cu\{H_3CS(N^tBu)_2\}]_2$ (**5**)	$[Cu\{H_5C_6S(NSiMe_3)_2\}]_2$-[5d]	$[Cu\{(SC_8H_5)S(N^tBu)_2\}]_2$ (**11**)
S–N$_{av}$	163.06(18)	161.9(3)	161.7(2)
N–S–N	109.79(9)	110.4(1)	115.35(11)
Cu···Cu	269.40(6)	270.2(1)	278.52(6)
Cu–N$_{av}$	187.82(17)	187.4(2)	188.15(2)
N–Cu–N	178.91(8)	178.6(1)	178.37(9)
N1–N2A	266.8	266.0	273.2

In all three structures the negative charge is delocalised over the chelating SN$_2$-backbone, indicated by almost identical S–N distances, located between the values for a S–N single and S=N double bond. The Cu–N bond lengths are in the typical range for Cu–N bonds (diagram 2).

Bonding Cu⋅⋅⋅Cu contacts could not be detected in the investigated systems, the Cu⋅⋅⋅Cu distances are about 30 pm too long to be regarded as bonding interactions. **5** and [Cu{H₅C₆S(NSiMe₃)₂}]₂ are very similar in the listed geometric properties, whereas **11** is differing from the two systems. Most remarkable, the longer Cu⋅⋅⋅Cu distance with 278.52(6) pm, the long N1⋅⋅⋅N2A distance (273.2 pm) and the expansion of the N-S-N angle of about 5° in comparison with **5** and [Cu{H₅C₆S(NSiMe₃)₂}]₂.
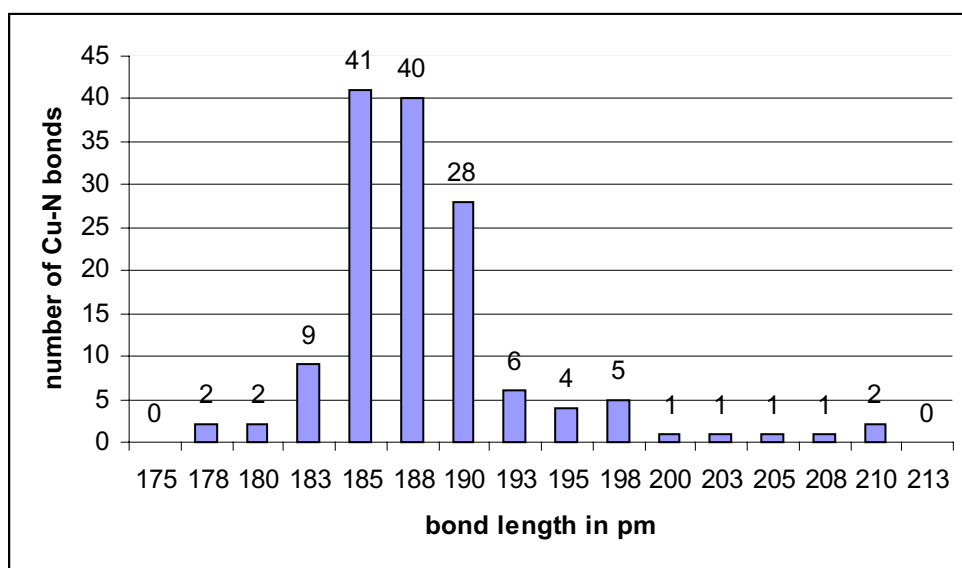
Diagram 2: Cu–N bond lengths from CCDC.

2.5   Aryl-bis-(diimidosulfinate)

2.5.1   Introduction

Recently *Walfort* reported the synthesis of [{(thf)Li₃[(*t*BuN)₂SCHS(N*t*Bu)₂]}₂].[6a] It is the first time, that two sulfurdiimide moieties are connected *via* a carbon bridge. [{(thf)Li₃[(*t*BuN)₂SCHS(N*t*Bu)₂]}₂ is the product of the addition reaction of the alkylenediimidosulfite [(thf)Li₂{H₂CS(N*t*Bu)₂}]₂ and sulfurdiimide. The acidity of the hydrogen atom at the bridging CH₂ group is so high, that it can be deprotonated by present [(thf)Li₂{H₂CS(N*t*Bu)₂}]₂.

In chapter 2.3 monosubstituted aryl systems have been shown. Why shouldn't it be possible to lithiate the aryldiimidosulfinate [(thf)Li₂{(H₃CNC₄H₃)S(N*t*Bu)₂}₂] (**8**)

a second time and react the resulting lithium organyl with a second equivalent of sulfurdiimide? Or is it possible to dilithiate other heteroaromatic systems and react them in a one-pot reaction with two equivalents of sulfurdiimide?
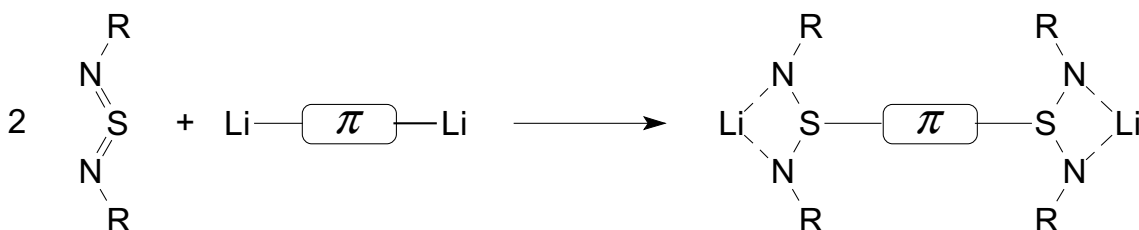
Scheme 16: Reaction pathway to aryl-bis-(diimidosulfinates).

Heteroaromatic systems like furan, thiophene, selenophene, dithiophene and methylpyrrole have been tested in this thesis.

One of the main aims was to see, if the heteroatom of the aromatic ring is included in the coordination sphere, resulting in a monoanionic tripodal or a dianionic pentapodal ligand.
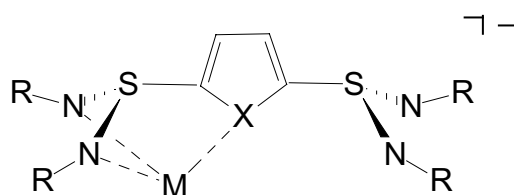
Scheme 17: Possible coordination mode of aryl-bis-(diimidosulfinates) (X = O, S, Se, NCH₃).

Thiophene is commonly known to coordinate either through the entire π system (η^5) or through the sulfur atom ($\eta^1(S)$) only.[68] Thiophene has also been reported to coordinate to metals through a single C=C bond (η^2)[69] or through both C=C bonds (η^4).[70] Similar coordinating properties have been found for selenophene.[71]

The second aim was to examine, if the aromatic system participates in the stabilisation of the negative charge. Hints might be changes in the bond lengths of the heteroarene and the NSN systems.

The third aim was to study the obtained molecules regarding their potential to undergo oxidation to radical species, because this radicals should be able to facilitate single electron transfer over the conjugated system.

Those molecules would be multidentate ligands with new electrochemical and geometrical properties.

2.5.2 Preparation of 12 - 14

Dimetalation of thiophene and selenophene with subsequent addition to two sulfurdiimides led to the novel class of bis-diimidosulfinates. The two diimidosulfinate units are connected *via* a heteroarene (**12** - **14**).

12: R = ^{t}Bu; E = S

13: R = SiMe$_3$; E = S

14: R = ^{t}Bu; E = Se
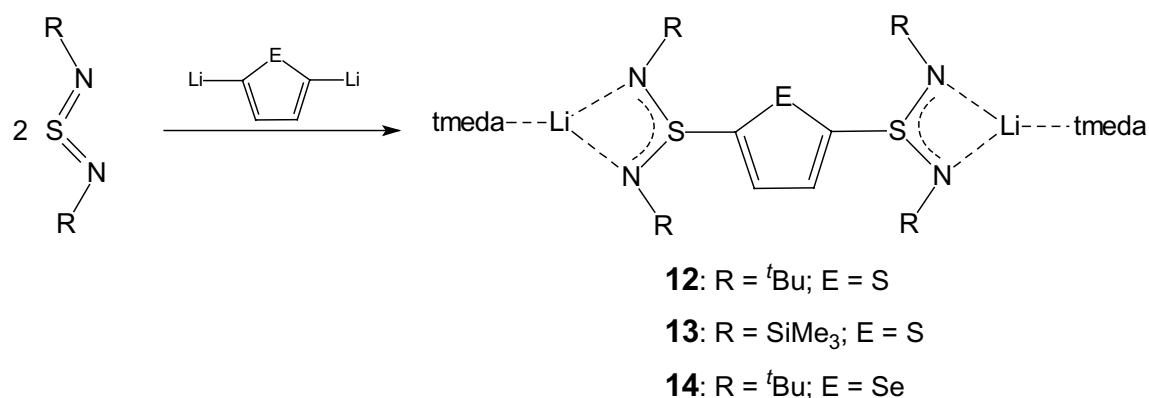
*Scheme 18: Preparation of **12** - **14**.*

Similar experiments have been performed with other dilithiated heteroarenes like 2,5-dilithiofuran[60] and 1,4-dilithiobenzene,[72] but failed in both cases. Problems might be the high reactivity of the furan species and the insolubility of 1,4-dilithiobenzene.

2.5.3 Crystal structure of [(tmeda)$_2$Li$_2${(^{t}BuN)$_2$S(SC$_4$H$_2$)S(N^{t}Bu)$_2$}] (12)

Figure 23 shows compound **12** in the solid state. Each diimidosulfinate unit coordinates one lithium atom with both nitrogen atoms. The tetrahedral coordination of each lithium cation is completed by one tmeda molecule. The two diimidosulfinate units are staggered by 61.8° in the N-S-N bisectors.

Figure 23: Solid state structure of [(tmeda)$_2$Li$_2${(^{t}BuN)$_2$S(SC$_4$H$_2$)S(N^{t}Bu)$_2$}] (12) (coordinating tmeda omitted for clarity).

Table 13: Selected bond lengths [pm] and angles [°] of 12.

S1 – N1	161.63(14)	S1 – C17	179.90(17)	N1 – S1 – C17	103.44(7)
S1 – N2	161.48(14)	S2 – C20	179.29(17)	N2 – S1 – C17	105.83(7)
S2 – N3	162.61(14)	N1 – S1 – N2	99.99(7)	N3 – S2 – C20	96.54(7)
S2 – N4	160.98(14)	N3 – S2 – N4	105.31(7)	N4 – S2 – C20	104.39(8)

The negative charge in each sulfinate unit is completely delocalised over the chelating N-S-N unit (S–N (av.): 161.67 pm), similar to the monosubstituted phenyl derivative PhS(NSiMe$_3$)$_2^-$.[5c] The average S–C$_{aromatic}$ bond length of 179.60(17) pm is in the usual range normally detected for S–C$_{aromatic}$ bonds.

The S2–N3 bond is special. It is in plane with the thiophenyl ring system and is with 162.61(14) pm 1.25 pm longer than all the other S–N bonds in 12. Furthermore it seems interesting to note that the S1-N2-C5 angle of 117.07(11)° is the widest among the S-N-C angles in the molecule. This indicates a gradual transition of a predominately sp^2-hybridised nitrogen atom N2 to the

predominantly sp^3-hybridized N3 *via* the intermediate N1 and N4. The 2,5-S(N^{t}Bu)$_2$ disubstitution seems not to affect the bonding in the SC$_4$-perimeter at all as the bond lengths and angles in the heteroaromatic ring of **12** are almost identical to those in parent thiophene.[73] If the standard S–C$_{aromatic}$ bond lengths are taken into consideration as well, it has to be concluded, that no electronic interaction occurs between the aromatic ring and the sulfinate units.

2.5.4 Crystal structure of [(tmeda)$_2$Li$_2${(Me$_3$SiN)$_2$S(SC$_4$H$_2$)S(NSiMe$_3$)$_2$}] (13)
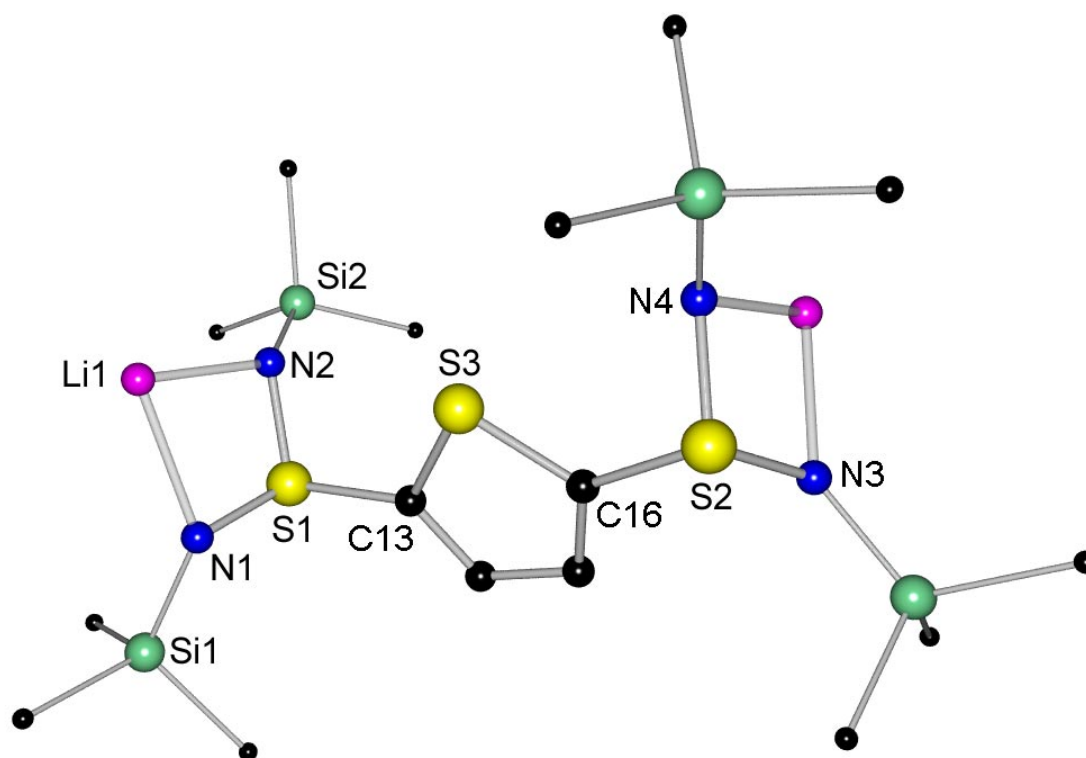
Figure 24: Solid state structure of [(tmeda)$_2$Li$_2${(Me$_3$SiN)$_2$S(SC$_4$H$_2$)S(NSiMe$_3$)$_2$}] (13) (coordinating tmeda omitted for clarity).

Table 14: Selected bond lengths [pm] and angles [°] of 13.

S1 – N1	159.6(4)	C15 – C16	133.6(6)	N1 – S1 – C13	104.02(18)
S1 – N2	160.9(3)	S1 – C13	179.8(4)	N2 – S1 – C13	102.26(18)
S2 – N3	160.0(4)	S2 – C16	180.9(4)	N3 – S2 – C16	101.39(18)
S2 – N4	160.1(3)	N1 – S1 – N2	104.45(18)	N4 – S2 – C16	101.51(17)
C13 – C14	135.2(6)	N3 – S3 – N4	105.33(18)		

A formal exchange in [(tmeda)$_2$Li$_2${(^{t}BuN)$_2$S(SC$_4$H$_2$)S(N^{t}Bu)$_2$}] (**12**) of the *tert*.-butyl groups against SiMe$_3$ groups led to [(tmeda)$_2$Li$_2${(Me$_3$SiN)$_2$S(SC$_4$H$_2$)-S(NSiMe$_3$)$_2$}] (**13**). This replacement has only little effects on the structural features. The S–N bond lengths (av. 160.2(4) pm) are slightly shorter and the N–Li bond lengths (av. 205.7(8) pm) are marginally longer than in the *tert*.-butyl substituted compounds (S–N: **12** av. 161.67(14), **14** av. 161.89(18), **15** av. 161.92(18) pm; N–Li: **12** av. 204.3(3), **14** av. 204.9(4), **15** av. 203.8(4) pm). The S–C$_{aromatic}$ bonds are with 179.8(4) pm and 180.9(4) pm in the standard range for S–C$_{aromatic}$ single bonds. The bisectors of the SN$_2$ moieties are rotated against each other by 67.6°. In **13**, different to **12**, no S–N bond is in the plane defined by the thiophenyl bridge.

Compared to thiophene (electron diffraction data), with a C=C bond length of 137.0 pm,[73] slight bond shortening of the C=C double bonds in the aromatic ring of **13** could be detected (about 1.5 and 3.3 pm) (see scheme 20).

But even for **13** no conjugation of the aromatic ring with the sulfinate substituents is ascertainable.

2.5.5 Crystal structure of [(tmeda)$_2$Li$_2${(^{t}BuN)$_2$S(SeC$_4$H$_2$)S(N^{t}Bu)$_2$}] (14)
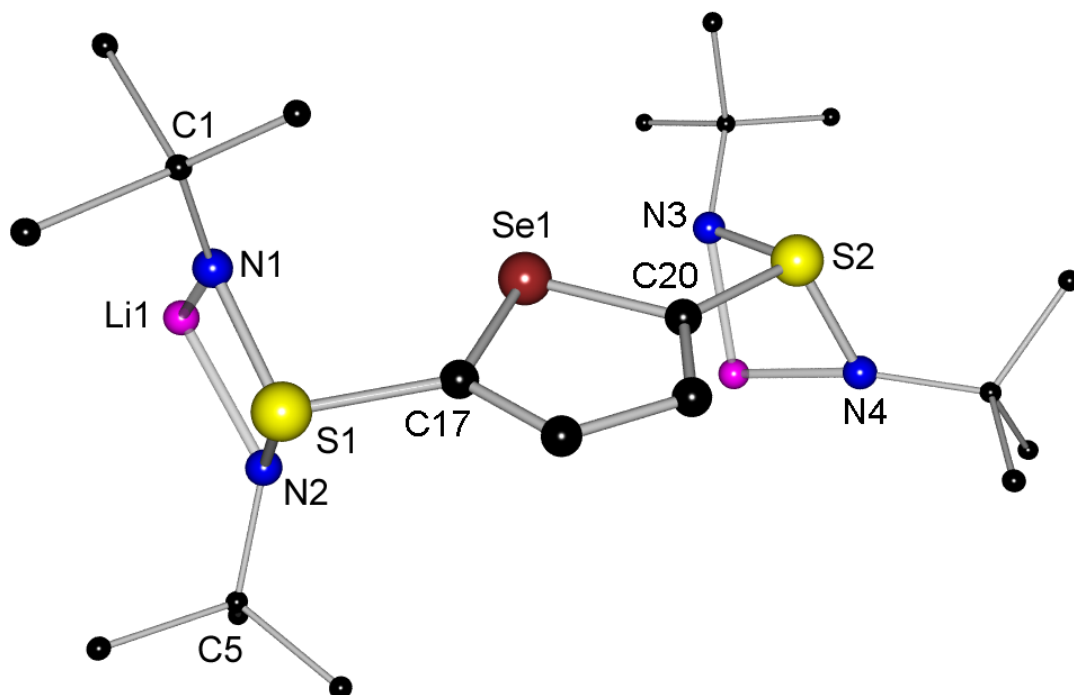
*Figure 25: Solid state structure of [(tmeda)$_2$Li$_2${(^{t}BuN)$_2$S(SeC$_4$H$_2$)S(N^{t}Bu)$_2$}] (**14**) (coordinating tmeda omitted for clarity).*

*Table 15: Selected bond lengths [pm] and angles [°] of **14**.*

S1 – N1	161.50(18)	S1 – C17	179.3(2)	N1 – S1 – C17	105.50(10)
S1 – N2	161.76(18)	S2 – C20	178.9(2)	N2 – S1 – C17	103.52(10)
S2 – N3	162.98(17)	N1 – S1 – N2	99.84(9)	N3 – S2 – C20	96.14(9)
S2 – N4	161.34(18)	N3 – S3 – N4	105.34(9)	N4 – S2 – C20	104.70(10)

Figure 25 shows $[(\text{tmeda})_2\text{Li}_2\{(^t\text{BuN})_2\text{S}(\text{SeC}_4\text{H}_2)_2\text{S}(\text{N}^t\text{Bu})_2\}]$ (**14**) in the solid state. Compound **14** is isostructural to $[(\text{tmeda})_2\text{Li}_2\{(^t\text{BuN})_2\text{S}(\text{SC}_4\text{H}_2)\text{S}(\text{N}^t\text{Bu})_2\}]$ (**12**). The formal replacement of the thiophenyl by a selenophenyl substituent has no significant effects on the structural properties. Both diimidosulfinate units of **14** coordinate with their two nitrogen atoms one lithium atom each. The tetrahedral coordination of each lithium cation is completed by one tmeda molecule each. The two diimidosulfinate units are rotated 59.3° about the S1-S2 axis with respect to each other. The presence of two different Se–N bond lengths in the selenophenyl ring is striking (Se1–C17: 188.7(2)pm; Se1–C20: 186.0(2) pm), whereas the CC bond lengths in the ring (C17–C18: 135.7(8); C18–C19: 142.4(3); C19–C20: 135.4(3) pm) match those for five membered heteroarenes (see scheme 20).

2.5.6 Preparation of $[(\text{tmeda})_2\text{Li}_2\{(^t\text{BuN})_2\text{S}(\text{SC}_4\text{H}_2)_2\text{S}(\text{N}^t\text{Bu})_2\}]$ (15)

The conjugated system can be extended by dimetalation of one equivalent of dithiophene and subsequent addition of two equivalents of sulfurdiimide, resulting in dithiophene-2,2'-bis-diimidosulfinate $[(\text{tmeda})_2\text{Li}_2\{(^t\text{BuN})_2\text{S}-(\text{SC}_4\text{H}_2)_2\text{S}(\text{N}^t\text{Bu})_2\}]$ (**15**).
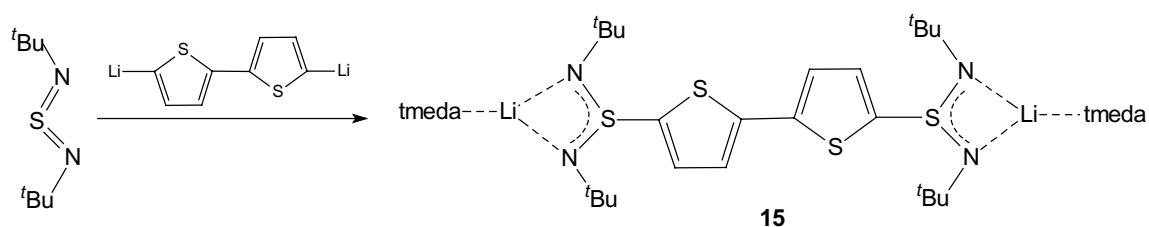
*Scheme 19: Preparation of $[(\text{tmeda})_2\text{Li}_2\{(^t\text{BuN})_2\text{S}(\text{SC}_4\text{H}_2)_2\text{S}(\text{N}^t\text{Bu})_2\}]$ (**15**).*

2.5.7   Crystal structure of [(tmeda)$_2$Li$_2${(^{t}BuN)$_2$S(SC$_4$H$_2$)$_2$S(N^{t}Bu)$_2$}] (15)
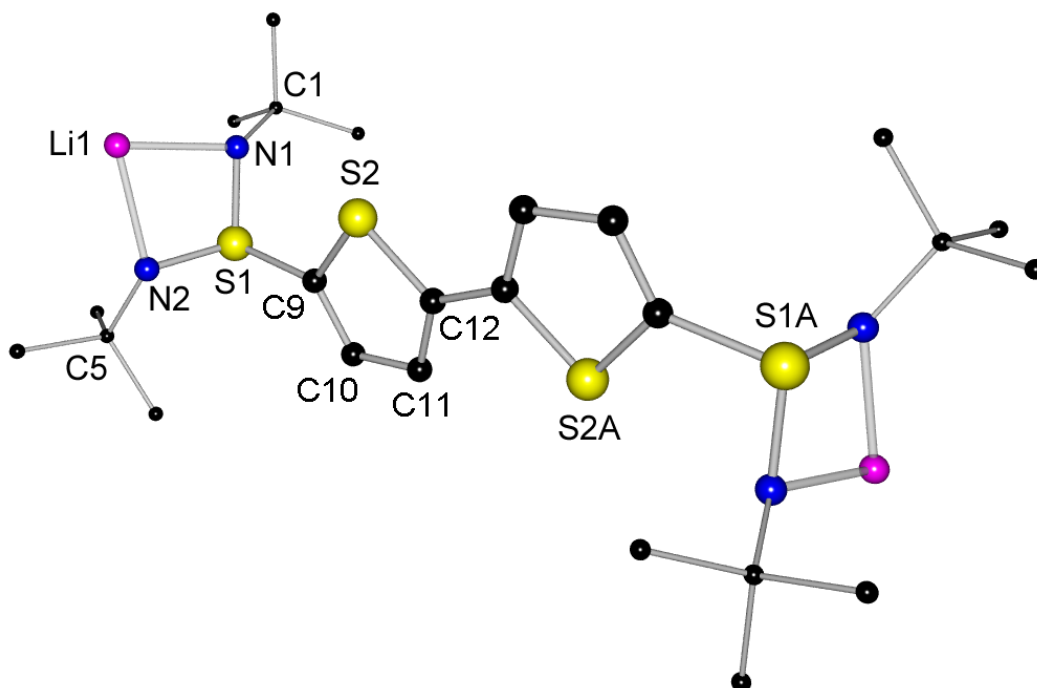
Figure 26: Solid state structure of [(tmeda)$_2$Li$_2${(^{t}BuN)$_2$S(SC$_4$H$_2$)$_2$S(N^{t}Bu)$_2$}] (15) (coordinating tmeda omitted for clarity).

Table 16: Selected bond lengths [pm] and angles [°] of 15.

S1 – N1	162.19(17)	S2 – C9	172.85(19)	N1 – S1 – N2	102.02(9)
S1 – N2	161.66(18)	S2 – C12	174.05(19)	N1 – S1 – C9	102.06(9)
S1 – C9	179.82(19)	C9 – C10	136.0(3)	N2 – S1 – C9	105.35(9)
Li1 – N1	203.4(4)	C10 – C11	142.0(3)		
Li1 – N2	204.2(2)	C11 – C12	137.8(3)		
		C12 - C12A	145.3(4)		

Figure 26 shows the obtained structure of compound **15**. The two diimidosulfinate units are connected by the dithiophenyl bridge with an inversion centre between C12–C12A. This causes the thiophenyl groups to be arranged in the E-configuration. The average S–N bond length of 161.93(18) pm, the S–C$_{aromatic}$ bond length of 179.82(19) pm and the still present alternation of single and double bonds in the thiophenyl moiety indicate, that the negative charge is located in the diimidosulfinate moieties. On the other hand, the intensive orange colour of the substance points to a conjugation. C1 and C5 are located 73.65

pm out of the SN_2 plane, evidently presenting a tetrahedral conformation with sp^3-hybridisation for the donating nitrogen atoms.

In $[(tmeda)_2Li_2\{(^tBuN)_2S(SC_4H_2)_2S(N^tBu)_2\}]$ (**15**) the aromatic S–C bonds are about 3 pm shorter than in parent dithiophene, whereas the formal double bond C11–C12 in **15** is lengthened by about 6 pm.[74]

2.5.8   Comparison of compounds 12 - 15

$[(tmeda)_2Li_2\{(^tBuN)_2S(SC_4H_2)S(N^tBu)_2\}]$
(**12**)

$[(tmeda)_2Li_2\{(Me_3SiN)_2S(SC_4H_2)S(NSiMe_3)_2\}]$
(**13**)
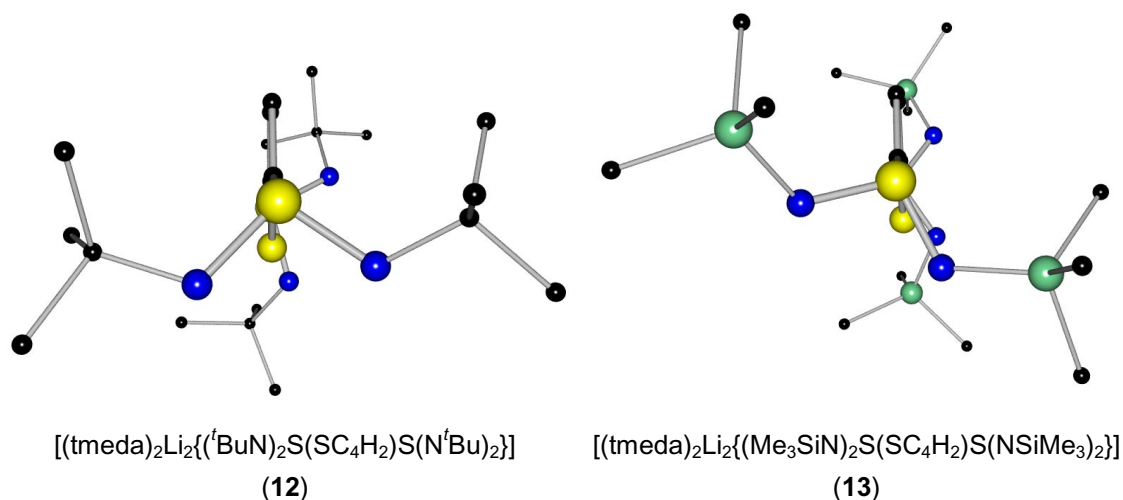
Figure 27: Comparison of 12 with 13 (12 as representative of 14). View along the S1···S2 axis.

First of all, the different arrangement of the S–N bonds with respect to the heteroaryl ring is evident. In $[(tmeda)_2Li_2\{(^tBuN)_2S(SC_4H_2)S(N^tBu)_2\}]$ (**12**) and $[(tmeda)_2Li_2\{(^tBuN)_2S(SeC_4H_2)S(N^tBu)_2\}]$ (**14**) as well one S–N bond is located in the plane of the aromatic system and moreover all S–N bonds are arranged in one hemisphere (figure 27, left). In $[(tmeda)_2Li_2\{(Me_3SiN)_2S(SC_4H_2)$-$S(NSiMe_3)_2\}]$ (**13**) no S–N bond is positioned in the plane of the aromatic ring, whereas two of the S–N bonds are orientated eclipsed to each other (figure 27, right). Unlike in **12** and **14**, the S–N bonds of **13** are arranged in a spherical way, with angles between the S–N bonds of about 120°.
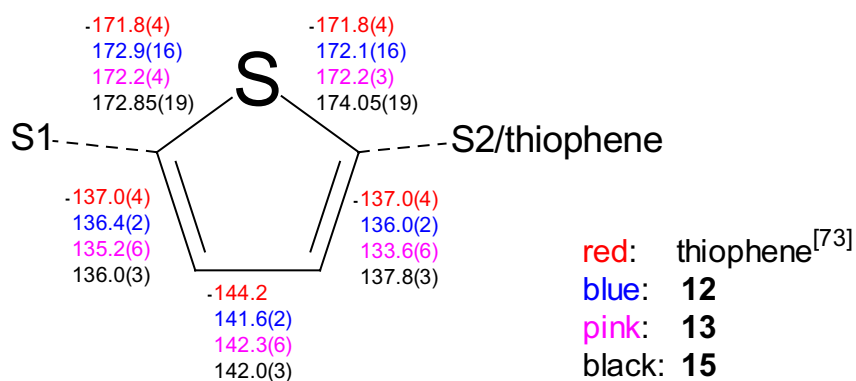
Scheme 20: Bond lengths in pm of substituted thiophenes.

As can be seen in scheme 20, the influence of the sulfinate substituents at thiophene on the geometrical properties of the heteroarene is marginal. In general the two so called C=C double bonds and the C–C bonds are shortened, whereas the heteroatom–C bonds are slightly lengthened. The same results are valid for **14**, the selenophene system.
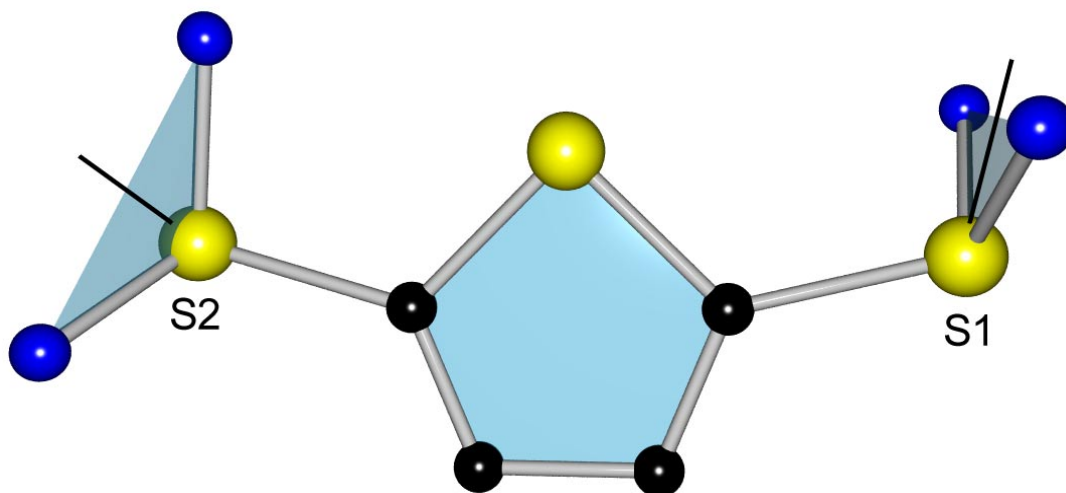
Figure 28: Planes and bisectors of compound [(tmeda)$_2$Li$_2${(^{t}BuN)$_2$S(SC$_4$H$_2$)S(N^{t}Bu)$_2$}] (**12**).

In [(tmeda)$_2$Li$_2${(^{t}BuN)$_2$S(SC$_4$H$_2$)S(N^{t}Bu)$_2$}] (**12**), [(tmeda)$_2$Li$_2${(Me$_3$SiN)$_2$S-(SC$_4$H$_2$)S(NSiMe$_3$)$_2$}] (**13**) and [(tmeda)$_2$Li$_2${(^{t}BuN)$_2$S(SeC$_4$H$_2$)S(N^{t}Bu)$_2$}] (**14**) the two SN$_2$ groups are arranged different with respect to the heteroaryl bridge. The S1N$_2$-unit, with its bisector almost in plane with the aromatic ring system, is positioned almost perpendicular to the heteroaromatic ring (**12**: 90.5°; **13**: 102.5°; **14**: 90.0°). The angle between the heteroarene plane and the S2N$_2$-

plane is in contrast always widened (**12**: 107.4°; **13**: 111.9°; **14**: 107.9°). In [(tmeda)$_2$Li$_2${(^{t}BuN)$_2$S(SC$_4$H$_2$)$_2$S(N^{t}Bu)$_2$}] (**15**) no SN$_2$ bisector is in plane with the thiophenyl plane and consequently the angle between the dithiophenyl plane and the SN$_2$ moiety is widened to 105.1°.

Table 17: Selected bond lengths [pm], angles [°] and other parameters of 12 - 15.

	12	13	14	15
S1 – N1	161.63(14)	159.6(4)	161.50(18)	162.19(17)
S1 – N2	161.48(14)	160.9(3)	161.76(18)	161.66(18)
S2 – N3	162.61(14)	160.0(4)	162.98(17)	-
S2 – N4	160.98(14)	160.1(3)	161.34(18)	-
N1 – Li1	202.7(3)	208.4(7)	200.0(4)	203.4(4)
N2 – Li1	200.3(3)	202.9(8)	203.2(4)	204.2(4)
N3 – Li2	204.6(3)	205.0(8)	206.9(4)	-
N4 – Li2	209.5(3)	206.6(8)	209.5(4)	-
S1 – C	179.90(17)	179.8(4)	179.3(2)	179.82(19)
S2 – C	179.29(17)	180.9(4)	178.9(2)	-
C = C(ar.)	136.2(2)	134.2(6)	135.6(3)	136.9(3)
C – C(ar.)	141.6(2)	142.3(6)	142.4(3)	142.0(3)
C1 – (SN$_2$)$_{plane}$	81.97	92.93 (Si1)	24.39	72.91
C5 – (SN$_2$)$_{plane}$	13.09	80.02 (Si2)	79.15	74.27
C9 – (SN$_2$)$_{plane}$	115.25	80.80 (Si3)	115.02	-
C13 – (SN$_2$)$_{plane}$	80.01	114.40 (Si4)	73.27	-
N1 – S1 – N2	99.99(7)	104.45(18)	99.84(9)	102.02(9)
N3 – S – N	105.31(7)	105.33(18)	105.34(9)	-
S/Se$_{aromatic}$–C	172.79(16)	172.2(4)	188.7(2)	172.85(19)
S/Se$_{aromatic}$–C	172.10(16)	172.2(3)	186.0(2)	174.05(19)
Ar$_{plane}$–(S1N$_2$)$_{bisec}$	5.0	27.1	8.3	35.3
Ar$_{plane}$–(S2N$_2$)$_{bisec}$	66.7	97.4	67.7	-
Ar$_{plane}$–(S1N$_2$)$_{plane}$	90.5	102.5	90.0	105.1
Ar$_{plane}$–(S2N$_2$)$_{plane}$	107.4	111.9	107.9	-

2.6 [(thf)Li$_2${(SC$_4$H$_2$)S(N^{t}Bu)$_2$}]$_2$ (16)

2.6.1 Preparation of [(thf)Li$_2${(SC$_4$H$_2$)S(N^{t}Bu)$_2$}]$_2$ (16)

The intention was to prepare a thiophenylsulfinate, carrying the sulfinate unit in the 3-position rather than in the 2-position of the heteroaromatic ring (chapter 2.3). The synthesis starts from one equivalent of nBuLi, 3-bromothiophene and sulfurdiimide each.[75] But the crystal structure of the crystallised product showed not the expected result. The thiophene substituent was added in the 3-position to the sulfurdiimide as anticipated, but in addition the thiophenyl substituent had been deprotonated in the 2-position. Two possible reaction mechanisms are plausible. In the first the thiophene was dimetalated in the 2- and 3-position and subsequently added in the 3-position to the S–N double bond in sulfurdiimide. The second reaction pathway involves selective single metalation in the 3-position, addition of the thiophenyl substituent to the sulfurdiimide and subsequent metalation.
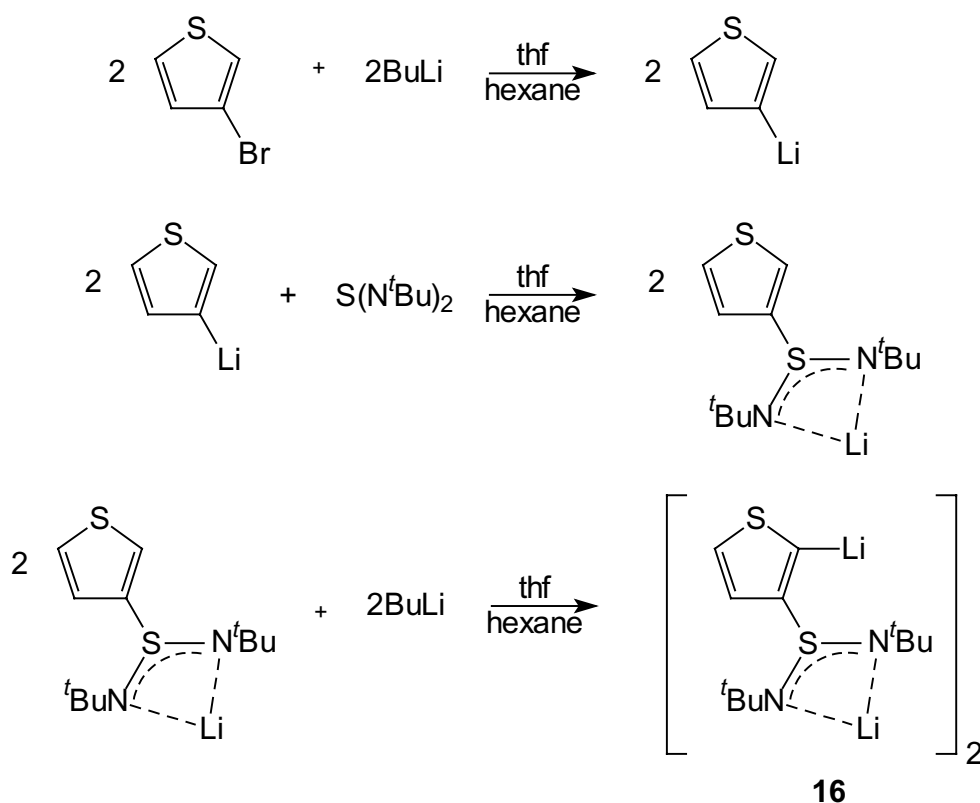
Scheme 21: Possible reaction pathway to [(thf)Li$_2${(SC$_4$H$_2$)S(N^{t}Bu)$_2$}]$_2$ (16).

However, the first mechanism can be excluded as the addition reaction would have taken place in the 2-position due to the higher charge concentration at that position. The related product was not observed. Therefore the second pathway seems much more favourable, because the CH acidity of the 2-position is increased by the added sulfur substituent, facilitating the second metalation.

2.6.2   Crystal structure of [(thf)Li$_2${(SC$_4$H$_2$)S(N^{t}Bu)$_2$}]$_2$ (16)
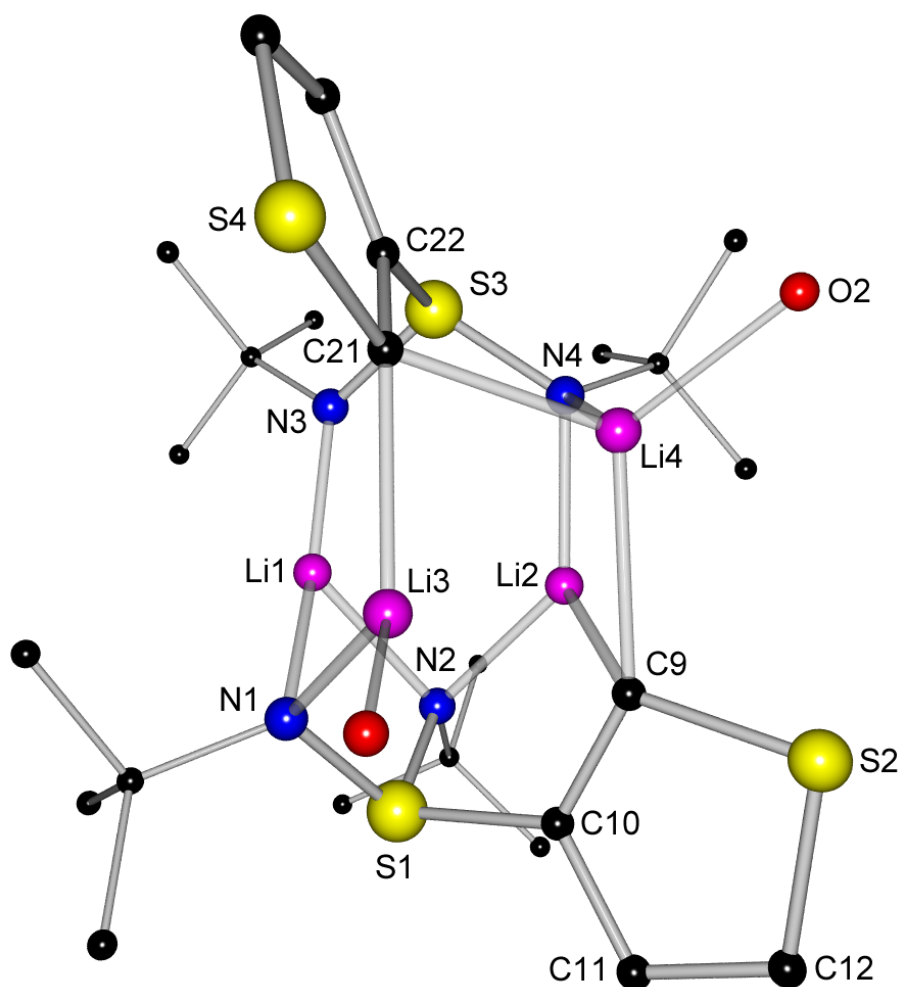
Figure 29: Solid state structure of [(thf)Li$_2${(SC$_4$H$_2$)S(N^{t}Bu)$_2$}]$_2$ (16) (thf carbon atoms omitted for clarity).

Compound **16** shows in analogy to the known triimidosulfites,[4j,51] triimidoselenites,[32]   triimidotellurites,[76]   alkylenediimidosulfites[6]   and alkylenetriimidosulfates[7] a dimeric structure. Both tripodal ligands face each other with their concave sites in a staggered conformation. The complete

structure can be deduced from the thf adduct of the triimidosulfite [Li$_4${(N^{t}Bu)$_3$S}$_2$][4j] by addition of another thf to Li3 inducing bond cleavage of Li3–C9 and bond formation of C9–Li4 (figure 29).
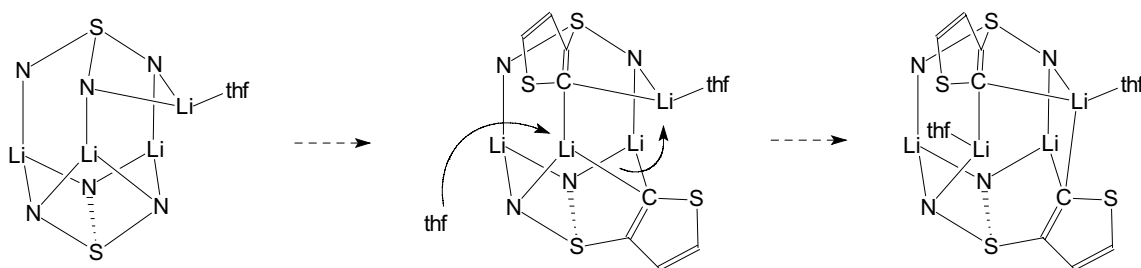
*Scheme 22: Structural deduction of compound **16** from the thf adduct of triimidosulfite (^{t}butyl groups are omitted for clarity).*

The replacement of one N^{t}Bu group with the thiophenyl group widens the bite of the tripodal dianion considerably. The sum of distances from the centre of the triangle N1, N2, C9 to the related nitrogen and carbon atoms in **16** (512.0 pm) is 60-70 pm longer in comparison to the methylenediimidosulfite [(thf)Li$_2${H$_2$CS(N^{t}Bu)$_2$}]$_2$ (454.4 pm) and triimidosulfite [Li$_4${(N^{t}Bu)$_3$S}$_2$] (441.7 pm), respectively.

*Table 18: Selected bond lengths [pm] and angles [°] of **16**.*

S1 – N1	163.68(18)	C9 – Li2	222.8(5)	N1 – S1 – N2	102.34(9)
S1 – N2	164.40(19)	C9 ⋯ Li3	240.3(5)	N3 – S3 – N4	106.59(9)
S1 – C10	179.4(2)	C9 – Li4	232.4(4)	N1 – S1 – C10	101.49(10)
N1 – Li1	207.0(4)	C21 – Li3	219.0(4)	N2 – S1 – C10	103.05(10)
N1 – Li3	201.9(4)	C21 – Li4	219.0(5)	N3 – S3 – C22	105.98(10)
N2 – Li1	205.5(5)	S2 – C9	173.0(2)	N4 – S3 – C22	101.15(10)
N2 – Li2	199.6(4)	S2 – C12	171.7(2)		
N3 – Li1	190.5(4)	C9 – C10	138.8(3)		
N4 – Li2	198.3(4)	C10 – C11	142.1(3)		
N4 – Li4	204.5(4)	C11 – C12	136.0(3)		

The average value for the S–N bond lengths of 163.88(19) pm is between typical values for S–N single- and double-bonds. The S–C$_{aromatic}$ bonds (av. 179.6(2) pm) match the standard values for S–C$_{aromatic}$ single bonds.

The C9–C10 and C21–C22 (av. 138.6(3) pm) bond lengths are 3 pm longer than the other C=C double bonds of the thiophenyl ring (C11–C12/C23–C24) with averaged 135.6(3) pm. These results point to an electronic interaction between the heteroaryl- and the sulfinate-unit.

One negative charge is delocalised over the SN$_2$ backbone and one is mainly localised at the β-atom. Therefore compound **16** can be seen, like methylenediimidosulfite [Li$_2${H$_2$CS(NR)$_2$}]$_2$, as a dianionic sulfur ylide,[77] strictly speaking a sulfur(IV)-β-ylide. The reactivity of **16** should be similar to the reactivity of the methylenediimidosulfites, thus addition reactions at the metalated carbon atom should be feasible to expand the conjugated system.

Looking at the Li bonding modes, it is evident, that they all have different coordination modes. The coordination number of Li1, Li2 and Li3 is three, whereas the coordination number of Li4 is four. Li1 is only coordinated by three nitrogen atoms, Li2 by two nitrogen atoms and one carbon atom and Li3 by one nitrogen, one carbon and one oxygen atom. The Li3···C9 distance is with 240.3(5) pm too long to be regarded as a bonding interaction. Li4 is the only fourfold coordinated Li atom, with one nitrogen, two carbon and one oxygen atom in the coordination sphere.

The Li1–N3 bond with 190.5(4) pm is the shortest among the Li–N bonds of compound **16**, and as well among the shortest ever found in crystal structures (diagram 3). The explanation is simple: N3 coordinates only one Li atom, not like all the others two Li atoms, resulting in a significantly shorter Li–N bond length.
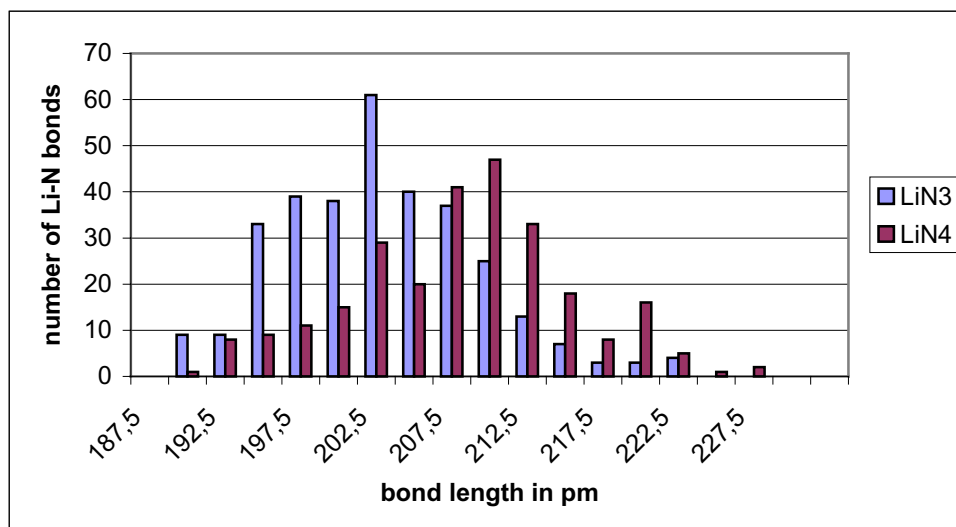
Diagram 3: Frequency of various Li–N-bond distances in the CCDC.

2.6.3   NMR-Data of [(thf)Li$_2${(SC$_4$H$_2$)S(N^{t}Bu)$_2$}]$_2$ (16)

As elucidated in chapter 2.6.2, each lithium cation in compound **16** has a different environment. Therefore in non-donating solvents a Li-NMR spectrum should ideally resolve the four specific sites for the magnetically different lithium cations. A variable temperature ^{7}Li-NMR-spectrum of **16** has been recorded and gave the results shown in figure 30.
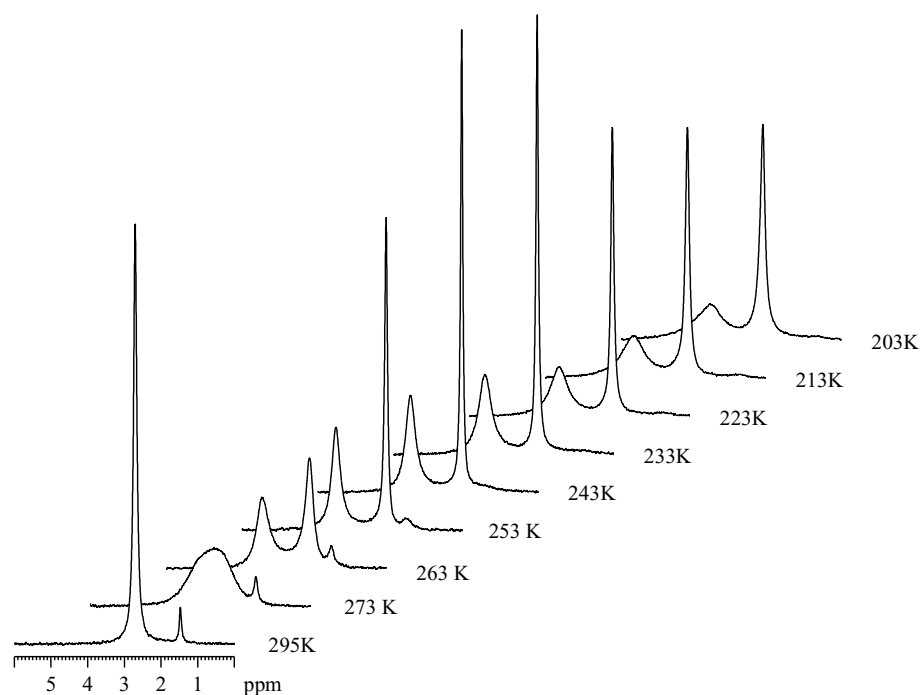
*Figure 30: ^{7}Li-NMR spectrum of **16** at different temperatures (in C$_7$D$_8$).*

*Table 19: Chemical shift of **16** at different temperatures.*

T	Li–thf (Li1/Li2)	Li–trigonal(Li3/Li4)	Integration
RT	2.70		4
273K	2.62		4
263K	2.07	3.38	2/2
253K	2.07	3.42	2/2
243K	2.07	3.48	2/2
233K	2.08	3.52	2/2
223K	2.10	3.59	2/2
213K	2.13	3.63	2/2
203K	2.14	3.57	2/2

At room temperature only one peak for the different lithium environments could be obtained. The small peak at 1.45 ppm vanishes upon cooling. The coalescence point is reached at 273 K and at 263 K two signals could be observed. A broad one at 3.38 ppm, which could be assigned to the trigonal coordinated lithium atoms Li1 and Li2. The second one at 2.07 ppm is sharp and could be assigned to the tetrahedral coordinated Li3 and Li4, where an additional thf is coordinated to lithium (for Li3···C9 a bonding interaction is assumed). It is not possible to distinguish all four different lithium environments, because the standard ^{7}Li-NMR techniques are not sensitive enough.

3   S(VI)-Compounds

3.1   Introduction

Until recently the direct reaction of thiols with chloroamines or better bromoamines was the only known synthetic access to S-alkyltriimido-sulfonates.[78] *Fleischer* developed a new straightforward synthetic route which involves the nucleophilic addition of lithium alkyls to the formal S=N double bond of sulfurtriimides.[23] Due to the steric crowding in the products of the few known sulfurtriimides (S(NR)$_3$, R = ^{t}Bu, SiMe$_3$), till now only sterically less demanding alkyls could be added (e. g. MeLi). Addition reactions with *n*BuLi and *t*BuLi failed. In principle, the resulting [MeS(NR)$_3$]$^-$ anion possesses C$_{3v}$ symmetry, prompting feasible tripodal cap shaped metal coordination. While the triimidosulfite S(NR)$_3{}^{2-}$ and triimidosulfate OS(NR)$_3{}^{2-}$ dianions show this anticipated tripodal behaviour even in mixed metal complexes,[51] only dipodal SN$_2$ chelation has been observed for the [MeS(NR)$_3$]$^-$ anion[23] and in [(thf)$_2$Li{(N^{t}Bu)$_3$SCCPh}].[26]

It seemed a rewarding aim to extend possible addition reactions to the sulfurtriimide by lithiated heteroarenes and to answer the following questions:

- Is the synthesis possible and are the sterical arguments used so far reliable?

- Is there any change in the coordination mode in comparison to [(thf)$_2$Li{(N^{t}Bu)$_3$SCCPh}][26] and [MeS(NR)$_3$]$^-$?[23]

- Is the heteroatom of the aromatic ring involved in metal coordination?

- Is there any conjugation of the sulfonate system with the heteroarene?

- How will this new class of sulfonates perform in their reactivity?

3.2   Aryltriimidosulfonates

3.2.1   Preparation of Aryltriimidosulfonates

In analogy to the syntheses of aryldiimidosulfinates ArS(NR)$_2^-$ and methyl
N,N',N'' tris(*tert*.-butyl)triimidosulfonate, [(thf)$_2$Li{(H$_3$CNC$_4$H$_3$)S(N^{t}Bu)$_3$}] (**17**),
[(tmeda)Li{(SC$_4$H$_3$)S(N^{t}Bu)$_3$}] (**18**) and [(tmeda)Li{(SeC$_4$H$_3$)S(N^{t}Bu)$_3$}] (**19**) are
obtained in the addition reaction of lithium aryls to one S=N double bond of
S(N^{t}Bu)$_3$.
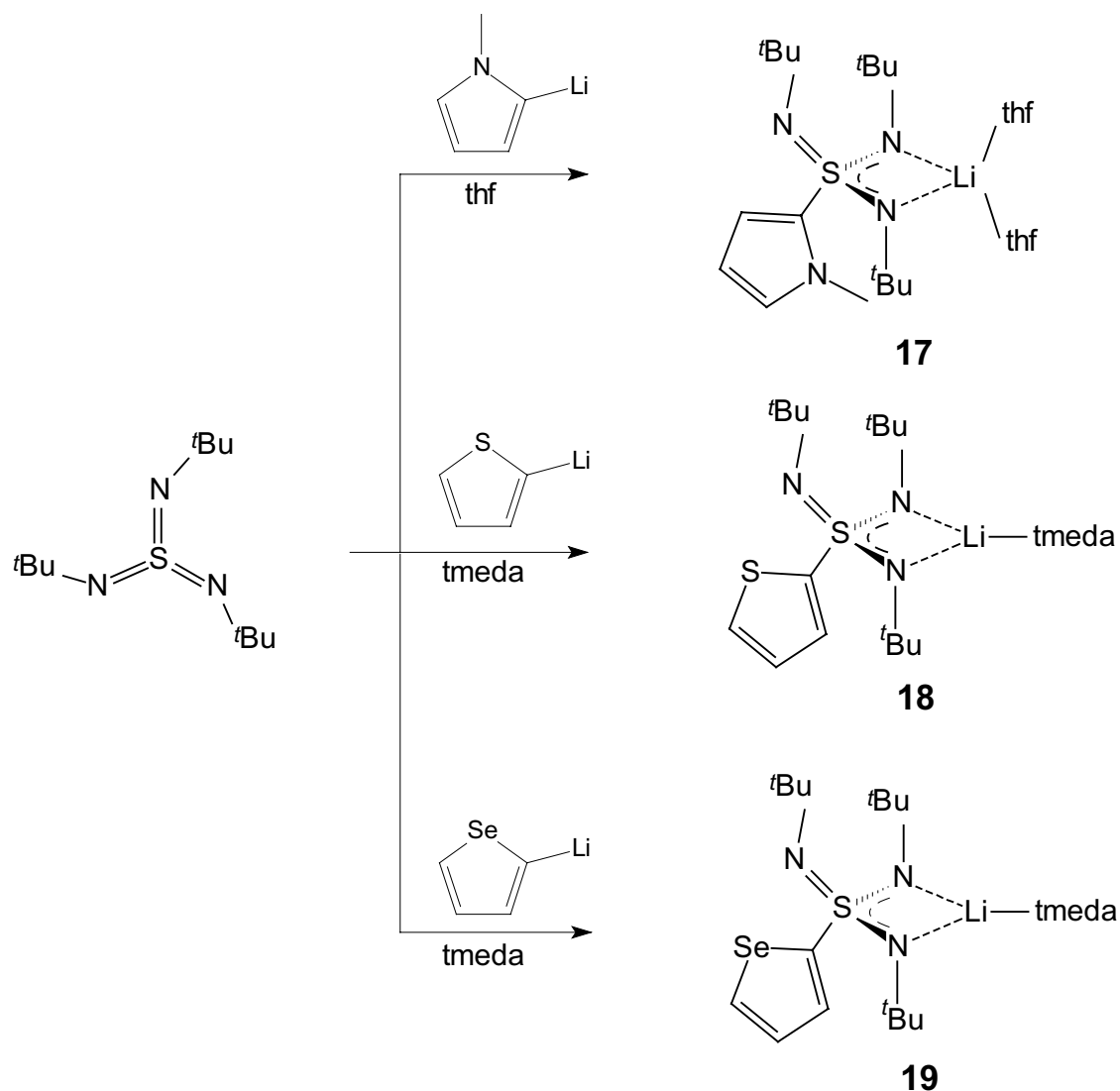
*Scheme 23: Preparation of **17** - **19**.*

Older results appeared to show, that addition reactions of sulfurtriimides are just practicable with sterically less demanding lithium organics. Our new findings indicate, that in some cases, like thiophene, selenophene and methylpyrrole, it is possible anyway. It has to be remarked, that all attempts to add 2-lithium furan to sulfurtriimide failed.

This results fit with experimental charge density studies of sulfurtriimide, carried out by *Leusser* in our group.[79] Figure 31 shows the isosurface defined by the zero-value of the Laplacian of $S(N^tBu)_3$. This visualises areas of relative charge depletions and indicates the most probable directions for a nucleophilic attack (reactive surface).

The reactive surface at the sulfur atom in $S(N^tBu)_3$ shows areas of strong depletion of charge located in the SN_3 plane at the bisections of the N–S–N angles.
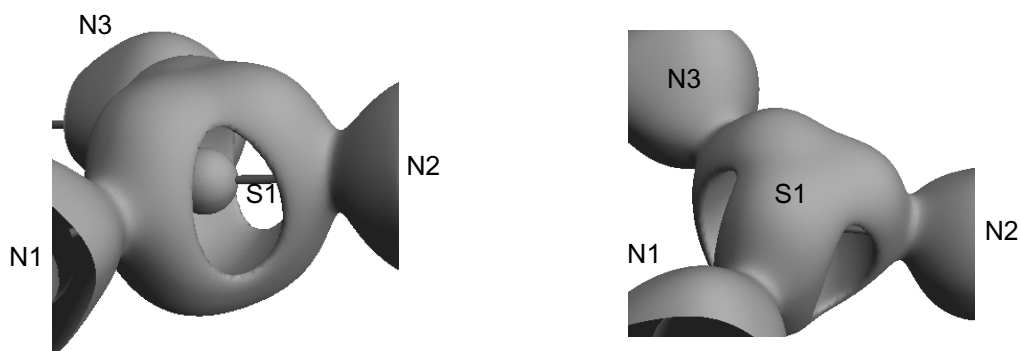
Figure 31: Isosurface representation of the reactive surface ($\nabla^2\rho(\mathbf{r}) = 0$) in $S(N^tBu)_3$.

Interestingly, there is no hole on top of the sulfur atom. A nucleophilic attack orthogonal to the SN_3 plane is precluded by the electron density distribution. This, in fact explains the reactivity of the sulfurtriimide: $S(N^tBu)_3$ reacts smoothly with 2-lithium-methylpyrrole, 2-lithium-thiophene, 2-lithium-selenophene, MeLi[18] or PhCCLi but not with ^nBuLi or ^tBuLi.[26] The carbanionic nucleophile has to approach the sulfurtriimide in an angle of about 45° and that is only feasible by small or flat carbanions, which can slot in between the N^tBu groups of $S(N^tBu)_3$ and approach the electron-depleted regions. Large anions can not reach the holes, as they only can approach the molecule in a wider angle. The

steric argument is not valid if a direct orthogonal attack is anticipated, as there is enough room in the planar molecule to reach the sulfur atom at a direct orthogonal line.

3.2.2   Crystal structures of [(thf)$_2$Li{(H$_3$CNC$_4$H$_3$)S(N^{t}Bu)$_3$}] (17), [(tmeda)Li{(SC$_4$H$_3$)S(N^{t}Bu)$_3$}] (18) and [(tmeda)Li{(SeC$_4$H$_3$)S(N^{t}Bu)$_3$}] (19)

*Figure 32: Superposition plot of the solid state structures of [(thf)$_2$Li{(H$_3$CNC$_4$H$_3$)S(N^{t}Bu)$_3$}] (**17**), [(tmeda)Li{(SC$_4$H$_3$)S(N^{t}Bu)$_3$}] (**18**) and [(tmeda)Li{(SeC$_4$H$_3$)S(N^{t}Bu)$_3$}] (**19**).*

The solid state structures of the lithium S-aryl-tri(*tert*.-butyl)triimidosulfonates **17**, **18** and **19** (figure 32) show that neither tripodal coordination nor additional coordination of the aromatic heteroatom does occur to the lithium cations.

*Table 20: Selected bond lengths [pm], angles [°] and other parameters of **17** – **19**.*

	17 R = N-methylpyrrole	**18** R = thiophene	**19** R = selenophene
S1 – C13	179.6(3)	179.2(3)	179.29(19)
C13 – C14	137.4(5)	140.2(4)	138.5(3)
C14 – C15	142.0(6)	143.5(4)	142.4(3)
C15 – C16	135.6(6)	134.8(5)	134.2(3)
C16 – E	137.0(5) (E = N4)	170.0(4) (E = S2)	186.5(2) (E=Se1)
E – C13	138.5(5) (E = N4)	171.1(3) (E = S2)	186.11(17) (E=Se1)
S1 – N1	158.4(3)	157.8(2)	157.94(15)
S1 – N2	158.5(3)	157.6(2)	157.88(15)
S1 – N3	153.6(3)	154.3(2)	154.72(14)
Li1 – N1	201.9(7)	198.9(5)	198.5(3)
Li1 – N2	196.9(6)	201.3(5)	201.6(3)
Li1 – O1/N4	202.1(7)	219.0(5)	220.0(3)
Li1 – O1/N5	197.1(6)	214(2)	214.0(3)
N1 – S1 – N2	96.52(15)	97.85(9)	97.63(8)
N2 – S1 – N3	122.03(6)	122.46(11)	122.14(8)
N1 – S1 – N3	123.79(17)	121.77(12)	121.71(8)
C13 – S1 – N1	109.24(15)	109.34(12)	109.54(8)
C13 – S1 – N2	108.97(16)	108.97(12)	109.61(8)
C13 – S1 – N3	95.85(16)	96.04(12)	95.99(8)
N1 – Li – N2	72.7(2)	72.91(16)	72.88(12)
C13 – S1 – Li1	121.44(18)	119.22(13)	119.54(9)

Similar to the coordination of PhS(NSiMe$_3$)$_2^-$,[5c] [(thf)Li$_2${(H$_3$CNC$_4$H$_3$)S(N^{t}Bu)$_2$}$_2$] (**8**) and [(tmeda)Li{(SC$_8$H$_5$)S(N^{t}Bu)$_2$}] (**9**) and as well PhCCS(N^{t}Bu)$_3^{2-}$,[26] the ligand is coordinated to one hemisphere of the metal, leaving the two thf donor molecules coordinated to the other in **17**. In **18** and **19** the tetrahedral coordination sphere is completed by one tmeda molecule each. Like the methyl

derivatives, this anions coordinate bidentate with only two nitrogen atoms orientated towards the metal.[23] No further coordination *via* the N3 group could be detected. In both molecules one *tert.*-butyl group is turned away from the heteroaromatic group down to the N_3 face, so one nitrogen atom is blocked from conceivable tripodal metal coordination.

The central sulfur atom is tetrahedrally coordinated and slightly displaced from the centre of the tetrahedron towards the N_3 face (av. N-S-N angle: **17** (114.1°), **18** (114.0°), **19** (113.8°); av. N-S-C angle: **17** (104.7°), **18** (104.7°), **19** (105.0°)).

The negative charge is delocalised over the chelating SN_2 backbone, indicated by the almost ideal planar arrangement of the C1-N1-S1-N2-C5-Li1 moiety (mean deviation from best plane only 4.6 pm for **17**, 8.31 pm for **18** and 8.45 pm for **19**) and the S–N bonds, marginally shorter than the compounds mentioned in chapter 2.3 as the higher oxidation state of the sulfur causes shorter bonds (**17**: av. 158.5(3) pm; **18**: av. 157.7(2) pm; **19**: av. 157.91(15) pm). The noncoordinated nitrogen atoms show much shorter S–N distances (**17**: 153.6(3) pm; **18**: 154.3(2) pm; **19**: 154.72(14) pm). They are comparable to the S=N double bond in $S(N^tBu)_2$ (153.2 pm), but significantly longer than in $S(N^tBu)_3$ (151.5 pm). In comparison to the bidentate sulfonate unit in $[(thf)Li\{(N^tBu)_3SMe\}]_2$ (av. SN_{coord}: 157.8(2) pm; $SN_{noncoord}$: 153.5(3) pm),[23] no significant deviations in the bond lengths could be detected.
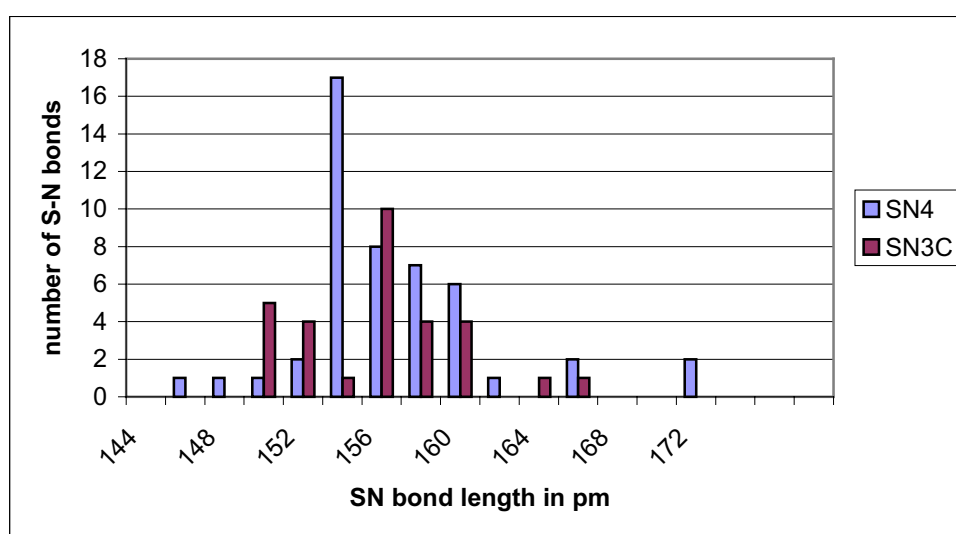
Diagram 4: S–N bond lengths from CCDC (red: SN_3C-compounds; blue: SN_4-compounds).

In general the S–N bonds in **17**, **18** and **19** are in a standard range for S(VI)–N bonds (diagram 4, red graph). The S–N bond lengths of the noncoordinating nitrogen atoms are in the range of 150 – 156 pm, and the S–N bond lengths of the coordinating nitrogen atoms are located between 156 – 168 pm.

The S–C bond lengths with 179.6(3) pm in **17**, 179.2(3) pm in **18** and 179.29(19) pm in **19** are in the standard range for typical S–C$_{aromatic}$ single bonds.

The S-methylsulfonates [Me$_2$Al{(N^{t}Bu)$_3$SMe}] and [Zn{(N^{t}Bu)$_3$SMe}$_2$] have slightly different S–N bond lengths and N-S-N angles, but this can be assigned to the different coordinated metals. The S1–N$_{coord}$ bonds of av. 160.32(19) pm (Al) and 159.75(3) pm (Zn), respectively are about 2 pm longer than in **17** - **19**, while their S1–N3 bonds are shorter (Al: 150.72(18) pm; Zn: 151.9(3) pm).

While the S–N distances of the coordinated nitrogen atoms in **17** – **19** show no significant differences, two different Li–N distances (Li1–N1: 201.9(7) and Li1–N2: 196.9(6) pm) and different Li–O distances (Li1–O1: 202.1(7) and Li1–O2: 197.1(6) pm) could be identified in **17**. In **18** and **19** this differences are much smaller. In both cases Li1 is situated approximately in plane with the N1-S1-N2 triangle, arranged only 9.29 pm in **17**, 3.4 pm in **18** and 4.84 pm in **19** above this plane.
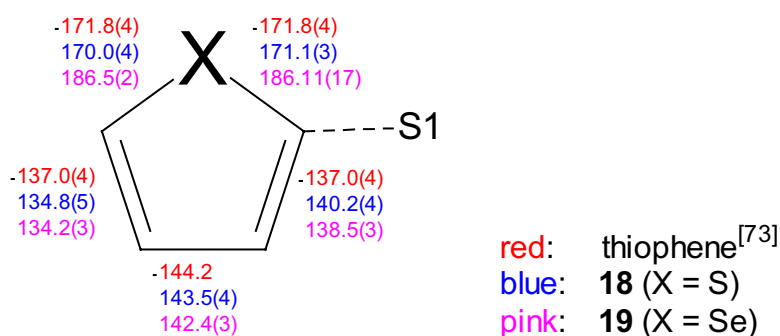
Scheme 24: Bond lengths in pm of sulfonate-substituted heteroarenes.

Comparison of the three structures reveals, that the heteroaromatic planes and the planes determined by S1, N3 and the N3-bonded tertiary carbon atom are almost coplanar. On closer examination of scheme 24, the bond shortening of the C=C double bond arranged opposite to the triimidosulfonate unit is obvious.

These facts witness an electronic interaction between the sulfonate units and the heteroaryls in **18** and **19**.

The heteroarenes in **17** - **19** are orientated in different ways, as can be seen in figure 32. The sulfur atom in **18** and the selenium atom in **19** are pointing towards the pending ^{t}Bu group, whereas the NCH$_3$ group in **17** is orientated away from the pending N^{t}Bu group. The reason for this arrangement might be the avoidance of steric strain.

Comparison of **17**, **18** and **19** reveals, that the geometrical features of the ES(N^{t}Bu)$_3{}^-$ unit (i.e. S-N distances, N-S-N angles and S-N-C angles) are almost invariant to the nature of the aromatic system.

In all currently known metal complexes the alkyltriimidosulfonate chelates as a bidentate ligand, although tripodal coordination occurs with the triimidosulfite[12] and the oxotriimidosulfate OS(N^{t}Bu)$_3{}^{2-}$.[18] In this dianions, tripodal coordination is facilitated by all *tert.*-butyl groups pointing towards the lone pair of the sulfur atom, leaving all lone pairs of the nitrogen atoms pointing in the opposite direction.

The comparison to the tripodal OS(N^{t}Bu)$_3{}^{2-}$ dianion (see chapter 3.3) proves, that tripodal coordination is primarily caused by the higher negative charge rather than by steric or electronic effects. Obviously for a single negative charge in the triimidosulfonates it is sufficient to be delocalised in two S–N bonds, while for a double negative charge in the triimidosulfite and the oxotriimidosulfate three S–N bonds are required.

Another question still remains open: Why is there no evident electronic communication of the heteroaromatic substituent and the sulfonate moiety and how can this be achieved?

3.3   Reactions of Aryltriimidosulfonates

3.3.1   Preparation of [Cu{OS(N^{t}Bu)$_3$}]$_2$ (20)

The initial intention was to transmetalate **17** with CuBr to get a till now unknown copper arylsulfonate species (scheme 25, top), but the reaction failed. In the reaction of [(thf)$_2$Li{(H$_3$CNC$_4$H$_3$)S(N^{t}Bu)$_3$}] (**17**) with CuBr and small amounts of H$_2$O [Cu{OS(N^{t}Bu)$_3$}]$_2$ (**20**) is the only characterised product.
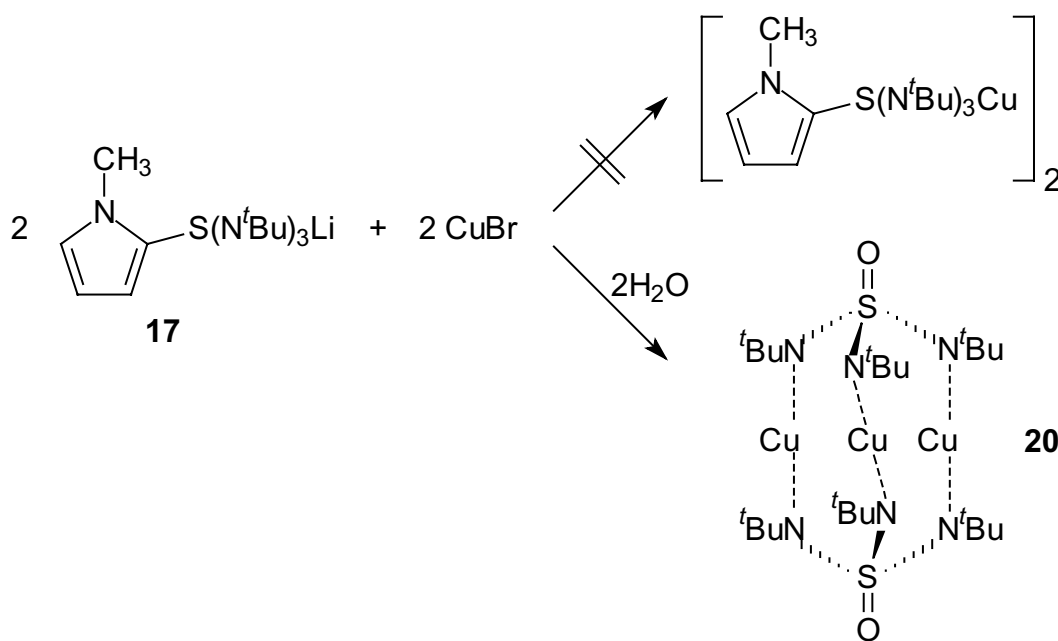
*Scheme 25: Reaction of **17** with CuBr and H$_2$O to [Cu{OS(N^{t}Bu)$_3$}]$_2$ (**20**) (occupation of each Cu: 2/3).*

The desired lithium-copper exchange occurred in the reaction sequence and furthermore Cu(I) was oxidised to Cu(II). In addition methylpyrrole was replaced by an oxygen atom (scheme 25, bottom).

This seems plausible as *Walfort* gained a similar result in the reaction of [(tmeda)$_2$Li$_2${(CH$_2$)S(N^{t}Bu)$_3$}] with small amounts of water: here the methylene substituent left the SN$_3$ unit as methane gas and the trimeric oxotriimidosulfate [(tmeda)Li$_2${OS(N^{t}Bu)$_3$}]$_3$ was obtained as the mayor product.[7]

3.3.2   Crystal structure of [Cu{OS(N^{t}Bu)$_3$}]$_2$ (20)
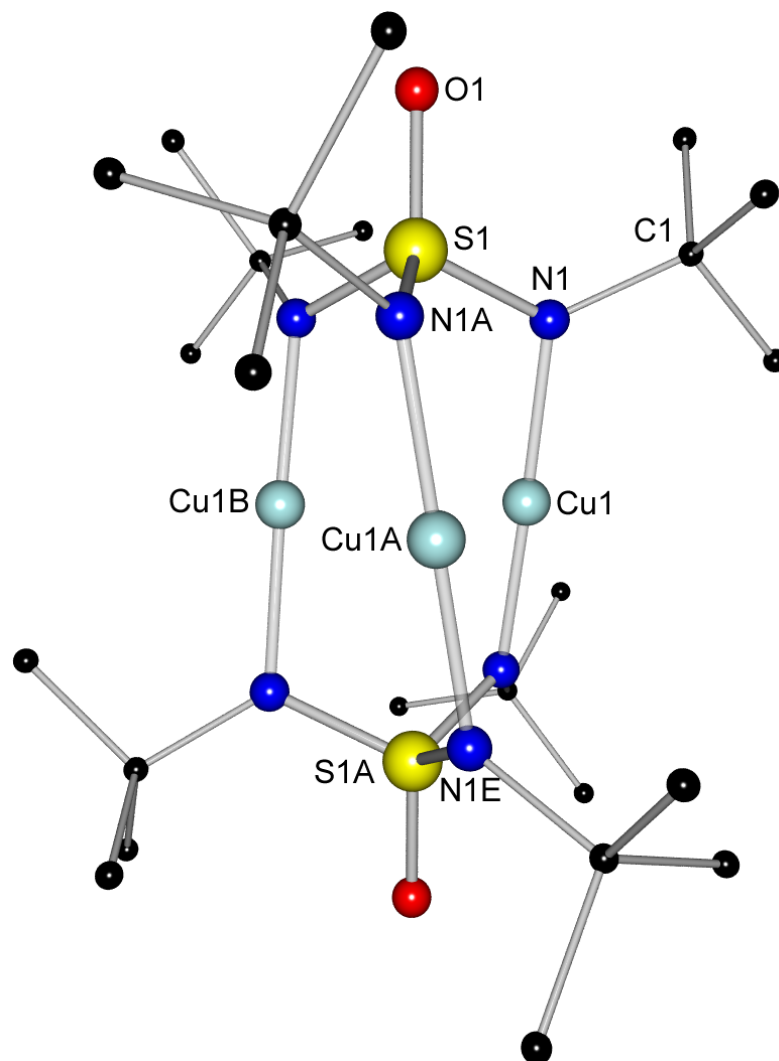
*Figure 33: Structure of [Cu{OS(N^{t}Bu)$_3$}]$_2$ (**20**) in the solid state.*

*Table 21: Selected bond lengths [pm] and angles [°] of **20**.*

S1 – N1	160.21(17)	N1 – S1 – N1A	105.59(8)
S1 – O1	144.5(2)	N1 – Cu1 – N1A	178.08(10)
C1 – N1	149.7(3)	N1 – S1 – O1	113.11(7)
Cu1 – Cu1A	254.78(9)	S1 – N1 – Cu1	111.67(10)
Cu1 – N1	189.92(18)		

Compound **20** crystallises in the centrosymmetric, hexagonal space group
P$\bar{3}$1c. The complete molecule contains six times the asymmetric unit. The side
occupation factor for Cu1 has been refined freely to 0.333, therefore two copper

cations are present in $[Cu\{OS(N^tBu)_3\}]_2$ (**20**). Thus each of the three copper positions is occupied by two thirds. Even though linear coordination is preferred by Cu(I) species, it is assumed that Cu(II) is present in structure **20**, facilitating charge balance.

Like the only other known triimidosulfoxide $[(thf)_3Li_3(\mu_3\text{-}I)\{(N^tBu)_3SO\}]$,[18] the solid state structure of **20** shows a dimer in which the two cap-shaped $OS(N^tBu)_3^{2-}$ ligands are connected *via* copper cations. The central sulfur atom of each cap is tetrahedrally coordinated and slightly displaced from the centre of the tetrahedron towards the oxygen top (N-S-N: 105.59(8)°; N-S-O: 113.11(7)°).

The copper atoms are located central between two nitrogen atoms and are each coordinated by one nitrogen atom of each triimidosulfate unit in a linear fashion, as can be seen by the N-Cu-N angle of 178.08(10)°. The Cu–N distance is 189.92(18) pm, almost exactly as long as in $[Cu\{H_5C_6S(SiMe_3)_2\}]_2$,[5d] $[Cu\{H_3CS(N^tBu)_2\}]_2$ (**5**) and $[Cu\{(SC_8H_5)S(N^tBu)_2\}]_2$ (**11**).

Only at first sight it seems that the N^tBu moieties are all orientated in an eclipsed arrangement, but the two $OS(N^tBu)_3^{2-}$ units are staggered. This can be realised at the angle of 24.8° between the two planes O1-S1-N1 and O1A-S1A-N1E.

The negative charge is completely delocalised in the $S(N^tBu)_3^{2-}$ system, as indicated by equally long S–N bonds (160.21(17) pm). The average S–N distance in $[(thf)_3Li_3(\mu_3\text{-}I)\{(N^tBu)_3SO\}]$[18] is 157.8 pm, thus about 2 pm shorter than in **20**. In $[(thf)Li_2\{O_2S(N^tBu)_2\}]_8\cdot2LiOH\cdot2LiCl$ (av. S–N: 155.0(4) pm) and $[(thf)_2Li_2\{O_2S(N^tBu)_2\}\cdot(thf)LiCl]_2$ (av. S–N: 155.7(2) pm) the S–N bonds are about 5 pm shorter.[80]

The S1–O1 bond length with 144.5(2) pm is equal to the S–O distance in $[(thf)_3Li_3(\mu_3\text{-}I)\{(N^tBu)_3SO\}]$ with 145.5(5) pm. In the sulfate anion SO_4^{2-} with 149.0 pm,[81] and the two bis(*tert.*-butyl)diimidosulfoxides $[(thf)Li_2\{O_2S(N^tBu)_2\}]_8\cdot2LiOH\cdot2LiCl$ (av. S–O: 150.1(3) pm) and $[(thf)_2Li_2\{O_2S(N^tBu)_2\}\cdot(thf)LiCl]_2$ (av. S–O: 150.89(17) pm), the S–O bonds are significantly longer.[80]

Again, it has been shown, that tripodal coordination is primarily caused by the higher negative charge than by steric or electronic effects. Obviously for a double negative charge in the triimidosulfites and oxotriimidosulfates three S–N bonds are required.

3.4   Aryl-bis-(triimidosulfonate)

3.4.1   Preparation of [(tmeda)$_2$Li$_2${(^{t}BuN)$_3$S(SC$_4$H$_2$)S(N^{t}Bu)$_3$}] (21a) and [(thf)$_2$Li$_2${(^{t}BuN)$_3$S(SC$_4$H$_2$)S(N^{t}Bu)$_3$}] (21b)

In analogy to the syntheses of **12** - **15** the reactions with S(N^{t}Bu)$_3$ instead of S(N^{t}Bu)$_2$ have been carried out. First the thiophene has been dilithiated with butyllithium and was subsequently reacted with two equivalents of sulfurtriimide.
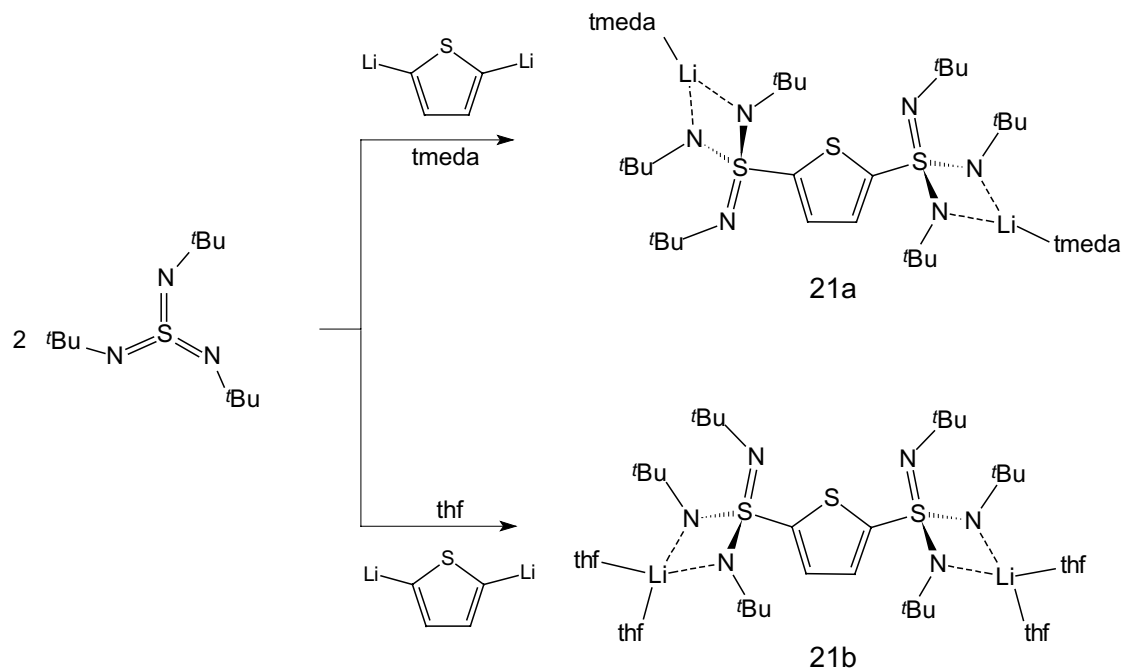
*Scheme 26: Preparation of **21a** and **21b**.*

Even though the steric crowding of the triimidosulfonate was previously believed to be very high, even this synthesis worked. Dependent on the donor base used in the reaction, two different structures (**21a** and **21b**) were obtained (scheme 26).

3.4.2 Crystal structures of [(tmeda)$_2$Li$_2${(^{t}BuN)$_3$S(SC$_4$H$_2$)S(N^{t}Bu)$_3$}] (21a) and [(thf)$_2$Li$_2${(^{t}BuN)$_3$S(SC$_4$H$_2$)S(N^{t}Bu)$_3$}] (21b)
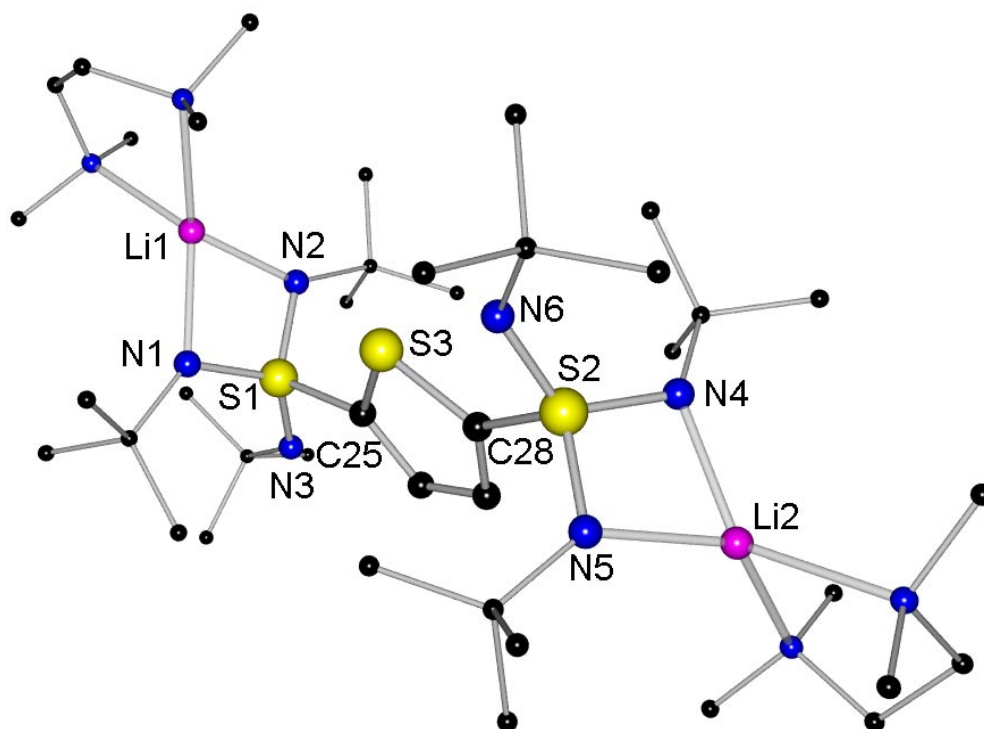
Figure 34: Solid state structure of [(thf)$_2$Li$_2${(^{t}BuN)$_3$S(SC$_4$H$_2$)S(N^{t}Bu)$_3$}] (21a).
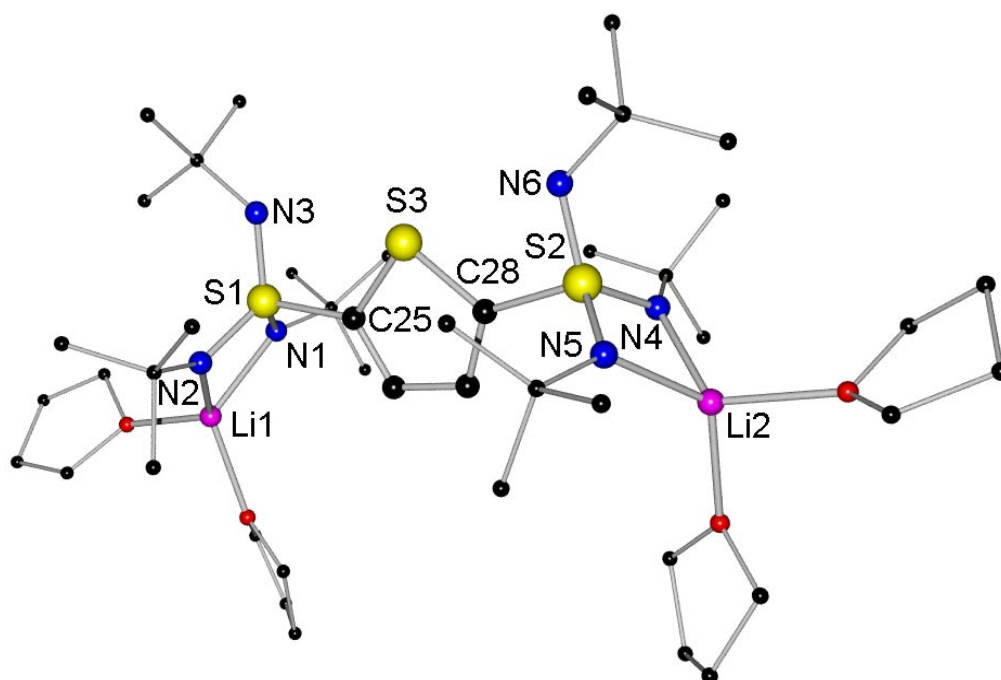
Figure 35: Structure of [(thf)$_2$Li$_2${(^{t}BuN)$_3$S(SC$_4$H$_2$)S(N^{t}Bu)$_3$}] (21b) in the solid state.

*Table 22: Selected bond lengths [pm], angles [°] and several parameters of **21a** and **21b**.*

	21a	21b
S1 – N1	156.5(3)	157.4(5)
S1 – N2	156.9(3)	157.0(5)
S1 – N3	149.4(3)	153.3(5)
S1 – C25	178.8(4)	180.1(5)
S2 – N4	156.9(3)	156.9(5)
S2 – N5	156.3(3)	157.1(5)
S2 – N6	153.4(3)	154.4(5)
S2 – C28	178.2(4)	178.7(6)
N1 – S1 – N2	98.02(17)	97.0(2)
N1 – S1 – N3	122.42(19)	122.6(3)
N2 – S1 – N3	122.64(19)	122.7(3)
N4 – S2 – N5	97.91(17)	97.9(3)
N4 – S2 – N6	121.97(17)	121.6(3)
N5 – S2 – N6	123.13(18)	121.1(3)
N1 – S1 – C25	107.42(18)	108.4(4)
N2 – S1 – C25	107.98(17)	108.7(3)
N3 – S1 – C25	97.32(19)	96.7(3)
N4 – S2 – C28	108.52(18)	108.9(3)
N5 – S2 – C28	108.39(17)	109.3(3)
N6 – S2 – C28	96.16(17)	97.6(3)

Each triimidosulfonate unit coordinates one lithium atom with two nitrogen atoms. The tetrahedral coordination of each lithium cation is completed by one tmeda molecule or two thf molecules, respectively. One difference between **21a** and **21b** is obvious: the different arrangement of the N*t*Bu groups. In **21a** the pending N*t*Bu groups are arranged opposite to each other. In **21b** however, the noncoordinating N*t*Bu groups are pointing exactly in the same direction; with respect to the thiophenyl ring in the direction of S3.

The S1–N3 and the S2–N6 bond of both molecules are in the plane, defined by the thiophenyl ring. In addition the N1-S1-N2 and the N4-S2-N5 bisectors are almost in plane with the thiophenyl substituent.

The negative charge in each sulfonate unit is completely delocalised over the chelating N-S-N unit (S–N (av.): **21a** 156.7(3) pm; **21b** 157.2(5) pm), and therefore the S–N bonds are equal to those in the monosubstituted aryltriimidosulfonates **17** - **19**. The S–N bonds of the pending N^{t}Bu are much shorter than the other S–N bonds (S–N(av.): **21a** 151.4(3); **21b** 153.8(5) pm). Most remarkably, the S1–N3 bond in **21a** of 149.4(3) pm is the shortest ever determined S–N bond in SN_3C_1 moieties (diagram 4).

The S–C$_{aromatic}$ bond length is 178.2(4) pm (av.) for **21a** and 179.4(6) pm (av.) for **21b**, and thus in the usual range for S–C$_{aromatic}$ single bonds. Moreover, no changes of the geometrical features in the thiophenyl ring of **21a** and **21b** could be detected, the bond lengths and angles are similar to those in parent thiophene.[73] Again, not even in this molecules conjugation of the sulfonate units and the heteroaromatic ring occurred.

The first alkylene-bis-(triimidosulfonate) $[(thf)_2Li_2\{((N^tBu)_3S)_2CH_2\}]$[7a] has a completely different constitution. This can be explained by the different coordination mode of lithium in $[(thf)_2Li_2\{((N^tBu)_3S)_2CH_2\}]$. Herein the lithium atoms are coordinated by one nitrogen atom of each sulfonate unit, whereas in **21a** and **21b** each lithium is coordinated by two nitrogen atoms of one sulfonate unit. The S–N bond lengths of $[(thf)_2Li_2\{((N^tBu)_3S)_2CH_2\}]$ are not affected by this change of the geometry. The averaged S–N$_{coord}$ bond lengths with 156.93 pm and the averaged SN$_{noncoord}$ bond lengths with 152.3 pm are in the same range as in **21a** and **21b**.

4   Conclusion and Prospects

4.1   The thermodynamically sink [thf$_6$Li$_6\{\mu_6$S$\}\{$(NR)$_3$S$\}_2$]

In all reactions, that have been carried out to obtain a triimidosulfite with three
(or two) different residues at nitrogen, the final product was always the dilithium
sulfide adduct.

$$RNSNR' + 2R''NHLi \quad \xrightarrow{\quad\not\quad} \quad Li_2S(NR)(NR')(NR'') + H_2NR''$$

R = ^{t}Bu, SiMe$_3$
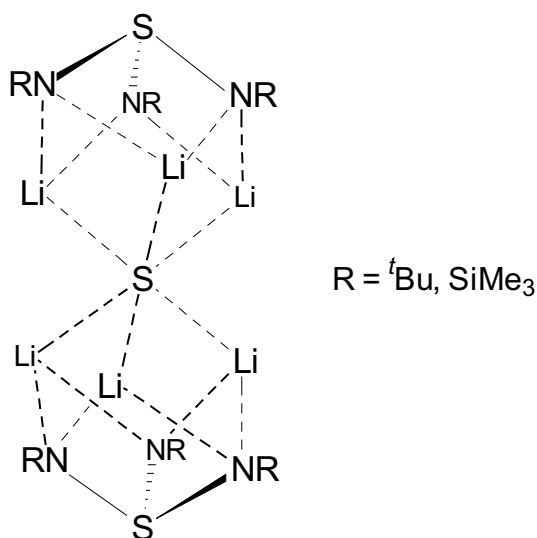
One aim of the further investigations in this field has to be the avoidance of
redox processes in the reaction pathway, otherwise each attempt will lead to the
dilithium sulfide adduct. The presence of elemental sulfur in the starting
products should strictly be avoided.

4.2   Alkylenediimidosulfites

The structures of the alkylenediimidosulfites are not influenced by the different
substituents at nitrogen and carbon, respectively. In each case the doublecubic
structure is received.
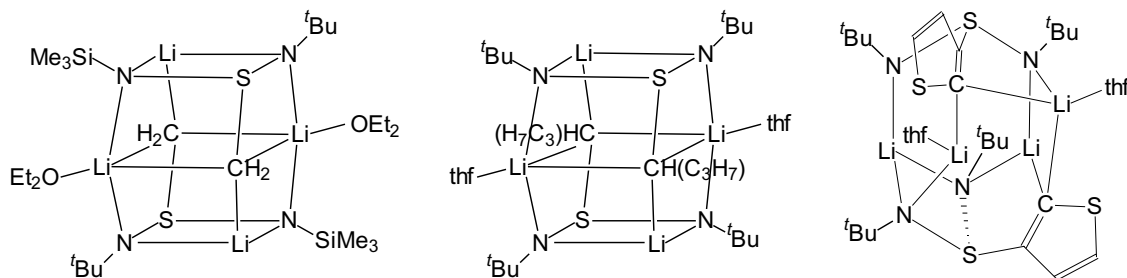
The structure of the sulfur-β-ylide resembles more the structure of triimidosulfite $[Li_4\{(N^tBu)_3S\}_2]$.[4j] The structural change from alkylenediimidosulfite to the sulfur-β-ylide can be described as cleavage of two N–Li bonds and one C–Li bond.

Due to the carbanionic character of the α-carbon atom of the alkylene-diimidosulfites, addition reactions are feasible. Furthermore *Wittig* type reactions of the new dianionic S-ylides, thus the transfer of CH_2 groups to ketons and aldehydes resulting in the generation of alkenes and oxodiimidosulfites, seem promising.
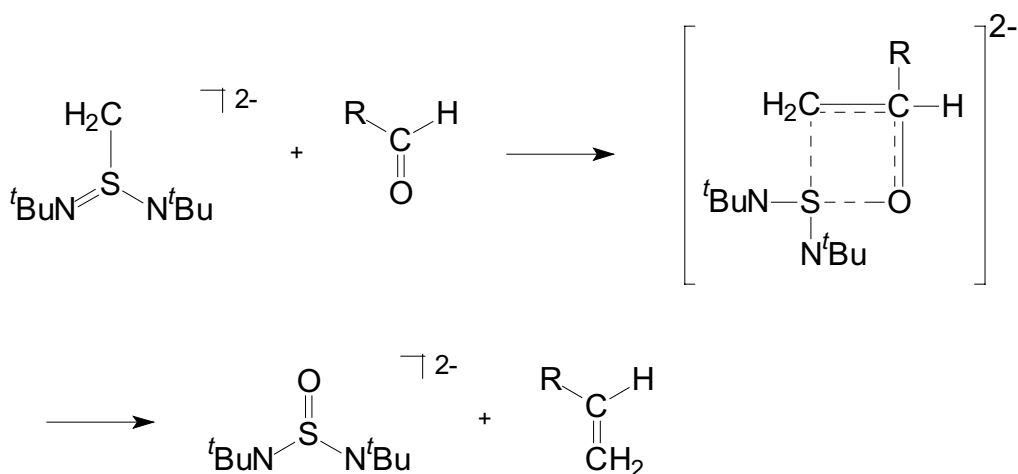
The C=C bond formation ability of *Corey's* S-ylides ($R_2(O)S^{+}\text{-}^{-}CR_2$) has been investigated in detail.[82] As one of the driving forces the high bonding energy of the resulting S=O bond (about 525 kJ/mol) is quoted.

If C=C bond formation reactions follow a stereoselective pathway, they are particularly suitable for the preparation of important biologically active compounds like carotenoids (vitamin A) and pheromones.

For this purpose chiral S-Ylides, like [(Et$_2$O)Li$_2${H$_2$CS(NSiMe$_3$)(N^{t}Bu)}]$_2$ (**6**) seem useful.
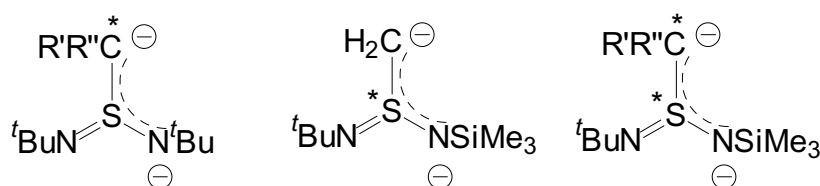
It can be supposed that the SN-chemistry, investigated in our group, is as well transferable to systems like (RC)$_x$S(NR)$_y$ (x=1,y=2; x=2,y=1).

For further work the following reaction sequence is suggested:
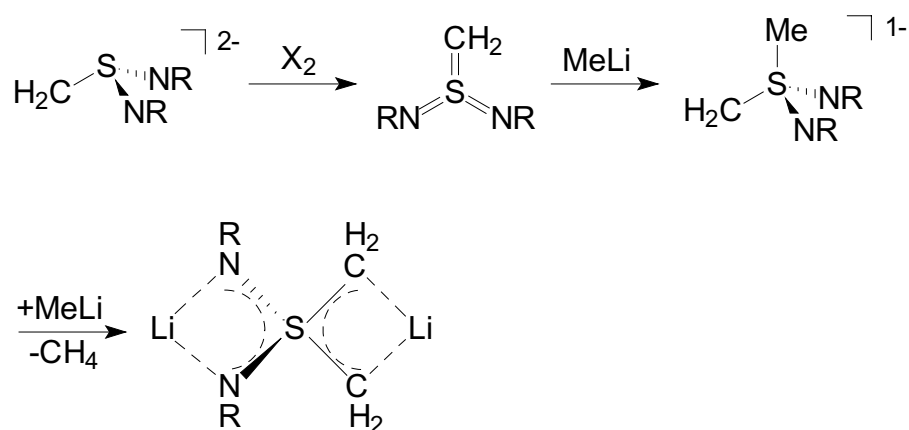
First of all the alkylenesulfurdiimide can be prepared. The various alkylenediimidosulfites seem to be good starting materials for this aim. By means of elemental halogens the oxidation to alkylenesulfurdiimides should be practicable, resulting in prochiral molecules. This sulfur(VI) species should be promising synthons for the generation of dialkylenediimidosulfates *via* addition of one equivalent of alkyl lithium and subsequent deprotonation of the carbon atom by a second equivalent of alkyl lithium.

The isoelectronic principle might be applicable to introduce the PR-group:
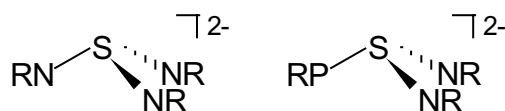
It is certainly advantageous to use the synergetic effect of imides and phoshides in catalysis.

The reaction of sulfurdiimides with lithium-cyclohexylphosphanide led to P_4-rings. Maybe the formation of phosphorous rings can be avoided by the direct insertion of a sulfurdiimide into a P–P bond.[83]

4.3   Aryl-sulfinates and -sulfonates

4.3.1   Aryldiimidosulfinates

The successful syntheses of the first heteroarenesulfinates methylpyrrole-diimidosulfinate and benzothiophenediimidosulfinate uncovered a lot of new structural features, among them a till now unknown monomeric structure type for the latter.
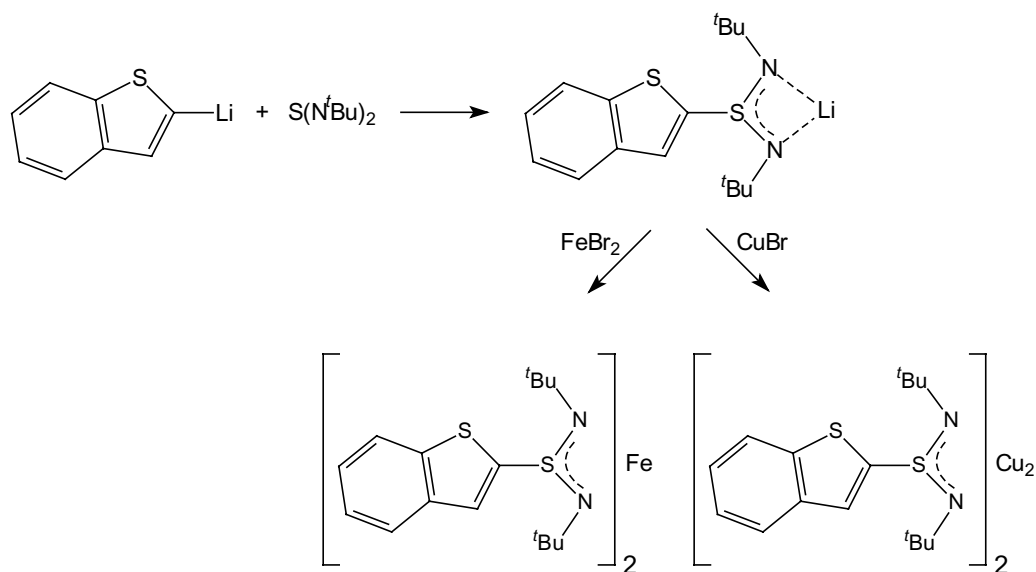
The transmetalation of lithium-benzothiophenediimidosulfinate worked with $FeBr_2$ and as well with CuBr.

4.3.2   Aryl-bis-(diimidosulfinates)

The first members of a completely new class of compounds were synthesised. In the bis-diimidosulfinates two SN_2 units are connected *via* a heteroaromatic linker, containing a potential donor centre in metal coordination.

R = ^{t}Bu; E = S; n = 1, 2

R = SiMe$_3$; E = S; n = 1

R = ^{t}Bu; E = Se; n = 1
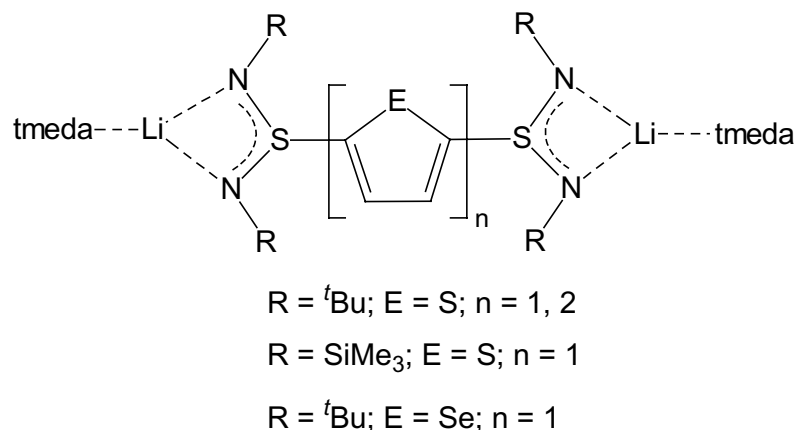
They represent, like the known alkyldiimidosulfinates, dipodal monoanionic ligands. The negative charge is delocalised in both molecules over the NSN-backbone, what can be realised by the identical S–N bond lengths of the sulfinate units. Unfortunately no conjugation of the sulfinate units and the heteroarene linker could be detected so far.

One idea to be realised in the future is the extension of the aromatic system to diselenophenes, dipyrroles, mixed heteroaromatic systems and others.

Aryl-bis-(diimidosulfinates) might be the starting materials for electrically conductive polymers. During the last 30 year, numerous applications have been considered for electrically conductive polymers (e. g. as corrosion-resistant coatings, as electrodes in rechargeable batteries, as sensors and as nonlinear optics).[84] *Scherer*[85] showed, that various SN-polymers with *p*-phenylenegroups are conductive polymers, in case that they are doped with acceptors like I$_2$, Br$_2$ or AsF$_5$. *Wudl* connected thiophene and selenophene, respectively, *via* NSN bridges and got conducting polymers without additional doping.[86]

A second aim would be to enable the participation of the aromatic heteroatom in metal coordination, resulting in a triopodal monoanionic or a pentapodal dianionic ligand.

The exchange of each lithium atom in **12**, **13**, **14** and **15** by dications should lead to diimidosulfinate polymers, connected alternatively by the organic group and the metal.
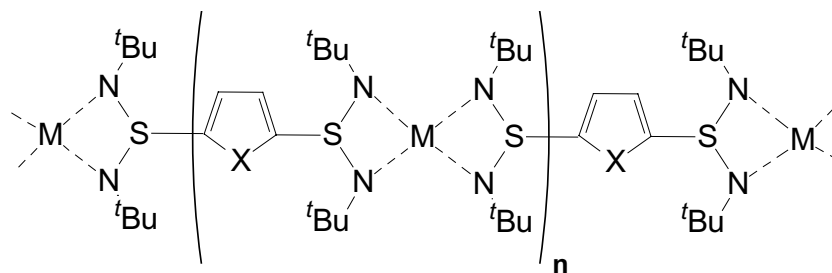
4.3.3   Aryltriimidosulfonates

In the field of sulfur (VI) chemistry the syntheses of aryltriimidosulfonates were successful. Hitherto it was believed, that only spatial less demanding lithium organics could be added to a S=N double bond in $S(N^tBu)_3$. This assumption was confirmed by the fact that methyl- and phenylacetylene-triimidosulfonate were the only known alkylsulfonates. Nevertheless, the addition of several lithiumheteroarenes to sulfurtriimide worked without difficulties. If the shape of the nucleophile permits to slot in between the N^tBu substituents and to approach the electrophilic sulfur in the sulfurtriimide from the side rather than in an orthogonal angle, the addition reaction works smoothly. The lithiumhetero-aromatics employed in this thesis meet this requirements.

$X = NCH_3$; donor = 2 thf
$X = S, Se$; donor = tmeda
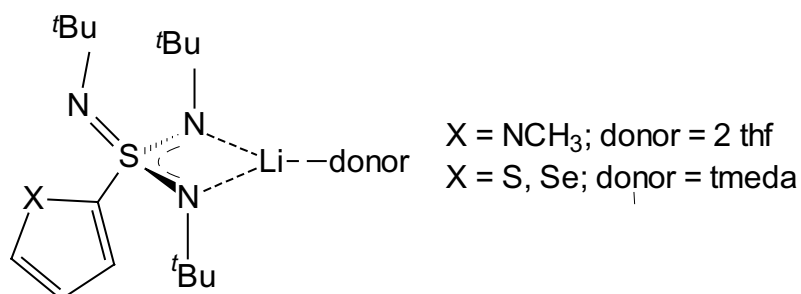
In all to date known complexes the triimidosulfonate monoanion exclusively chelates the metal fragments rather than coordinates in a tripodal fashion. The two adjacent ^tBu substituents are in plane with the SN_2M four membered ring while the third is twisted towards the open N_3 face.

The transmetalation-oxidation product of methylpyrrolesulfonate, $[Cu\{OS(N^tBu)_3\}]_2$, showed, that tripodal coordination is only necessary if two negative charges have to be accommodated. For one negative charge η^2 coordination is sufficient, as can be seen in the aryltriimidosulfonates.

4.3.4 Aryl-bis-(triimidosulfonate)

Although the steric demand of the tris(*tert.*-butyl)triimidosulfonate unit is very high, the synthesis of thiophene-bis-(triimidosulfonate) worked. Here as well, the sulfonate moieties function as dipodal ligands.

$$(^{t}BuN)_{3}S \underset{}{\overset{S}{\diagup\!\!\!\!\diagdown}} S(N^{t}Bu)_{3} \quad \rceil^{\,2-}$$
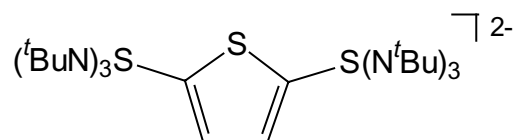
Depending on the donor base two different structure types could be detected:

N^{t}Bu = noncoordinating
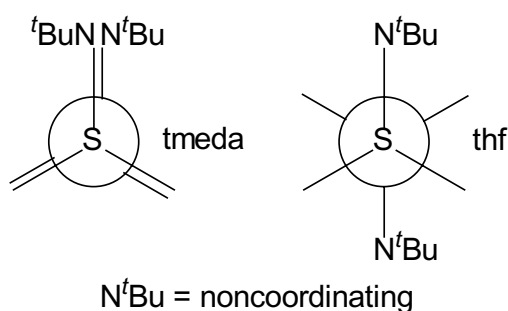
The pending N^{t}Bu-groups in the tmeda product are arranged in an ecliptic order, whereas in the thf product they are arranged anti.

Even in this systems no conjugation of the heteraromatic ring and the sulfonate-units could be detected.

The future aims will be the extension of the aromatic system and the integration of the aromatic heteroatom and the aromatic ring itself into the coordination sphere of the ligand.

5   Zusammenfassung

Die zu den Schwefelsauerstoffverbindungen SO_x isoelektronischen Schwefelstickstoffverbindungen $S(NR)_x$ stellen unser langjähriges Forschungsgebiet dar.

$$O=S(=O)O \qquad NR_3=S(NR_1)(NR_2) \qquad CR_3R_4=S(R_1N)(NR_2) \qquad CR_4R_5=S(R_1N)(CR_2R_3)$$
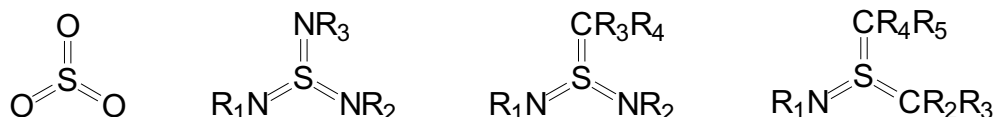
Hierbei sind wir vor allem an Triimidosulfiten $S(NR)_3^{2-}$, Alkyldiimidosulfinaten $RS(NR)_2^{-}$, Schwefeltriimiden $S(NR)_3$, Tetraimidosulfaten $S(NR)_4^{2-}$ und Alkyltriimidosulfonaten $RS(NR)_3^{-}$ interessiert. Das Isoelektronie-Prinzip wurde mittlerweile auf CR_2-Gruppen erweitert, wodurch die neuen Klassen der Alkylendiimidosulfite $(H_2C)S(NR)_2^{2-}$ und der Alkylentriimidosulfate $(H_2C)S(NR)_3^{2-}$ entstanden.

Ein Ziel der Arbeit war es, unsymmetrisch substituierte Triimidosulfite und die entsprechenden Schwefeltriimide darzustellen. Dazu sollte nach dem angegebenen Reaktionsschema vorgegangen werden, das zum Tris(*tert.*-butyl)triimidosulfit geführt hatte.

$$S(NR)_2 + 2\,LiHNR' \longrightarrow Li_2S(NR)_2(NR') + H_2NR'$$
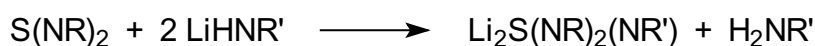
Durch Ersatz des Restes R durch Silyl-, Cyclohexyl- oder aromatische Gruppen sollte die Synthese eines gemischt substituierten Triimidosulfits gelingen. Dieser Ansatz führte nicht zum Erfolg, in einer Vielzahl von Versuchen gelangte man zum Dilithiumsulfid Addukt.

Enthielt die Reaktionssequenz eine *t*Bu-Gruppe, wurde das *t*Bu Sulfid Addukt erhalten, war hingegen keine *t*Bu Gruppe vorhanden, jedoch $SiMe_3$-Gruppen, so entstand ausschließlich das $SiMe_3$ Sulfid Addukt.

$R = {}^{t}Bu, SiMe_3$
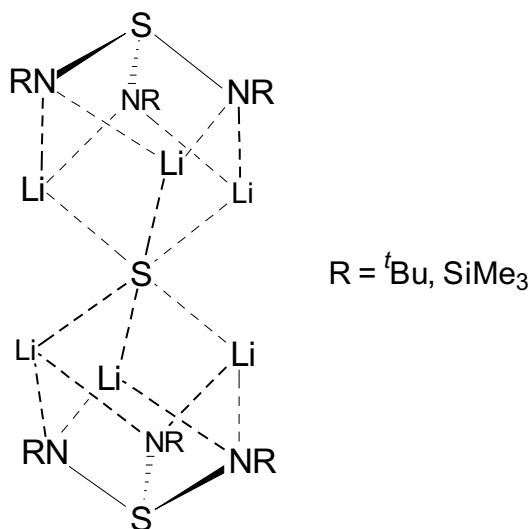
Ausgehend von den bekannten Alkyldiimidosulfinaten können die Alkylendiimidosulfite durch Deprotonierung des α-Kohlenstoffatoms mit einem Äquivalent MeLi bzw. BuLi synthetisiert werden.

$R = {}^{t}Bu; R' = C_3H_7$
$R = SiMe_3; R' = H$
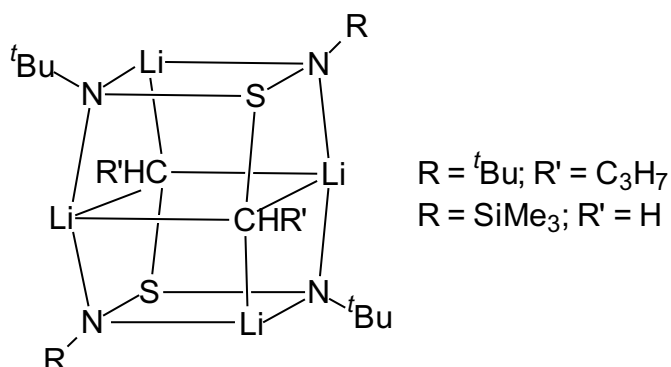
Diese besitzen jeweils Doppelkubusstruktur, wie das von *Walfort* dargestellte $[(thf)Li_2\{H_2CS(N{}^{t}Bu)_2\}]_2$.

Somit gelang die Darstellung chiraler Alkylendiimidosulfite, mit einem chiralen S-Atom im Fall des Methylen(trimethylsilyl)(*tert*.-butyl)diimidosulfits beziehungsweise mit einem chiralen C-Atom im Fall des Butylenbis(*tert*.-butyl)-diimidosulfits. Beide Verbindungen werden in Form ihrer Racemate isoliert.

Die S–C Bindung in diesen Molekülen entspricht S–C-Einfachbindungen und die negative Ladung ist jeweils über das NSN-Gerüst delokalisiert. Somit liegen in diesen Molekülen, wie in den bekannten S-Yliden, ein positiv geladenes Schwefel-Atom neben einem carbanionischen Zentrum vor.
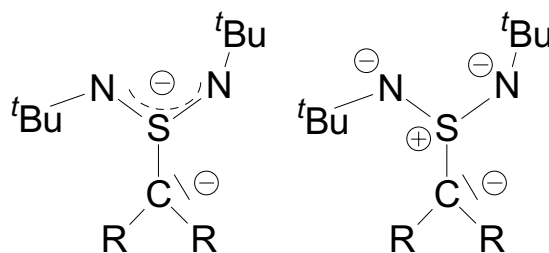
Diese Schwefel-α-Ylide stellen die Carba/Imido-Analoga von SO_3^{2-} und SO_4^{2-} dar.

Ein weiteres Molekül, welches ähnliche strukturelle Eigenschaften aufweist, ist das Di-lithium-thiophenyldiimidosulfit. Thiophen wurde in 3-Position an das Schwefeldiimid addiert und die 2-Position, aufgrund der hierdurch erhöhten CH-Acidität, deprotoniert. Das carbanionische Zentrum liegt somit in β-Position zum SN_2-Gerüst, so dass dieses Molekül als erstes dianionisches Schwefel-β-Ylid bezeichnet werden kann.
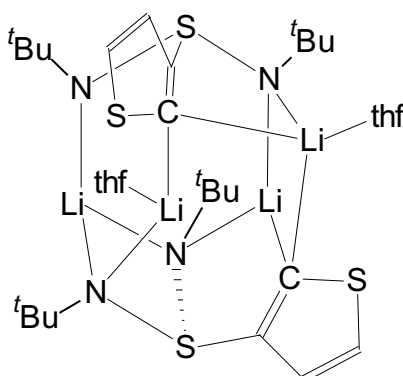
Denkbar ist die Anwendung der gezeigten S-Ylide zur stereoselektiven C=C Bindungsknüpfung, analog zu *Coreys* S-Yliden.

Es gelang erstmals die Synthese zweier Heteroarensulfinate: Methylpyrrol-diimidosulfinat und Benzothiophendiimidosulfinat. Dabei trat neben der bereits bekannten Twist Tricyclus Struktur im Methylpyrroldiimidosulfinat, auch ein neuer Strukturtyp auf, das monomere Benzothiophendiimidosulfinat.

Transmetallierungs-Reaktionen wurden mit Lithium-benzothiophenyldiimido-sulfinat durchgeführt. Dabei gelang der vollständige Lithiumaustausch gegen Fe^{2+} mittels $FeBr_2$ beziehungsweise gegen Cu^+ mittels CuBr. Dies ist insbesondere deshalb bemerkenswert, da bei den Transmetallierungs-

versuchen mit Triimidosulfit bislang entweder Zersetzung oder unvollständiger Metallaustausch auftrat.
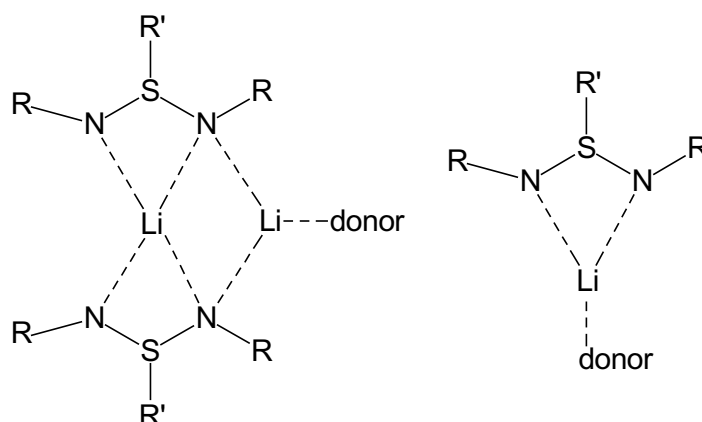
Die Klasse der Aryl-bis-(diimidosulfinate) wurde neu erschlossen. Dabei handelt es sich um Systeme, in denen heteroaromatische Brücken zwei Diimidosulfinat-Einheiten verbinden.

Sie sind, wie die bisher bekannten Alkyldiimidosulfinate, dipodale monoanionische Liganden. Die negative Ladung ist jeweils über das NSN-Gerüst delokalisiert, was sich in den identischen S–N Bindungslängen der Sulfinat-Einheiten zeigt.

R = ^{t}Bu; E = S; n = 1, 2

R = SiMe$_3$; E = S; n = 1

R = ^{t}Bu; E = Se; n = 1
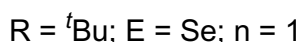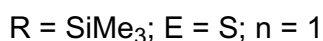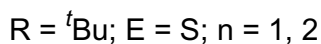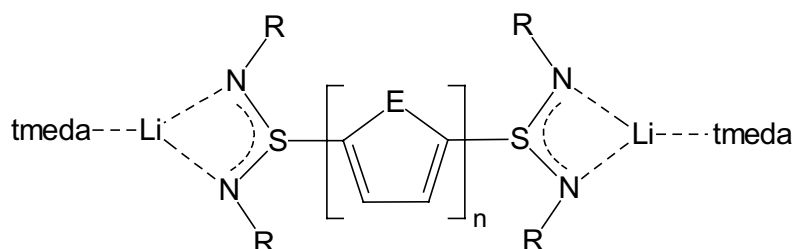
Aufgrund des Elektronenreichtums im heteroaromatischen Ring sollte man annehmen, daß es zu einer Konjugation zwischen dem Aromaten und der Sulfinat-Einheit/den Sulfinat-Einheiten kommt. Dies konnte jedoch nur im Falle des Methylpyrroldiimidosulfinats in geringem Maße beobachtet werden. Ansonsten konnte weder im Falle des Benzothiophendiimidosulfinats, noch im

Falle der Aryl-bis-diimidosulfinate eine Konjugation beobachtet werden. Wichtigstes Kriterium war hierbei die Länge der S–C$_{Aromat}$ Bindung, die jeweils im Bereich einer S–C$_{Aromat}$ Einfachbindung lag. Das zweite wichtige Kriterium war die Veränderung der Bindungsverhältnisse im Aromaten, was jedoch nicht beobachtet werden konnte. Eine Beteiligung des aromatischen Heteroatoms an der Metall-Koordination konnte bislang in keinem Fall beobachtet werden. Durch die Variation der heteroaromatischen Substituenten ließ sich keine Modifikation der Struktur erreichen, lediglich der Substituentenwechsel am Stickstoff führte zu einer veränderten Anordnung der Sulfinat-Einheiten gegenüber dem Heteroaromaten.

Bisher wurde angenommen, dass nur sterisch wenig anspruchsvolle Systeme an eine N–S Doppelbindung des S(N^{t}Bu)$_3$ addiert werden können. So existierten bisher nur das Methyl- und das Phenylacetylen-triimidosulfonat. In dieser Arbeit gelang jedoch die Darstellung diverser Aryltriimidosulfonate. Eine Additionsreaktion ist dann problemlos möglich, wenn die Geometrie des Lithiumorganyls es erlaubt, in die Lücke zwischen den N^{t}Bu Substituenten zu gelangen und sich das Nucleophil somit dem elektrophilen Schwefel von der Seite annähern kann.

X = NCH$_3$; LM = 2 thf
X = S, Se; LM = tmeda
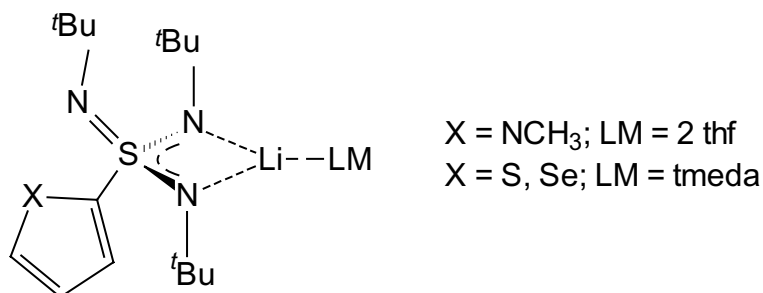
Wie schon im Falle des Tetraimidosulfats und der genannten Sulfonate, tritt keine Koordination über alle drei Stickstoffatome auf, sondern die Sulfonat-Einheit koordiniert das Metallkation η^2-chelatisierend. Die dritte *tert.*-Butyl Gruppe ist zur offenen N$_3$-Ebene gerichtet, wodurch das freie Elektronenpaar am Stickstoffatom abgeschirmt ist und sich nicht an der Koordination des gleichen Metallkations beteiligen kann.

Bei der Umsetzung des Methylpyrrol-triimidosulfonates mit CuBr und Spuren von Wasser gelangt man zum Kupferoxotriimidosulfat, wobei das Cu(I) im Reaktionsverlauf zu Cu(II) oxidiert wurde. Hier tritt trotz des an das Schwefel-atom gebundenen Sauerstoffatom, eine tripodale Koordination auf. Dabei zeigt sich, dass für die tripodale Koordination zwei negative Ladung notwendig sind. Die beiden OS(N^{t}Bu)$_3$-Kappen stehen nicht exakt ekliptisch zueinander, sondern sind leicht gegeneinander verdreht.

$$
\begin{array}{c}
O \\
\parallel \\
S \\
{}^t\text{BuN} \quad \text{N}^t\text{Bu} \quad \text{N}^t\text{Bu} \\
\text{Cu} \quad \text{Cu} \quad \text{Cu} \\
{}^t\text{BuN} \quad {}^t\text{BuN} \quad \text{N}^t\text{Bu} \\
S \\
\parallel \\
O
\end{array}
$$
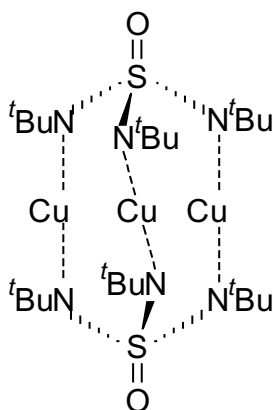
Trotz des hohen sterischen Anspruchs der Triimidosulfonat-Einheit, gelang die Synthese des Thiophen-bis-triimidosulfonats.

$$
(^t\text{BuN})_3\text{S}-\!\!\!\!\left\langle \text{Thiophen} \right\rangle\!\!\!\!-\text{S}(\text{N}^t\text{Bu})_3 \Big]^{2-}
$$
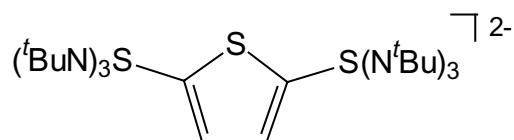
Die Sulfonat-Einheiten fungieren hier, wie bereits für die Aryltriimidosulfonate gezeigt, als dipodale Liganden, die dritte N^{t}Bu-Gruppe ist wiederum nicht an der Koordination beteiligt. Abhängig von der Donorbase konnten folgende Strukturtypen dargestellt werden:

$$
{}^t\text{BuN} \;\; \text{N}^t\text{Bu} \qquad\qquad \text{N}^t\text{Bu}
$$

S   tmeda   S   thf

N^{t}Bu   N^{t}Bu

N^{t}Bu = nicht koordinierend
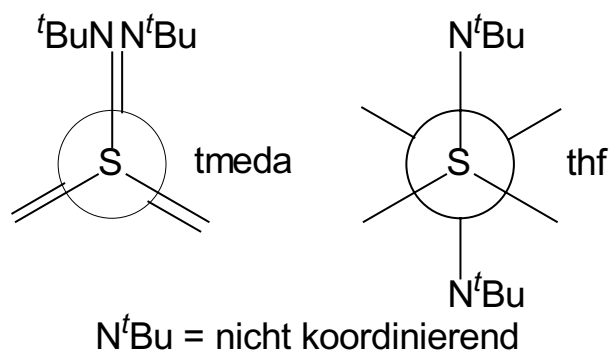
Im Fall des tmeda-Produktes stehen die nicht-koordinierenden N^{t}Bu-Gruppen verdeckt, im Fall des thf-Produktes stehen sie anti zueinander.

Leider trat hier ebenfalls keine Konjugation zwischen den Sulfonat-Einheiten und dem Heteroaromaten auf.

Die weiteren Ziele werden zum einen sein, das aromatische System auszudehnen, zum anderen auch die Einbeziehung des Heteroatoms in die Koordination zu ermöglichen, beziehungsweise den gesamten Heteroaromaten als η^5-Ligand zu nutzen.

6   Experimental Section

All experiments were performed under inert gas atmosphere of dry N_2 with Schlenk techniques or in an argon drybox. Reagents were used as received. $S(N^tBu)_2$,[87] $S(NSiMe_3)_2$,[88] $SNCy(SiMe_3)$,[89] $S(N^tBu)(SiMe_3)$,[90] $S(N^tBu)_3$,[18] and ^tBuNSO[38] were prepared according to literature procedures. Solvents were freshly distilled from sodium-potassium alloy prior to use.

Melting points and Decomposition temperatures: The determination of MP and DT was done in tight glass-capillary with a MEL TEMP II (MEL, marked separately), Laboratory devices, or on a DTA-apparatus, Du Pont Thermal Analyzer TA 9000 and a DSC-cell, in the analytical laboratory of the Department of Inorganic Chemistry at Würzburg. Melting points and Decomposition temperatures are uncorrected.

NMR-Spectra: The NMR spectra were obtained on a Jeol Lambda 300 spectrometer or on a Bruker AM 250, Bruker MSL 400, Bruker DRX 300, Bruker AMX 400 spectrometer. All spectra were measured at 25°C. Chemical shifts are reported in ppm, coupling constants in Hz. ^1H-, ^7Li-, ^{13}C- and ^{29}Si-NMR-spectra were recorded in C_6D_6 (^1H C_6HD_5: δ= 7.15; ^{13}C C_6D_6: δ= 128.0). The samples were externally referenced to 1.0 M LiCl for ^7Li-spectra and TMS for ^{29}Si.

Multiplicity: s = singlet, d = duplet, t = triplet, q = quartet, qi = quintet, m = multiplet, s_{br} = broad singlet.

X = -NCH$_3$, -S, -Se
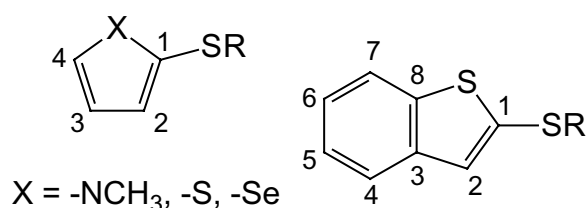
Elemental analysis: Elemental analysis were carried out by the analytical laboratory of the Department of Inorganic Chemistry in Würzburg.

$C_6H_{11}NSN^tBu$ (1):

A solution of butyllithium in hexane (1.6 M, 54.3 mmol, 33.92 mL) was added dropwise to N-cyclohexyl-N'-trimethylsilylamin (54.3 mmol, 9.3 g) at 0°C. The reaction mixture was allowed to warm to room temperature and stirred for 1 h. *tert.*-butylthionylimin (53.76 mmol, 6.4 g) was added at 0°C and the mixture was stirred overnight. The solvent was removed under vacuum (12 mbar) and the crude product was purified by distillation at 57°C/0.02 mbar to give $C_6H_{11}NSN^tBu$ as a yellow liquid. M = 200.34 g/mol. (yield 6.96 g, 65%). ^{1}H-NMR (400.13 MHz, C_6D_6): δ = 1.24 (s, 9H, CCH_3), 1.13 – 1.67 (m, 11H, $CH(CH_2)_5$); ^{13}C-NMR (100 MHz, C_6D_6): δ = 25.47 ($CHCH_2CH_2\underline{C}H_2(CH_2)_2$), 26.82 ($CHCH_2\underline{C}H_2(CH_2)_3$), 32.53 ($C(\underline{C}H_3)_3$), 34.70 ($CH\underline{C}H_2(CH_2)_4$), 58.79 ($\underline{C}(CH_3)_3$), 60.59 ($\underline{C}H(CH_2)_5$). Mp.: 3°C.

$[thf_6Li_6\{\mu_6S\}\{(NSiMe_3)_3S\}_2]$ (2):

N,N'bis(trimethylsilyl)sulfurdiimide (5 mmol, 1.03 g) was added to freshly cut lithium (10 mmol, 0.069 g) in 10 mL thf. After stirring overnight, the lithium is completely dissolved. The remaining solid was filtered and crystallisation from the deep red thf solution at –26°C gave colourless crystals. M = 1092.91 g/mol. (yield 1.2 g, 66%). ^{1}H-NMR (400.13 MHz, C_6D_6): δ = 0.39 (s, 9H, $SiMe_3$), 1.37 (qi, 4H, $O(CH_2C\underline{H}_2)_2$), 3.67 (t, 4H, $O(C\underline{H}_2CH_2)_2$); ^{13}C-NMR (100 MHz, C_6D_6): δ = 3.34 ($NSi\underline{Me}_3$), 25.48 ($O(CH_2\underline{C}H_2)_2$), 68.33 ($O(\underline{C}H_2CH_2)_2$); ^{7}Li-NMR (155.5 MHz, ext. sat. LiCl solution) δ = 1.62 (s); [29]Si: (60 MHz, C_6D_6): -10.0 ($\underline{Si}Me_3$). Elemental analysis found (calc) in %: C 45.17 (46.13), H 8.67 (9.4), N 7.66 (7.68), S 8.26 (8.79). Mp.: 139°C (dec.).

$[(thf)Li\{H_3CS(NSiMe_3)_2\}]_2$ (3):

A solution of methyllithium in diethyl ether (1.6 M, 5.0 mmol, 3.13 mL) was added slowly to a solution of N,N'bis(trimethylsilyl)sulfurdiimide (5.0 mmol, 1.03 g) in 5 mL thf at –78°C. The reaction mixture was allowed to warm to room temperature and stirred for 2 h. 3 d storage at –36°C yields colourless crystals. M = 600.34 g/mol. (yield 0.806 g, 57%). ^{1}H-NMR (300.4 MHz, C_6D_6): δ = 0.33

(s, 18H, SiMe$_3$), 1.28 (qi, 4H, O(CH$_2$CH$_2$)$_2$), 2.24 (s, 3H, SCH$_3$), 3.45 (t, 4H, O(CH$_2$CH$_2$)$_2$); ^{13}C-NMR (100 MHz, C$_6$D$_6$): δ = 2.60 (SiMe$_3$), 25.40 (O(CH$_2$CH$_2$)$_2$), 68.15 (O(CH$_2$CH$_2$)$_2$); ^{7}Li-NMR (155.5 MHz, ext. sat. LiCl solution) δ = 1.46 (s); ^{29}Si (60 MHz, C$_6$D$_6$): –3.81 (SiMe$_3$). Elemental analysis found (calc) in %: C 42.95 (43.96), H 9.47 (9.73), N 9.43 (9.32), S 10.34 (10.67). Mp.: 99°C.

[(Et$_2$O)Li{H$_3$CS(NSiMe$_3$)(NC$_6$H$_{11}$)}]$_2$ (4):

A solution of butyllithium in hexane (1.6 M, 4.64 mmol, 2.9 mL) was added to a solution of N-cyclohexyl-N'-trimethylsilyl-sulfurdiimide (4.6 mmol, 1.00 g) in 5 mL diethyl ether at –78°C. The reaction mixture was stirred 30 min at –78°C, then warmed up to room temperature and stirred for 1 h. 7 d storage at –36°C yielded colourless crystals. M = 624.44 g/mol. (yield 0.78 g, 54%). ^{1}H-NMR (300.4 MHz, C$_6$D$_6$): δ = 0.35 (s, 9H, SiMe$_3$), 1.33 (m, 6H, (O(CH$_2$CH$_3$)$_2$), 1.09 – 1.99 (m, 11H, C$_6$H$_{11}$), 2.33 (s, 3H, SCH$_3$), 3.49 (m, 4 H, (O(CH$_2$CH$_3$)$_2$); ^{13}C-NMR (100 MHz, C$_6$D$_6$): δ = 3.12 (SiMe$_3$), 25.50 (O(CH$_2$CH$_3$)$_2$), 26.56 (SCH$_3$), 26.70 (CHCH$_2$CH$_2$CH$_2$(CH$_2$)$_2$), 38.61 (CHCH$_2$CH$_2$(CH$_2$)$_3$), 51.02 (CHCH$_2$(CH$_2$)$_4$), 60.05 (CH(CH$_2$)$_5$), 68.12 (O(CH$_2$CH$_3$)$_2$); ^{7}Li-NMR (155.5 MHz, ext. sat. LiCl solution) δ = 1.56 (s); ^{29}Si-NMR (60 MHz, C$_6$D$_6$): δ = –7.1. Elemental analysis found (calc) in %: C 51.55 (53.81), H 9.87 (10.64), N 9.48 (8.96), S 9.97 (10.26). Mp.: 106°C.

[Cu{H$_3$CS(N^{t}Bu)$_2$}]$_2$ (5):

N,N'bis(*tert*.-butyl)sulfurdiimide (5.7 mmol, 1.0 g) was added to CuCl (5.7 mmol, 0.56 g) in 20 mL hexane. A solution of methyllithium in diethyl ether (1.6M, 5.7 mmol, 3.56 mL) was added slowly to the suspension at –40°C. The reaction mixture was allowed to warm to room temperature and stirred for 2 h. The insignificant white precipitate was filtered. The solution was stored at –36°C and after 5 d colourless crystals were obtained. M = 504.14 g/mol. (yield 0.51g, 36%). ^{1}H-NMR (400.13 MHz, C$_6$D$_6$): δ = 1.41 (s, 18H, C(CH$_3$)$_3$), 2.55 (s, 3H, SCH$_3$); ^{13}C-NMR (100.62 MHz, C$_6$D$_6$): δ = 34.50 (C(CH$_3$)$_3$), 52.47 (SCH$_3$), 56.40

($\underline{C}(CH_3)_3$). Elemental analysis found (calc) in %: C 42.15 (42.75), H 7.54 (8.37), N 10.52 (11.08), S 11.70 (12.68). Mp.: 84°C.

[(Et$_2$O)Li$_2${H$_2$CS(NSiMe$_3$)(N^{t}Bu)}]$_2$ (6):

A solution of methyllithium in diethyl ether (1.6 M, 5.25 mmol, 3.28 mL) was added drop by drop to a solution of N-*tert*.-butyl-N'-trimethylsilylsulfurdiimide (5.25 mmol, 1.00 g) in 5 mL diethyl ether at –78°C. The reaction mixture was allowed to warm to room temperature and stirred for 30 min. A second equivalent of methyllithium in diethyl ether (1.6 M, 5.25 mmol, 3.28 mL) was added to the solution at –78°C. The solution was warmed up to room temperature and stirred for 1 h. Colourless crystals were obtained directly from the reaction mixture upon 7 days storage at –36°C. M = 584.43 g/mol. (yield 1.25 g, 81%). ^{1}H-NMR (300.4 MHz, C$_6$D$_6$): δ = 0.32 (s, 9H, Si(C$\underline{H}_3$)$_3$), 1.08 (t, 6H, O(CH$_2$C$\underline{H}_3$)$_2$), 1.13 (s, 2H, SCH$_2$), 1.33 (s, 9H, C(C$\underline{H}_3$)$_3$), 3.25 (q, 4H, O(C$\underline{H}_2$CH$_3$)$_2$); ^{13}C-NMR (100 MHz, C$_6$D$_6$): δ = 1.36 (Si$\underline{Me}_3$), 15.04 (O(CH$_2$$\underline{C}H_3$)$_2$), 33.49 (C($\underline{C}H_3$)$_3$), 42.92 (S$\underline{C}H_2$), 52.32 ($\underline{C}$(CH$_3$)$_3$), 65.18 (O(CH$_2$$\underline{C}H_3$)$_2$); ^{7}Li (155.5 MHz, ext. sat. LiCl solution): δ = 3.00 (s); ^{29}Si-NMR (60 MHz, C$_6$D$_6$): δ = -2.1 + -4.5. Elemental analysis found (calc) in %: C 45.98 (49.29), H 9.09 (10.34), N 9.47 (9.58), S 9.33 (10.96). Mp.: 117°C (dec.).

[(thf)Li$_2${H$_8$C$_4$S(N^{t}Bu)$_2$}]$_2$ (7):

A solution of butyllithium in hexane (1.6 M, 11.47 mmol, 7.17 mL) was added dropwise to a solution of N,N'bis(*tert*.-butyl)sulfurdiimide (5.7 mmol, 1.00 g) in 5 mL thf and 1.7 mL tmeda and stirred for 12 h. Colourless crystals were obtained directly from the reaction mixture upon 7 d storage at +6°C. M = 632.54 g/mol. (yield 0.63 g, 35%). ^{1}H-NMR (300.4 MHz, C$_6$D$_6$): δ = 0.87 (m, 1H, S-C$\underline{H}$LiCH$_2$CH$_2$CH$_3$), 1.11 (t, 3H, S-CHLiCH$_2$CH$_2$C$\underline{H}_3$), 1.30 (qi, 4H, O(CH$_2$C$\underline{H}_2$)$_2$), 1.38 + 1.40 (s, 18H, C(C$\underline{H}_3$)$_3$), 1.49 (m, 2H, S-CHLiCH$_2$C$\underline{H}_2$CH$_3$)1.57 (m, 2H, S-CHLiC$\underline{H}_2$CH$_2$CH$_3$), 3.59 (t, 4H, (O(C$\underline{H}_2$CH$_2$)$_2$); ^{13}C-NMR (100 MHz, C$_6$D$_6$): δ = 14.58 (S-CHLiCH$_2$CH$_2$$\underline{C}H_3$), 25.32 (($\underline{C}H_2CH_2$)$_2$O), 27.40 (S-CHLiCH$_2$$\underline{C}H_2CH_3$), 33.78 (S-$\underline{C}H_2CH_2CH_2CH_3$), 34.04 + 34.30 (C($\underline{C}H_3$)$_3$), 52.01 + 52.29 ($\underline{C}$(CH$_3$)$_3$),

52.14 (S-C<u>H</u>LiCH$_2$CH$_2$CH$_3$), 68.57 (O(<u>C</u>H$_2$CH$_2$)$_2$); [7]Li (155.5 MHz, ext. sat. LiCl solution): δ = 2.42, 2.51 (2s, 1:1). Elemental analysis found (calc) in %: C 59.09 (60.74), H 10.23 (10.83), N 8.96 (8.85), S 9.44 (10.13). Mp.: 50°C.

[(thf)Li$_2${(H$_3$CNC$_4$H$_3$)S(N^{t}Bu)$_2$}$_2$] (8):

A solution of butyllithium in hexane (1.6M, 9.8 mmol, 6.125 mL) was added dropwise to a solution of N-methylpyrrole (9.8 mmol, 0.8 g) in 7 mL thf at −78°C. The reaction mixture was allowed to warm to room temperature and finally refluxed gently for 90 min. N,N'bis(*tert*.-butyl)sulfurdiimide (9.8 mmol, 1.72 g) was added to the suspension at 0°C. The solution was stirred for another 12 h. The solvent was removed under vacuum and the white precipitate was resolved in 10mL hexane and 3 mL thf. 4 d storage at −36°C yielded colourless crystals. M = 594.43 g/mol. (yield 1.46 g, 51%). ^{1}H-NMR (400.13 MHz, C$_6$D$_6$): δ = 1.22 (qi, 4H, O(CH$_2$C<u>H</u>$_2$)$_2$), 1.48 (s, 36H, C(C<u>H</u>$_3$)$_3$), 3.12 (m, 4H, O(C<u>H</u>$_2$CH$_2$)$_2$), 3.25 (s, 3H, NC<u>H</u>$_3$), 6.14 (d, 1H), 6.26 (d, 1H), 6.86 (m, 1H); ^{13}C-NMR (100 MHz, C$_6$D$_6$): δ = 25.19 (O(CH$_2$<u>C</u>H$_2$)$_2$), 33.54 (C(<u>C</u>H$_3$)$_3$), 34.91 (N<u>C</u>H$_3$), 54.16 (<u>C</u>(CH$_3$)$_3$, 67.50 (O(<u>C</u>H$_2$CH$_2$)$_2$), 106.89 (C3), 112.51 (C2), 124.41 (C4), 141.77 (C1); ^{7}Li-NMR (155.5 MHz, ext. sat. LiCl solution): δ = 1.46 (s, 2Li). Elemental analysis found (calc) in %: C 59.69 (60.58), H 9.19 (9.49), N 14.00 (14.13), S 10.36 (10.78). Mp.: 93°C.

[(tmeda)Li{(SC$_8$H$_5$)S(N^{t}Bu)$_2$}] (9):

A solution of butyllithium in hexane (1.6M, 4.08 mmol, 2.54 mL) was added dropwise to a solution of benzothiophene (4.08mmol, 0.55g) in 12 mL thf hexane and tmeda (8.0 mmol, 1.25 mL) at 0°C. The reaction mixture was allowed to warm to room temperature and stirred for 1 h. N,N'bis(*tert*.-butyl)sulfurdiimide (4.08 mmol, 0.71 g) was added to the suspension and stirred 3 h. The reaction mixture was stored at +6°C and after 3 d colourless crystals could be obtained. M = 430.28 g/mol. (yield 0.73 g, 51%). ^{1}H NMR (400 MHz, C$_6$D$_6$): δ = 1.45 (s, 18H; C(C<u>H</u>$_3$)$_3$), 2.08 (s, 16H; <u>Me</u>$_2$NC<u>H</u>$_2$C<u>H</u>$_2$N<u>Me</u>$_2$), 7.01 -

7.62 (m, H10-H15); ^{13}C NMR (100 MHz, C$_6$D$_6$): δ = 33.79 (C($\underline{C}$H$_3$)$_3$), 46.03 ($\underline{Me}_2$NCH$_2$CH$_2$N$\underline{Me}_2$), 52.83 ($\underline{C}$(CH$_3$)$_3$), 56.65 (Me$_2$N$\underline{C}$H$_2$$\underline{C}H_2NMe_2$), 122.65 - 124.43 (m, C2/C4 − C7), 141.10 (C3), 146.09 (C8), 160.24 (C1); ^{7}Li NMR (116.7 MHz, ext. sat. LiCl solution): δ = 0.98 (s). Elemental analysis found (calc) in %: C 57.50 (61.36), H 8.43 (9.13), N 11.38 (13.01), S 13.65 (14.89). Mp.: 55°C (dec).

[Fe{(SC$_8$H$_5$)S(N^{t}Bu)$_2$}$_2$] (10):

A suspension of **9** (1.16 mmol, 0.5 g), FeBr$_2$ (0.58 mmol, 0.125 g), 2 mL tmeda and 8 mL hexane was stirred at 0°C for 1 h and additionally stirred 12 h at RT. Volatile material was removed under vacuum and 10 mL pentane was added to the residue. After lithium bromide was filtered off, the solution was stored at − 24°C and after 2 d red crystals were obtained. M = 670.20 g/mol. No further analytical data could be obtained, due to the high air sensitivity of the compound.

[Cu{(SC$_8$H$_5$)S(N^{t}Bu)$_2$}]$_2$ (11):

A suspension of **9** (1.16 mmol, 0.5 g), CuI (1.16 mmol, 0.22 g), 8 mL thf and 2 mL tmeda was stirred at 0°C for 1 h and additionally stirred 3 d at RT. Volatile material was removed under vacuum and 10 mL pentane was added to the residue. After lithium iodide was filtered off, the solution was stored at +6°C and after 1 d colourless crystals were obtained. M = 740.12 g/mol. (yield 0.25 g, 58%). ^{1}H NMR (400 MHz, C$_6$D$_6$): δ = 1.29 (s, 18H, C(C$\underline{H}_3$)$_3$), 7.00 (m, 1H, H4), 7.08 (m, 1H, H7), 7.50 (m, 2H, H5/H6), 7.59 (d, 1H, H2); ^{13}C NMR (100 MHz, C$_6$D$_6$): δ = 33.86 (C($\underline{C}$H$_3$)$_3$, 56.40 ($\underline{C}$(CH$_3$)$_3$, 122.45 (C7), 124.23 (C4), 124.56 (C5), 124.74 (C6), 126.27 (C2), 140.57 (C3), 143.78 (C8), 159.44 (C1). Elemental analysis found (calc) in %: C 49.36 (51.79), H 6.07 (6.25), N 7.54 (7.55), S 15.03 (17.28). Mp.: 79°C.

[(tmeda)$_2$Li$_2${(^{t}BuN)$_2$S(SC$_4$H$_2$)$_2$S(N^{t}Bu)$_2$}] (12):

Thiophene (6.5 mmol, 0.55 g) was added slowly to a mixture of tmeda (13 mmol, 2 mL), 2 mL diethyl ether and a solution of butyllithium in hexane (1.6M, 13 mmol, 8.125 mL) and stirred for 30 min. N,N'bis(*tert.*-butyl)sulfurdiimide (13 mmol, 2.26 g) was added during 30 min and the solution was stirred for another 2 h. Crystals were obtained directly from the reaction mixture upon 3 days storage at +6°C. M = 676.52 g/mol (yield 1.76 g, 47%). ^{1}H NMR (400 MHz, C$_6$D$_6$): δ = 1.42 + 1.49 (s$_{br}$, 18H, C(CH$_3$)$_3$), 2.09 (s, 12H, Me$_2$NCH$_2$CH$_2$NMe$_2$), 3.25 (m, 4H, Me$_2$NCH$_2$CH$_2$NMe$_2$), 7.16 (d, 2H, H3/H4); ^{13}C NMR (100 MHz, C$_6$D$_6$): δ = 33.98 + 34.17 (C(CH$_3$)$_3$, 46.05 (Me$_2$NCH$_2$CH$_2$NMe$_2$), 52.93 (C(CH$_3$)$_3$), 57.88 (Me$_2$NCH$_2$CH$_2$NMe$_2$), 123.87 - 126.97 (m, C$_4$H$_2$S); ^{7}Li NMR (116.7 MHz, ext. sat. LiCl solution): δ = 1.01 (s), 1.08 (s). Elemental analysis found (calc) in %: C 55.24 (56.77), H 9.90 (10.42), N 15.43 (16.55), S 13.67 (14.61). Mp.: 94°C.

[(tmeda)$_2$Li$_2${(Me$_3$SiN)$_2$S(SC$_4$H$_2$)S(NSiMe$_3$)$_2$}] (13):

Thiophene (5.94 mmol, 0.5 g) was added slowly to a mixture of tmeda (11.89, 1.78 mL), 2 mL diethyl ether and butyllithium in hexane (1.6M, 11.89 mmol, 7.43 mL) and stirred for 2 h. N,N'bis(trimethylsilyl)sulfurdiimide (11 mmol, 1.92 g) was added during 30 min and the solution was stirred for another 2 h. The volume of the solution was reduced by a half, the reaction mixture was stored at –36°C and after 12 h colourless crystals were obtained. M = 740.42 g/mol (yield 2.44 g, 55%). ^{1}H NMR (300 MHz, C$_6$D$_6$): δ = 0.34 (s, 18H, SiMe$_3$), 2.02 (s, 12H, Me$_2$NCH$_2$CH$_2$NMe$_2$), 3.57 (t, 4H, Me$_2$NCH$_2$CH$_2$NMe$_2$), 6.98 (dd, 1H), 7.23 (dd, 1H); ^{13}C NMR (100 MHz, C$_6$D$_6$): δ = 3.16 (SiMe$_3$), 45.62 (Me$_2$NCH$_2$CH$_2$NMe$_2$), 56.33 (Me$_2$NCH$_2$CH$_2$NMe$_2$), 123.77 - 126.59 (C$_4$H$_2$S); ^{7}Li NMR (116.7 MHz, ext. sat. LiCl solution): δ = 1.10 (s). ^{29}Si-NMR (60 MHz, C$_6$D$_6$): δ = -6.91 (N(SiMe$_3$)$_2$). Elemental analysis found (calc) in %: C 44.34 (45.37), H 9.04 (9.52), N 14.07 (15.12), S 11.91 (12.97). Mp.: 75°C.

[(tmeda)$_2$Li$_2${(^{t}BuN)$_2$S(SeC$_4$H$_2$)S(N^{t}Bu)$_2$}] (14):

Selenophene (7.6 mmol, 1.0 g) in 2 mL hexane was added to a solution of tmeda (15.26 mmol, 2.29 mL) and butyllithium in hexane (1.6M, 15.2 mmol, 9.5 mL) at –78°C. The reaction mixture was allowed to warm to room temperature and stirred for 1 h. N,N'bis($tert$.-butyl)sulfurdiimide (15.26 mmol, 2.66 g) was added to the suspension at 0°C and stirred 3 h at room temperature. 10 mL hexane and 4.5 mL thf were added to solve the white precipitate. The reaction mixture was stored at +6°C and after 1 d colourless crystals were obtained. M = 724.47 g/mol. (yield 1.6 g, 29%). ^{1}H NMR (400 MHz, C$_6$D$_6$): δ = 1.44 + 1.48 (s, 18H, C(CH$_3$)$_3$), 2.10 (s, 12H, Me$_2$NCH$_2$CH$_2$NMe$_2$), 3.54 (t, 4H, Me$_2$NCH$_2$CH$_2$NMe$_2$), 7.37 (s$_{br}$, 2H, H2/H3); ^{13}C NMR (100 MHz, C$_6$D$_6$): δ = 34.01 + 34.20 (C(CH$_3$)$_3$), 46.07 (Me$_2$NCH$_2$CH$_2$NMe$_2$), 52.91 (C(CH$_3$)$_3$), 55.09 (Me$_2$NCH$_2$CH$_2$NMe$_2$), 125.50, 127.87, 128.11, 128.28 (C$_4$H$_2$Se); ^{7}Li NMR (116.7 MHz, ext. sat. LiCl solution): δ = 1.08 (s). Elemental analysis found (calc) in %: C 51.59 (53.09), H 9.17 (9.75), N 14.85 (15.48), S 8.21 (8.86). Mp.: 105°C.

[(tmeda)$_2$Li$_2${(^{t}BuN)$_2$S(SC$_4$H$_2$)$_2$S(N^{t}Bu)$_2$}] (15):

A solution of butyllithium in hexane (1.6 M, 15.6 mmol, 9.75 mL) was added dropwise to a solution of dithiophene (6.0 mmol, 1.0 g), tmeda (15.6 mmol, 1.8 g) and 15 mL thf at –40°C. The reaction mixture was allowed to warm to room temperature and refluxed gently, until the butane-formation had finished. N,N'bis($tert$.-butyl)sulfurdiimide (12 mmol, 2.09 g) was added at 0°C and the mixture was stirred overnight. After remaining solids were filtered, the volume of the solution was reduced to 10 mL. Orange crystals were grown by storage of the solution at –36°C for 7 d and used for structure determination M = 758.51 g/mol. (yield 0.86 g, 38%). ^{1}H NMR (400.13 MHz, C$_6$D$_6$): δ = 1.45 + 1.48 (s, 18H, (C(CH$_3$)$_3$), 2.06 (s, 12H, Me$_2$NCH$_2$CH$_2$NMe$_2$), 3.50 (m, 4H, Me$_2$NCH$_2$CH$_2$NMe$_2$), 6.97 + 7.06 (2d, 2H, H2/H3); ^{13}C-NMR (100 MHz, C$_6$D$_6$): δ = 33.5 + 33.93 (C(CH$_3$)$_3$), 46.03 (Me$_2$NCH$_2$CH$_2$NMe$_2$), 52.84 (C(CH$_3$)$_3$), 54.33 (Me$_2$NCH$_2$CH$_2$NMe$_2$), 122.92 (C2), 124.54 (C3), 138,76 (C4), 171.14 (C1); ^{7}Li

NMR (116.7 MHz, ext. sat. LiCl solution): δ = 1.00 (s). Elemental analysis found (calc) in %: C 55.21% (56.96%), H 8.68% (9.56%), N 13.17% (14.76%), S 16.03% (16.89%). Mp.: 87°C (dec).

[(thf)Li$_2${(SC$_4$H$_2$)S(N^{t}Bu)$_2$}]$_2$ (16):

To a solution of 3-bromothiophene (10 mmol, 1.63 g) in 15 mL hexane was dropped slowly a solution of butyllithium in hexane (1.6M, 10.56 mmol, 6.6 mL) at –40°C. 2 mL thf were added and the suspension was stirred 15 min. Supplementary 5 mL hexane were added to the suspension and heated up to room temperature. Subsequently N,N'bis(*tert*.-butyl)sulfurdiimide (10 mmol, 1.75 g) was added. The suspension was heated up instantaneous to solve the white precipitate. Storage of the solution for 10 min afforded colourless crystals. M = 684.82 g/mol. (yield 0.376 g, 22%). ^{1}H NMR (400 MHz, C$_6$D$_6$): δ = 1.27 (qi, 4H, (CH$_2$CH$_2$)$_2$O, 1.36 (s, 18H, C(CH$_3$)$_3$), 3.41 (t, 4H; (CH$_2$CH$_2$)$_2$O), 7.48 (d, 1H, C$_4$H$_2$S), 7.66 (d, 1H, C$_4$H$_2$S); ^{13}C NMR (100 MHz, C$_6$D$_6$): δ = 25.36 ((CH$_2$CH$_2$)$_2$O), 33.17 + 33.49 ((C(CH$_3$)$_3$), 54.15 + 54.55 (C(CH$_3$)$_3$), 68.41 ((CH$_2$CH$_2$)$_2$O), 125.64, 127.16, 132.33, 165.67 (C$_4$H$_2$S); ^{7}Li NMR (116.7 MHz, ext. sat. LiCl solution) RT: δ = 2.54 (s, 2Li); -30°C: δ = 2.07 (s, 1Li), 3.48 (s, 1Li). Elemental analysis found (calc) in %: C 55.54 (56.12), H 8.12 (8.24), N 8.19 (8.18), S 18.23 (18.73). Mp.: 94°C (dec).

[(thf)$_2$Li{(H$_3$CNC$_4$H$_3$)S(N^{t}Bu)$_3$}] (17):

A solution of butyllithium in hexane (1.6 M, 2.44 mmol, 1.52 mL) was added dropwise to a solution methylpyrrole (2.44 mmol, 0.2 g) in 3.5 mL thf at –78°C. The reaction mixture was allowed to warm to room temperature and finally refluxed gently for 30 min. N,N',N''tris(*tert*.-butyl)sulfurtriimide (2.44 mmol, 0.6 g) was added to the solution and stirred 12 h. All volatile material was removed under vacuum and the residue was solved in 3 mL hexane and 1 mL thf. Crystallisation at –36°C gave colourless crystals. M = 476.37 g/mol. (yield 0.76 g, 65%). ^{1}H NMR (400 MHz, C$_6$D$_6$): δ = 1.31 (qi, 4H, (CH$_2$CH$_2$)$_2$O), 1.44 (s, 18H, C(CH$_3$)$_3$), 1.50 (s, 9H, C(CH$_3$)$_3$), 3.47 (t, 4H, (CH$_2$CH$_2$)$_2$O), 3.52 (s, 3H, NCH$_3$),

6.02 (t, 1H, H2), 6.19 (t, 1H, H4), 6.83 (q, 1H, H3); ^{13}C NMR (100 MHz, C_6D_6): δ = 25.48 (($\underline{C}H_2CH_2O)_2$), 30.57 (C($\underline{C}H_3)_3$), 33.11 (C($\underline{C}H_3)_3$), 37.05 (N-$\underline{C}H_3$), 53.83 ($\underline{C}(CH_3)_3$, 54.82 ($\underline{C}(CH_3)_3$), 68.23 (($CH_2\underline{C}H_2O)_2$), 105.76 (C3), 114.91 (C4), 126.00 (C2), 128.28 (C1); ^{7}Li (155 MHz, C_6D_6): δ = 0.87. Elemental analysis found (calc) in %: C 60.69 (62.99), H 9.6 (10.36), N 12.77 (11.75), S 7.12 (6.73). Mp.: 60°C.

[(tmeda)Li{($SC_4H_3)S(N^tBu)_3$}] (18):

Thiophene (5 mmol, 0.42 g) was added slowly to a mixture of tmeda (5 mmol, 0.58 g), 2 mL diethyl ether and butyllithium in hexane (1.6M, 5 mmol, 3.125 mL) and stirred for 30 min. A solution of N,N',N''tris(*tert.*-butyl)sulfurtriimide (4.5 mmol, 1.1 g) in 2 mL hexane was added to the solution and stirred 12 h. After the small amount of precipitate was filtered off, 5 ml hexane and 1.5 mL thf were added. The solution was stored at +6°C and after 1 d colourless crystals were obtained. M = 451.34 g/mol. (yield 1.60 g, 70%). ^{1}H NMR (400 MHz, C_6D_6): δ = 1.42 (s, 18H, C($C\underline{H}_3)_3$), 1.74 (s, 9H, C($C\underline{H}_3)_3$), 1.82 (s_{br}, 4H, $Me_2NC\underline{H}_2C\underline{H}_2NMe_2$), 1.99 (s, 12H, $\underline{Me}_2NCH_2CH_2N\underline{Me}_2$), 6.80, 6.95, 7.26 ($C_4\underline{H}_3S$); ^{13}C NMR (100 MHz, C_6D_6): δ = 33.02 (C($\underline{C}H_3)_3$), 33.83 (C($\underline{C}H_3)_3$), 46.72 ($\underline{Me}_2NCH_2CH_2N\underline{Me}_2$), 51.82 ($\underline{C}(CH_3)_3$); 56.80 ($Me_2N\underline{C}H_2\underline{C}H_2NMe_2$); ^{7}Li (155 MHz, C_6D_6): δ = 0.64 (s). Elemental analysis found (calc) in %: C 55.63 (58.50), H 9.45 (10.26), N 14.11 (15.50), S 13.01 (14.20). Mp.: 141°C.

[(tmeda)Li{($SeC_4H_3)S(N^tBu)_3$}] (19):

A solution of selenophene (3.8 mmol, 0.5 g) in 4.77 mL hexane was added dropwise to a solution of tmeda (3.8 mmol, 0.45 g) and butyllithium in hexan (1.6M, 3.8 mmol, 2.4mL) at −78°C. The reaction mixture was allowed to warm to room temperature and stirred for 1 h. N,N',N''tris(*tert.*-butyl)sulfurtriimide (3.8 mmol, 0.94 g) in 1 mL hexane was added at 0°C. After 12 h stirring at room temperature, the small amount of precipitate was filtered off. Crystallisation from the resulting solution at +6°C yielded colourless crystals after 1 d. M = 499.30

g/mol. (yield 1.74 g, 91%). ^{1}H NMR (400 MHz, C_6D_6): δ = 1.45 (s, 18H, C(C$\underline{H}_3$)$_3$), 1.72 (s$_{br}$, 4H, Me$_2$NC$\underline{H}_2$C$\underline{H}_2$NMe$_2$), 1.80 (s, 9H, C(C$\underline{H}_3$)$_3$), 1.97 (s, 12H, $\underline{Me}_2$NCH$_2$CH$_2$N$\underline{Me}_2$), 7.15 (s$_{br}$, 1H, H2), 7.34 (s$_{br}$, 1H, H4), 7.66 (dd, 1H; H3); ^{13}C NMR (100 MHz, C_6D_6): δ = 33.69 (C($\underline{C}H_3$)$_3$), 33.98 (C($\underline{C}H_3$)$_3$), 46.71 ($\underline{Me}_2$NCH$_2$CH$_2$N$\underline{Me}_2$), 51.82 ($\underline{C}$(CH$_3$)$_3$), 53.17 ($\underline{C}$(CH$_3$)$_3$), 56.75 (Me$_2$N$\underline{C}H_2\underline{C}H_2NMe_2$), 127.87, 128.11, 128.35, 129.06 ($\underline{C}_4H_3$Se); ^{7}Li NMR (155.5 MHz, ext. sat. LiCl solution) δ = 0.62 (s). Elemental analysis found (calc) in %: C 49.21 (53.00), H 8.57 (9.30), N 13.62 (14.05), S 6.01 (6.43). Mp.: 134°C (dec).

[Cu{OS(N^{t}Bu)$_3$}]$_2$ (20):

17 (0.69 mmol, 0.3 g) and CuBr ((0.69 mmol, 0.1 g) in 1 mL tmeda, 8 mL thf and H_2O (0.69 mmol, 0.012 g) were refluxed for 12 h. The solvent was removed under vacuum and 10 mL pentane was added to the white precipitate. After the lithium bromide was filtered off, 1 mL tmeda was added. The solution was stored at +6°C and after 3 d colourless crystals could be obtained. M = 649.94 g/mol. (yield 0.1 g, 44%). ^{1}H-NMR (400.13 MHz, C_6D_6): δ = 1.52 (s, 18H, C(C$\underline{H}_3$)$_3$); ^{13}C-NMR (100 MHz, C_6D_6): δ = 32.64 (C($\underline{C}H_3$)$_3$), 48.37 ($\underline{C}$(CH$_3$)$_3$).

[(tmeda)$_2$Li$_2${(^{t}BuN)$_3$S(SC$_4$H$_2$)S(N^{t}Bu)$_3$}] (21a):

Thiophene (2.08 mmol, 0.18 g) was added slowly to a mixture of tmeda (4.15 mmol, 0.48 g), 2 mL diethyl ether and butyllithium in hexane (1.6M, 4.15 mmol, 2.60 mL) and stirred for 30 min. A solution of N,N',N''tris(*tert*.-butyl)sulfurtriimide (4.15 mmol, 1.0 g) in 1 mL hexane was added to the solution and stirred 3 d. The white precipitate was filtered of. The clear reaction mixture was stored at +6°C and after 1 d light yellow crystals could be obtained. M = 819.26 g/mol. (yield 1.46 g, 86%). ^{1}H-NMR (400.13 MHz, C_6D_6): δ = 1.55 (s, 18H, C(C$\underline{H}_3$)$_3$), 1.77 (s, 4H, Me$_2$NC$\underline{H}_2$C$\underline{H}_2$NMe$_2$), 1.83 (s, 9H, C(C$\underline{H}_3$)$_3$), 2.07 (s, 12H, $\underline{Me}_2$NCH$_2$CH$_2$N$\underline{Me}_2$), 6.95, 7.34 (2s, 2H, C$_4\underline{H}_2$S); ^{13}C-NMR (100 MHz, C_6D_6): δ = 33.10 + 33.92 (C($\underline{C}H_3$)$_3$), 46.58 ($\underline{Me}_2$NCH$_2$CH$_2$N$\underline{Me}_2$), 51.91 ($\underline{C}$(CH$_3$)$_3$), 53.58

($\underline{C}(CH_3)_3$), 55.03 (Me$_2$N$\underline{C}$H$_2$$\underline{C}H_2NMe_2$), 130.27, 130.69, 133.16, 148.89 ($\underline{C}_4$H$_2$S); ^{7}Li-NMR (155.5 MHz, ext. sat. LiCl solution) δ = 0.70 (s). Elemental analysis found (calc) in %: C 55.33 (58.64), H 10.42 (10.83), N 15.54 (17.10), S 10.98 (11.74). Mp.: 152°C (dec).

[(thf)$_2$Li$_2${(^{t}BuN)$_3$S(SC$_4$H$_2$)S(N^{t}Bu)$_3$}] (21b):

Thiophene (2.08 mmol, 0.18 g) was added slowly to a mixture of tmeda (4.15 mmol, 0.48 g), 2 mL diethyl ether and butyllithium in hexane (1.6M, 4.15 mmol, 2.60 mL) and stirred for 30 min. A solution of N,N',N''tris(*tert*.-butyl)sulfurtriimide (4.15 mmol, 1.0 g) in 1 mL hexane was added to the solution and stirred 3 d. The suspension was solved by addition of 4 mL thf and 1 d storage at +6°C yielded yellow crystals. M = 875.28 g/mol. (yield 1.43 g, 84%).

7   Crystallographic Section

A sample of the crystalline material was taken from the mother liquor, using standard Schlenk techniques and covered with an inert oil.[91] The crystals were prepared in the inert oil (rewashing of satellites and check for twinning under a microscope fitted with a polariser). A suitable crystal was mounted on the top of a glass fibre in a drop of inert oil and shock cooled in the N_2-stream on the diffractometer. All data were collected at low temperature.[92]

7.1   Data Collection

All data were measured using graphite monochromated MoK_α radiation (λ = 71.073 pm). Data of **2** were collected on a STOE IPDS diffractometer, the data of compounds **3** - **21b** were collected on a Bruker Smart Apex D8 diffractometer.

7.2   Procedure at the STOE IPDS diffractometer

After mounting the crystal and centring with a microscope, about 50 images were collected in a φ-range between 0° - 360° for screening the crystal quality and determining a provisional unit cell. Several parameters had to be stipulated: The φ increment, the starting and ending position concerning phi, depending on the symmetry restrictions and the desired redundancy, the detector distance, and the irradiation time to get an as high as possible $I/\sigma(I)$ ratio. The data collection was proceeded in a φ-scan mode with a 1.0° step size. Data integration was performed after determination of an exact unit cell and a sensible mosaic spread. With the obtained raw-file structure solution and refinement was processed.

7.3   Procedure at the Bruker Smart Apex CCD D8 Diffractometer

After mounting the crystal and centring by use of a video camera, a rotation frame was taken to align the beam centre relative to the CCD camera. A single run (usually 50 frames in the ω-scan mode with steps of 0.3°) was performed to check the quality of the crystal and to determine a preliminary unit cell. With the knowledge of the cell dimensions a useful strategy was planned to get a complete dataset and a redundancy of at least three for a successful empirical absorption correction. Data collection was performed depending on the strategy in the ω-scan mode with steps of 0.3°. The program SAINT-NT[93] was employed for integration of the frames. The obtained data were empirically absorption corrected applying SADABS2.[94] Structure solution and refinement was performed with the obtained *hkl*-file.

7.4   Structure solution and refinement

General: All structures were solved by Patterson or direct methods with SHELXS-97[95] and refined by full-matrix least-squares procedures on F^2, using SHELXTL-NT V5.1.[96] All non-hydrogen atoms were refined with anisotropic displacement parameters. Hydrogen atoms bonded to structure relevant atoms were located by difference Fourier synthesis and refined independently. All other hydrogen atoms of the molecules were refined using a riding model. The denoted *R*-values are defined as follows:

$$R1 = \frac{\sum \left\| F_o \right| - \left| F_c \right\|}{\sum \left| F_o \right|}.$$

$$wR2 = \sqrt{\frac{\sum w(F_o^2 - F_c^2)^2}{\sum w(F_o^2)^2}}.$$

$$w = \frac{1}{\sigma^2\left(F_o^2\right) + (g_1 P)^2 + g_2 P}; P = \frac{\left(F_o^2 + 2F_c^2\right)}{3}.$$

Relevant data of the compounds **2**-**21b** can be found in Chapter 7.5.

Disorder: Several disorders occurred in the structures. A typical phenomenon of disorder is the rotation around the N–C-axis of bonded *tert.*-butyl groups. In addition, twist disorders of coordinated thf molecules were observed. Another frequent disorder was a rotational disorder of $(CH_3)_2NCH_2$-groups in tmeda along the CH_2–CH_2 vector. For the refinement of disordered structures restraints are applied.

The SAME instruction fits 1,2 and 1,3 distances of chemically equal groups, the SADI instruction suits 1,2 distances, the SIMU instruction fits U_{ij} of neighboured atoms to be the same, and the DELU instruction equals components of the anisotropic displacement parameters in the direction of the bond to be equal with an effective standard deviation.

7.5   Structural Details

7.5.1   [thf$_6$Li$_6${μ$_6$S}{(NSiMe$_3$)$_3$S}$_2$] (2):

*Figure 36: Asymmetric unit of **2** in the solid state; anisotropic displacement parameters are depicted at the 50 % probability level.*

Compound **2** crystallises in the centrosymmetric, cubic space group Pa$\overline{3}$, with S1 and S2 at the three fold axis. S2 is additionally located at the inversion centre. The asymmetric unit contains one sixth molecule. The complete molecule is generated by inversion at the origin followed by (2, 1, 0) translation, by a C_3 axis anticlockwise at (1/3, 1/3, -1/3) with additional translation (0, 0, 1) and by a C_3 axis clockwise with following (1, -1, 0) translation.

7.5.2   [(thf)Li{H$_3$CS(NSiMe$_3$)$_2$}]$_2$ (3):

Compound **3** crystallises in the centrosymmetric, triclinic space group P$\overline{1}$. The asymmetric unit contains half the molecule. The complete molecule is generated by inversion at the origin followed by (0, 1, 0) translation.

*Figure 37: Asymmetric unit of **3** in the solid state; anisotropic displacement parameters are depicted at the 50% probability level.*

7.5.3   [(Et$_2$O)Li{H$_3$CS(NSiMe$_3$)(NC$_6$H$_{11}$)}]$_2$ (4):

*Figure 38: Asymmetric unit of **4** in the solid state; anisotropic displacement parameters are depicted at the 50% probability level.*

Compound **4** crystallises in the centrosymmetric, triclinic space group P$\bar{1}$. The asymmetric unit contains half the molecule. The complete molecule is generated by inversion at the origin followed by (1, 2, 0) translation. All carbon atoms were restrained using SIMU and DELU. The disordered Et_2O molecule coordinated to Li1 was refined using distance restraints (SAME) to split occupancies of 0.84/0.16.

7.5.4   [Cu{H$_3$CS(N^{t}Bu)$_2$}]$_2$ (5):

Compound **5** crystallises in the centrosymmetric, monoclinic space group P2$_1$/c. The H-atoms at C9 were located by difference Fourier synthesis and refined independently. The asymmetric unit contains half the molecule. The complete molecule is generated by inversion at the origin followed by (0, 2, 1) translation.

*Figure 39: Asymmetric unit of **5** in the solid state; anisotropic displacement parameters are depicted at the 50% probability level.*

7.5.5   [(Et$_2$O)Li$_2${H$_2$CS(NSiMe$_3$)(N^{t}Bu)}]$_2$ (6):

Compound **6** crystallises in the centrosymmetric, monoclinic space group C2/c. The H-atoms at C8 were located by difference Fourier synthesis and refined freely. The asymmetric unit contains half the molecule. The second moiety of the dimer is generated by inversion at the origin followed by (0, 2, 0) translation. All carbon and silicon atoms were restrained with SIMU and DELU. The disordered *tert.*-butyl- and trimethylsilyl-groups of the sulfurdiimide backbone were refined using distance restraints (SAME) to split occupancies of 0.76/0.24. The disordered Et$_2$O molecule at Li1 was refined using distance restraints (SADI) to split occupancies of 0.81/0.19.

*Figure 40: Asymmetric unit of **6** in the solid state; anisotropic displacement parameters are depicted at the 50% probability level.*

7.5.6   [(thf)Li$_2${H$_8$C$_4$S(N^{t}Bu)$_2$}]$_2$ (7):

Compound **7** crystallises in the centrosymmetric, monoclinic space group P2$_1$/n. The H-atoms at C9 were located by difference Fourier synthesis and refined freely. The asymmetric unit contains half of the molecule. The complete molecule is generated by inversion at the origin followed by (0, 1, 0) translation.

*Figure 41: Asymmetric unit of **7** in the solid state; anisotropic displacement parameters are depicted at the 50% probability level.*

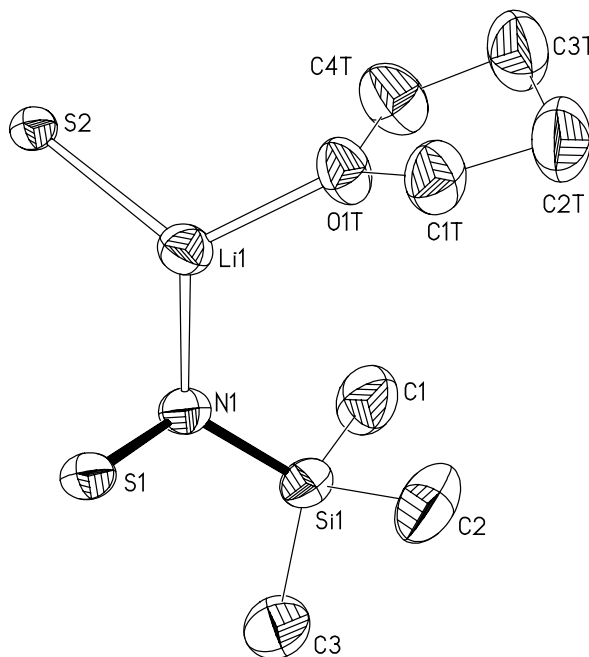### 7.5.7   [(thf)Li$_2$\{(H$_3$CNC$_4$H$_3$)S(N^{t}Bu)$_2$\}$_2$] (8):

*Figure 42: Asymmetric unit of **8** in the solid state; anisotropic displacement parameters are depicted at the 50% probability level.*

Compound **8** crystallises in the centrosymmetric, triclinic space group P$\bar{1}$. The asymmetric unit contains two independent molecules. The disordered thf molecule was refined using distance and adp restraints (SAME, SIMU, DELU) to split occupancies of 0.56/0.44. Methylpyrrole (C39 – C43) and *tert.*-butyl (C5 – C8) were refined using distance and adp restraints (SAME, SIMU, DELU).

7.5.8   [(tmeda)Li{(SC$_8$H$_5$)S(N^{t}Bu)$_2$}] (9):

*Figure 43: Asymmetric unit of **9** in the solid state; anisotropic displacement parameters are depicted at the 50% probability level.*

Compound **9** crystallises in the non centrosymmetric, orthorhombic space group Pna2$_1$. As the Flack x-parameter[97] refined to 0.43(7) the absolute structure could not be determined reliably. Neither refinement of the inverted structure, nor refinement as a racemic twin was successful. The asymmetric unit contains two molecules.

7.5.9   [Fe{(SC$_8$H$_5$)S(N^{t}Bu)$_2$}$_2$] (10):

Compound **10** crystallises in the centrosymmetric, triclinic space group P$\bar{1}$. The asymmetric unit contains the complete molecule and half a tmeda molecule.

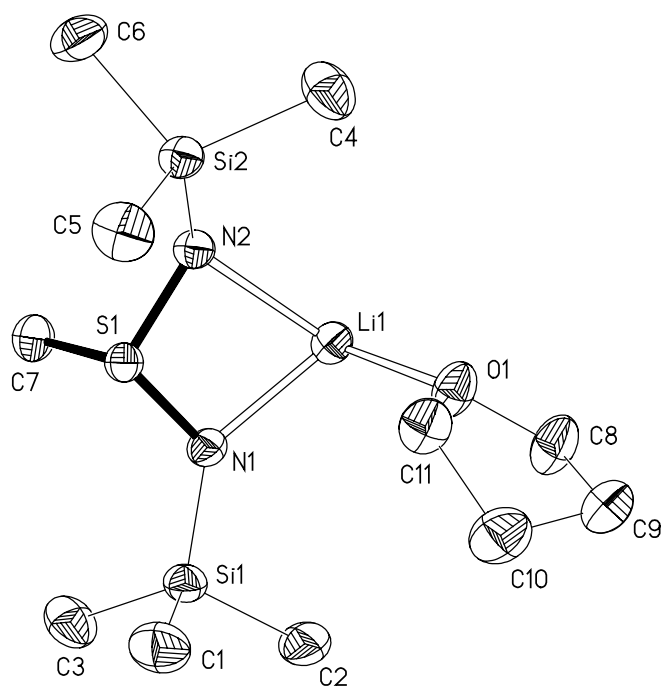The second moiety of tmeda is generated *via* inversion at the origin followed by (1, 1, 1) translation.

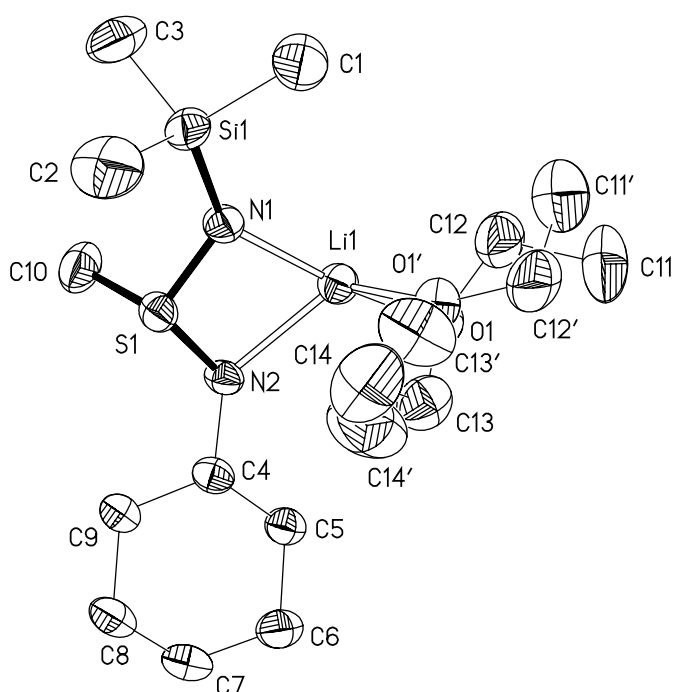*Figure 44: Asymmetric unit of **10** in the solid state; anisotropic displacement parameters are depicted at the 50% probability level.*

7.5.10 [Cu{(SC$_8$H$_5$)S(N^{t}Bu)$_2$}]$_2$ (11):

Compound **11** crystallises in the centrosymmetric, triclinic space group P$\bar{1}$. The asymmetric unit contains two half symmetry-independent molecules. The complete molecules are generated by inversion at the origin followed by (0, 1, 2) translation of the left moiety in figure 45 and (2, 2, 1) for the other respectively. All carbon atoms were restrained with SIMU and DELU. The disorder of the benzothiophene was refined using distance and adp restraints (SIMU, DELU, SADI) to split occupancies of 0.61/0.39 (S4 – C32), while those of the disordered sulfurdiimide backbone was refined to split occupancies 0.15/0.85 (S3, N3, N4). The disordered benzothiophene was refined using distance restraints (SAME) to split occupancies of 0.70/0.08/0.15/0.07 (S4 – C32). The disordered *tert.*-butyl-group was refined using distance restraints (SAME) to split occupancies of 0.8/0.2 (C18 – C20). One relatively high residual difference peak which is connected to the molecule could not be interpreted.
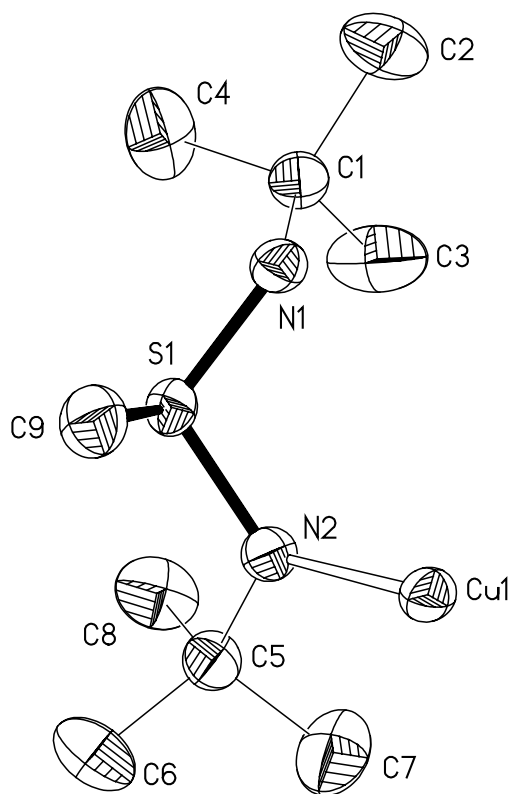
*Figure 45: Asymmetric unit of **11** in the solid state; anisotropic displacement parameters are depicted at the 50% probability level.*

7.5.11 [(tmeda)$_2$Li$_2${((^{t}BuN)$_2$S(SC$_4$H$_2$)$_2$S(N^{t}Bu)$_2$}] (12):

*Figure 46 Asymmetric unit of **12** in the solid state; anisotropic displacement parameters are depicted at the 50% probability level.*

Compound **12** crystallises in the centrosymmetric, monoclinic space group P2$_1$/n. The asymmetric unit contains the complete molecule. All disordered

molecules were refined using distance and adp restraints (SAME, SIMU, DELU). The tmeda molecules were refined to split occupancies of 0.67/0.33 (C21 – C23) and 0.88/0.12 (C30 – C32), the *tert.*-butyl group to 0.6/0.4 (C13 – C16), respectively.

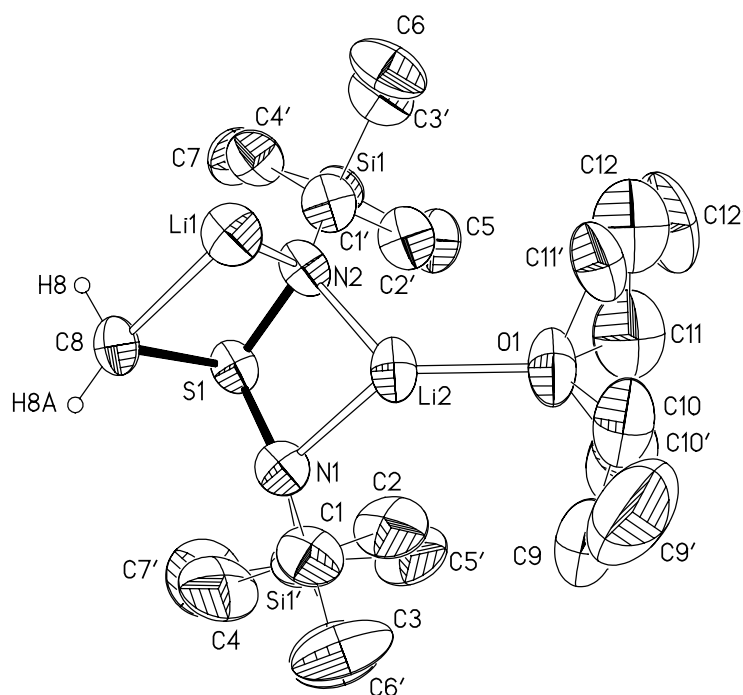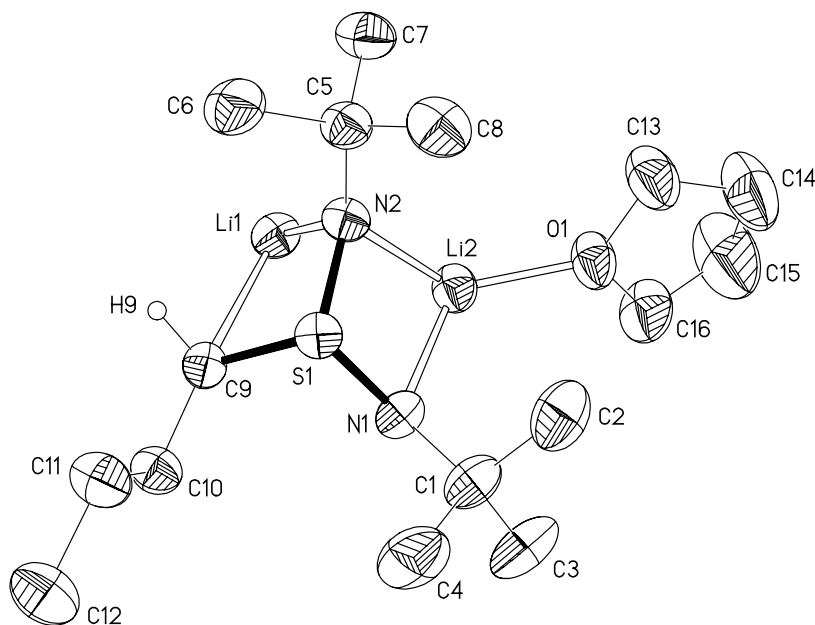### 7.5.12   [(tmeda)$_2$Li$_2${(Me$_3$SiN)$_2$S(SC$_4$H$_2$)S(NSiMe$_3$)$_2$}] (13):

*Figure 47: Asymmetric unit of **13** in the solid state; anisotropic displacement parameters are depicted at the 50% probability level.*

Compound **13** crystallises in the non-centrosymmetric, orthorhombic space group P2$_1$2$_1$2$_1$. The Flack x-parameter[97] refined to 0.11(11). Therefore the absolute structure could be determined unequivocally. The asymmetric unit contains the complete molecule. All disordered molecules were refined using distance and adp restraints (SAME, SIMU, DELU). The tmeda molecules were refined to split occupancies of 0.69/0.31 (C19 – C22) and 0.55/0.45 (C26 – C28), the trimethylsilyl-groups to 0.56/0.44.(Si3 – C9) and 0.62/0.38 (Si4 – C12), respectively. C9 had to be restrained by ISOR (*U$_{ij}$* values are restrained to lead to approximately isotropic thermal motion of the atoms).

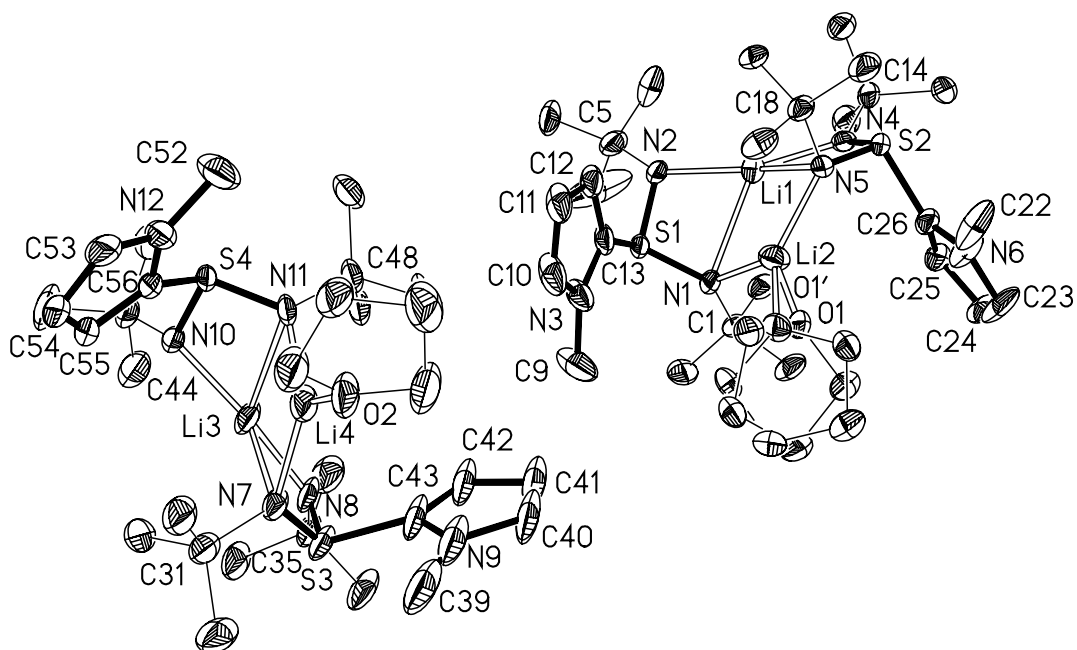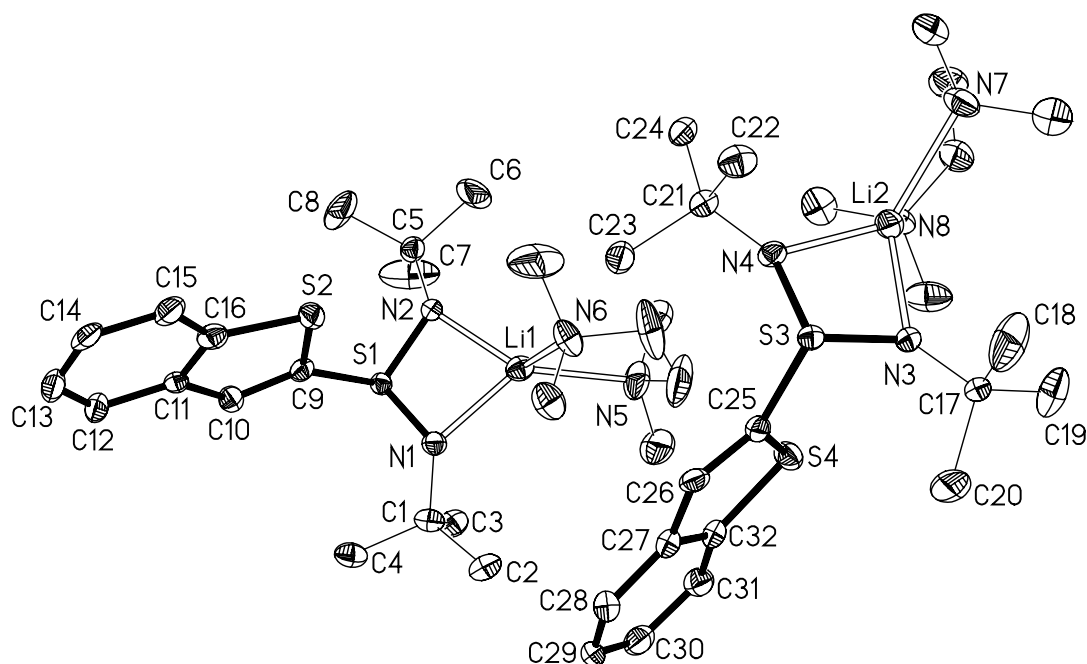### 7.5.13   [(tmeda)$_2$Li$_2$\{(^{t}BuN)$_2$S(SeC$_4$H$_2$)S(N^{t}Bu)$_2$\}] (14):

*Figure 48: Asymmetric unit of **14** in the solid state; anisotropic displacement parameters are depicted at the 50% probability level.*

Compound **14** crystallises in the centrosymmetric, monoclinic space group P2$_1$/n. The asymmetric unit contains the complete molecule. All disordered molecules were refined using distance and adp restraints (SAME, SIMU, DELU). The tmeda molecule was refined to split occupancies of 0.74/0.26 (C24 to C26), the *tert.*-butyl-groups to 0.70/0.30 (C2 to C4) and 0.64/0.36 (C14 to C16), respectively.

7.5.14   [(tmeda)$_2$Li$_2$\{(^{t}BuN)$_2$S(SC$_4$H$_2$)$_2$S(N^{t}Bu)$_2$\}] (15):

Compound **15** crystallises in the centrosymmetric, monoclinic space group P2$_1$/n. The asymmetric unit contains half the molecule. The complete molecule is generated by inversion at the origin followed by (2, 1, 0) translation.
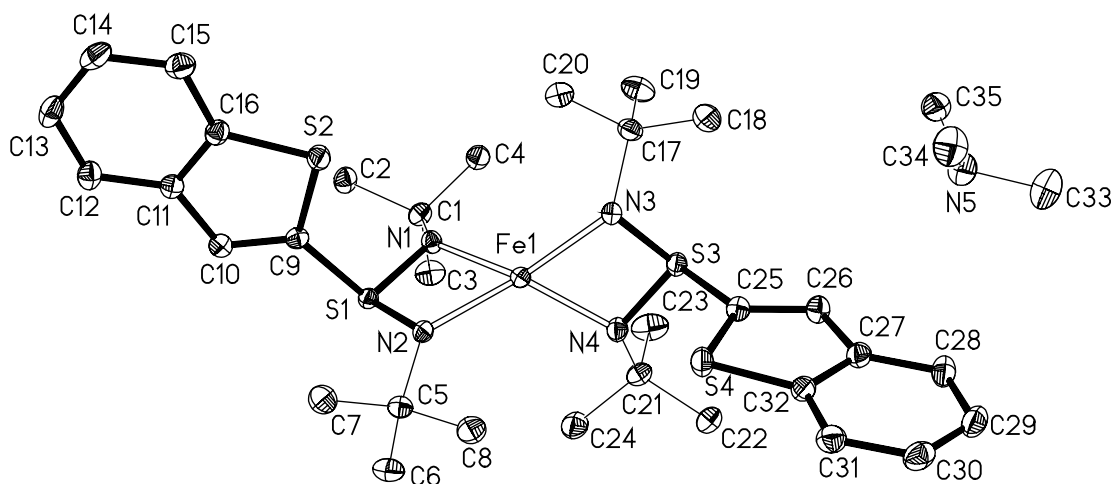
*Figure 49: Asymmetric unit of **15** in the solid state; anisotropic displacement parameters are depicted at the 50% probability level.*

7.5.15   [(thf)Li$_2${(SC$_4$H$_2$)S(N^{t}Bu)$_2$}]$_2$ (16):

*Figure 50: Asymmetric unit of **16** in the solid state; anisotropic displacement parameters are depicted at the 50% probability level.*

Compound **16** crystallises in the centrosymmetric, monoclinic space group P2$_1$/c. The asymmetric unit contains the complete molecule.

7.5.16 [(thf)$_2$Li{(H$_3$CNC$_4$H$_3$)S(N^{t}Bu)$_3$}] (17):

*Figure 51: Asymmetric unit of **17** in the solid state; anisotropic displacement parameters are depicted at the 50% probability level.*

Compound **17** crystallises in the centrosymmetric, monoclinic space group P2$_1$/n. The asymmetric unit contains the complete molecule.

7.5.17 [(tmeda)Li{(SC$_4$H$_3$)S(N^{t}Bu)$_3$}] (18):

Compound **18** crystallises in the centrosymmetric, monoclinic space group P2$_1$/n. The asymmetric unit contains the complete molecule. The disordered tmeda molecule was refined using distance and adp restraints (SAME, SIMU, DELU) to split occupancies of 0.51/0.49 (C20 – C22).
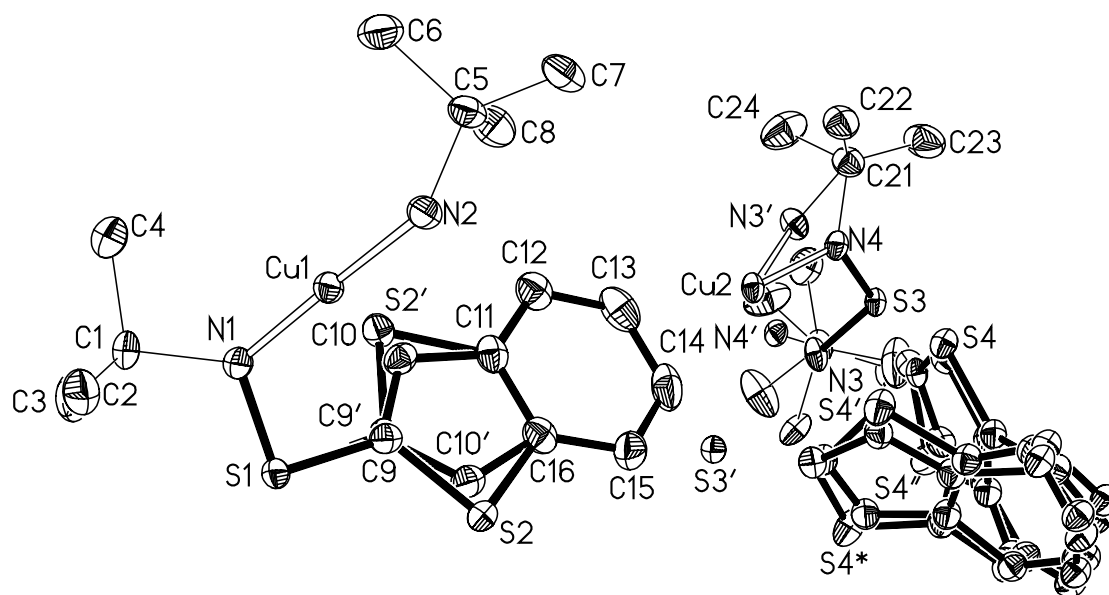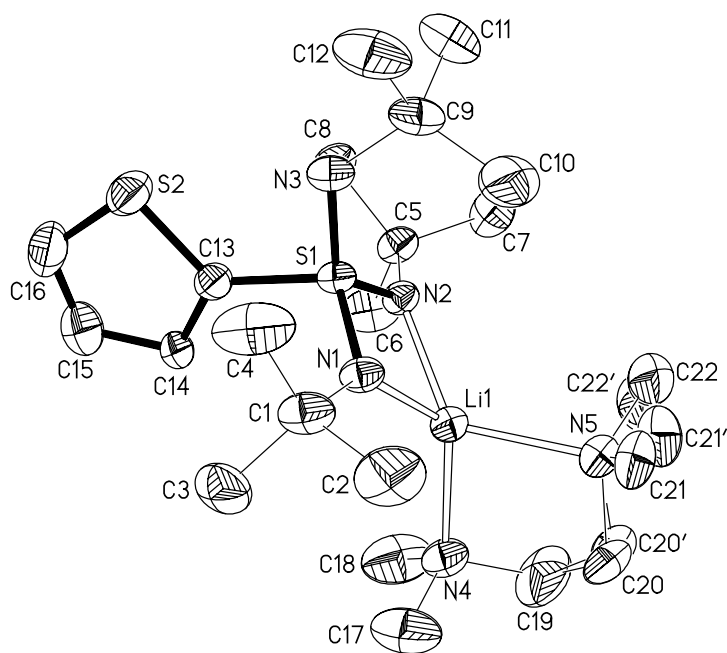
*Figure 52: Asymmetric unit of **18** in the solid state; anisotropic displacement parameters are depicted at the 50% probability level.*

7.5.18   [(tmeda)Li{(SeC$_4$H$_3$)S(N^{t}Bu)$_3$}] (19):
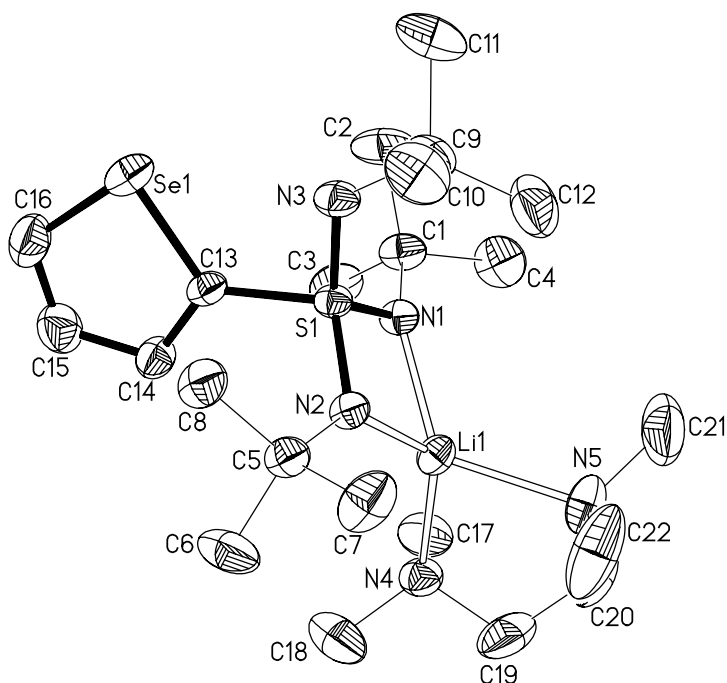
*Figure 53: Asymmetric unit of **19** in the solid state; anisotropic displacement parameters are depicted at the 50% probability level.*

Compound **19** crystallises in the centrosymmetric, monoclinic space group $P2_1/n$. The asymmetric unit contains the complete molecule.
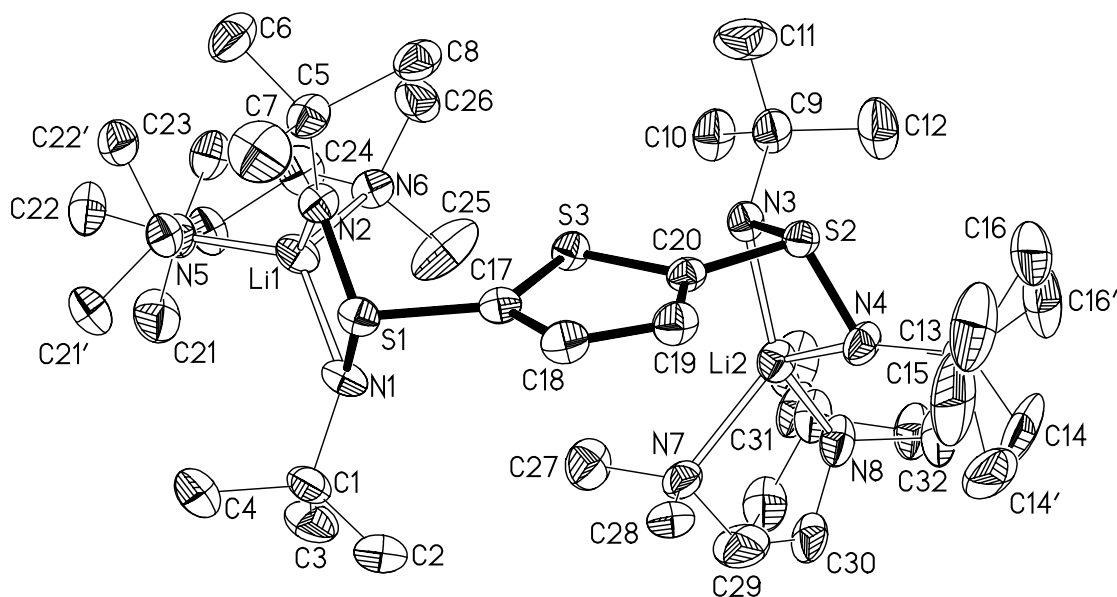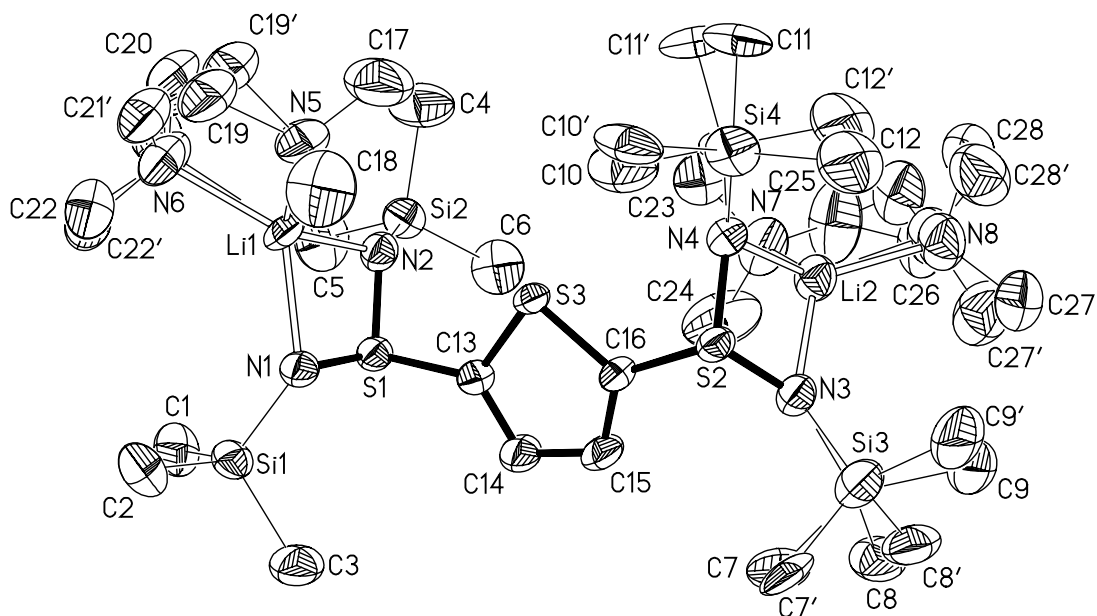
7.5.19   [Cu{OS(N^{t}Bu)$_3$}]$_2$ (20):
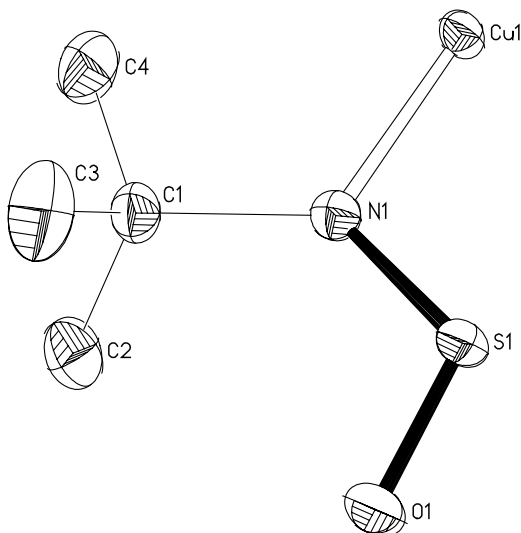
*Figure 54: Asymmetric unit of **20** in the solid state; anisotropic displacement parameters are depicted at the 50% probability level.*

Compound **20** crystallises in the centrosymmetric, trigonal space group $P\overline{3}1c$. The asymmetric unit contains one sixth of the complete molecule. The other moieties are generated by clockwise rotation along a C_3 axis at (0, 0, z) followed by (1, 0, 0) translation, by an anticlockwise rotation along a C_3 axis at (0,0,z) followed by (1, 1, 0) translation and by a C_2 axis at (x, -x, ¼) followed by (1, 1, 0) translation, respectively.

Side occupation factors of Cu have been refined freely to 0.333, therefore two copper cations are present in the structure. Thus in [Cu{OS(N^{t}Bu)$_3$}]$_2$ (**20**) each copper position is occupied only by two thirds. No electron density in the environment of the nitrogen atom is detectable, thus no hydrogen atom could be located there.

7.5.20   [(tmeda)$_2$Li$_2${(^{t}BuN)$_3$S(SC$_4$H$_2$)S(N^{t}Bu)$_3$}] (21a):

Compound **21a** crystallises in the centrosymmetric, monoclinic space group $P2_1/c$. The asymmetric unit contains the complete molecule. All disordered

groups were refined using distance and adp restraints (SAME, SIMU, DELU). The tmeda molecule was refined to split occupancies of 0.67/0.33 (C32 – C34), the *tert*.-butyl-groups to 0.85/0.15 (C5 – C8) and 0.69/0.31 (C13 – C16), respectively.
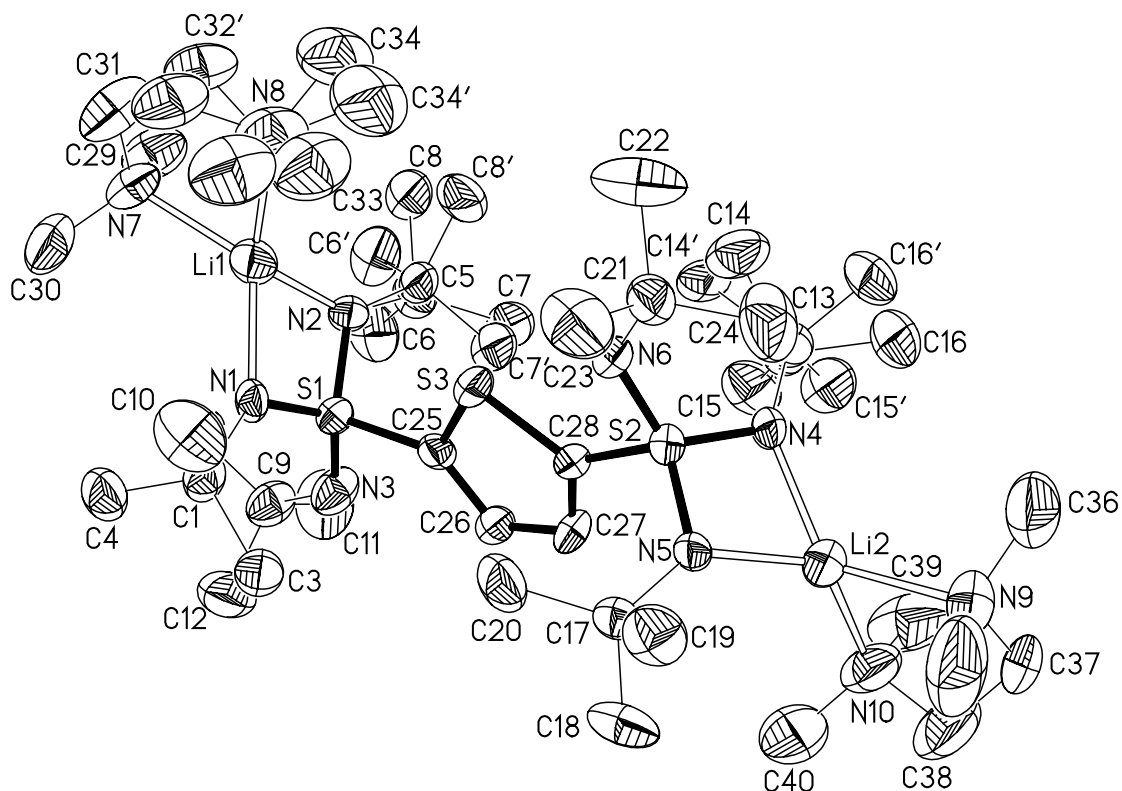
*Figure 55: Asymmetric unit of **21a** in the solid state; anisotropic displacement parameters are depicted at the 50% probability level.*

7.5.21 [(thf)$_2$Li$_2${(^{t}BuN)$_3$S(SC$_4$H$_2$)S(N^{t}Bu)$_3$}] (21b):

Compound **21b** crystallises in the centrosymmetric, monoclinic space group P2$_1$/c. The asymmetric unit contains the complete molecule. All disordered units were refined using distance and adp restraints (SAME, SIMU, DELU). The thf molecule was refined to split occupancies of 0.51/0.32/0.17 (O4 – C44), the *tert*.-butyl-groups to 0.51/0.49 (C2 – C4), 0.67/0.33 (C14 – C16) and 0.78/0.22 (C22 – C24), respectively.

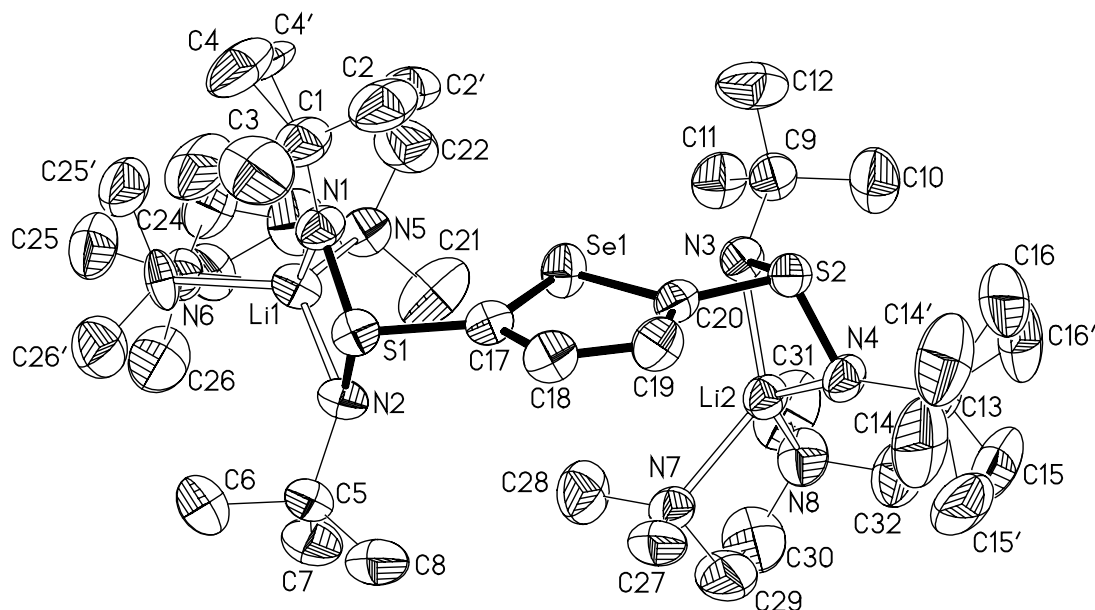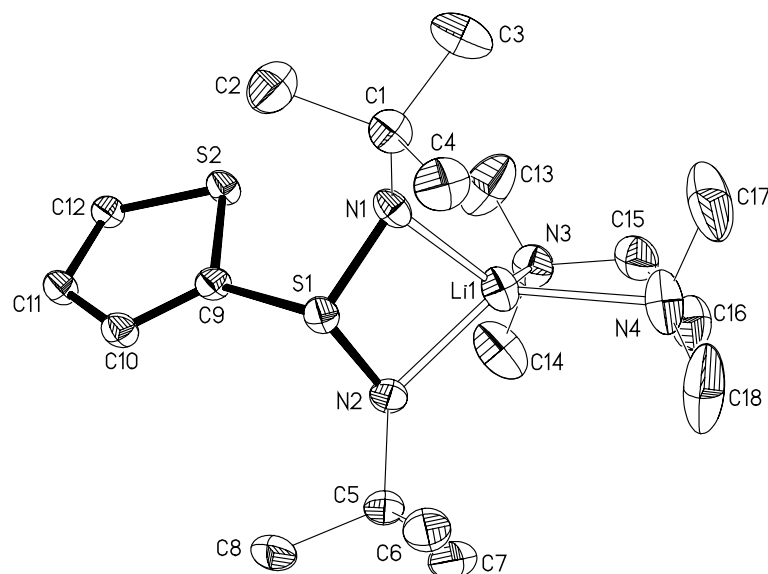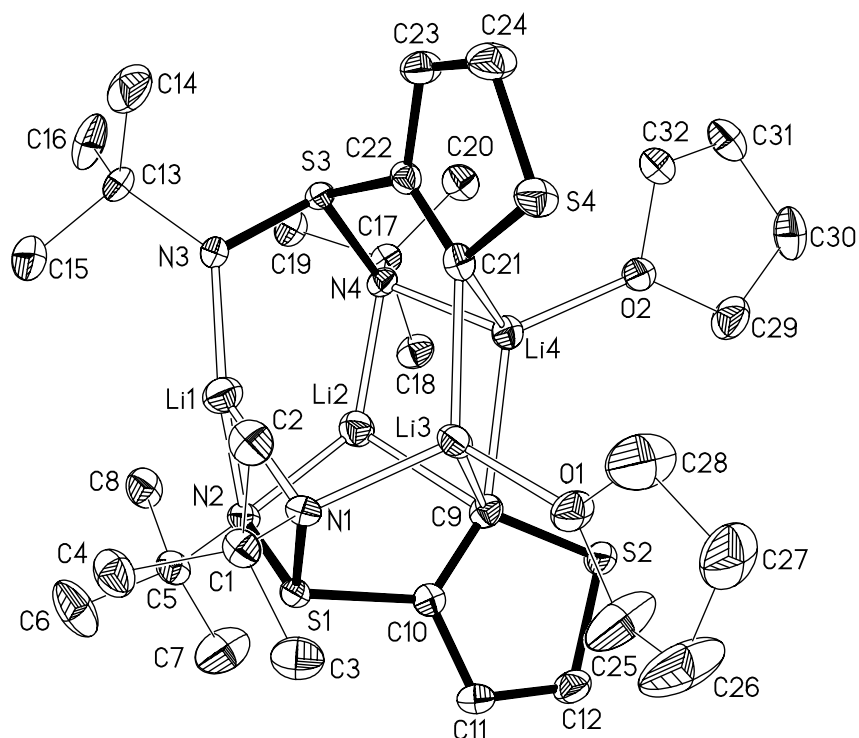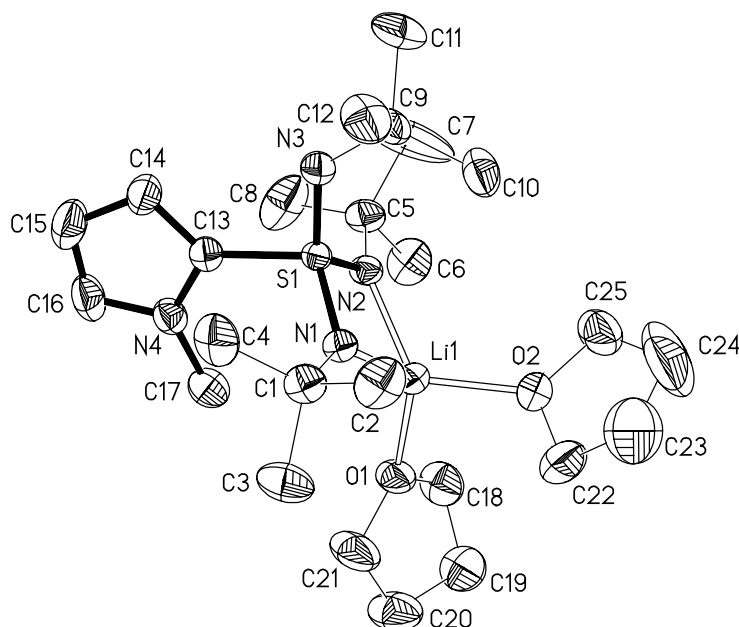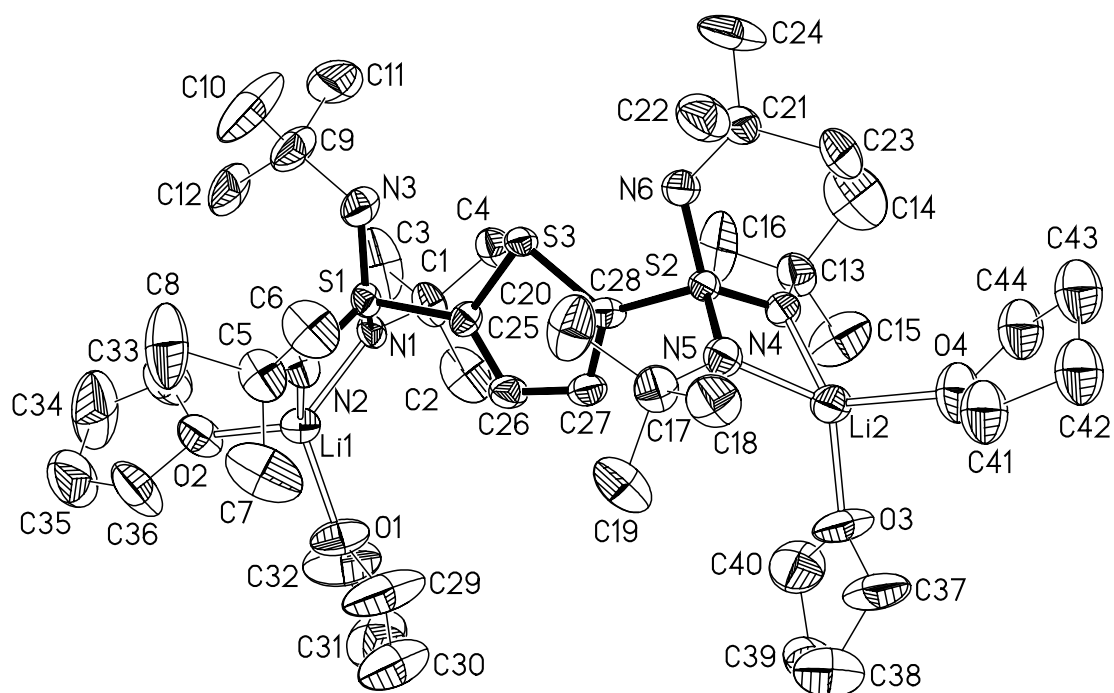*Figure 56: Asymmetric unit of **21b** in the solid state; anisotropic displacement parameters are depicted at the 50% probability level.*

7.6   Crystallographic Data

*Table 23: Crystal data and structure refinements for **2**, **3** and **4***

compound number	**2**	**3**	**4**
formula	$C_{42}H_{102}Li_6N_6O_6S_3Si_6$	$C_{11}H_{29}LiN_2OSSi_2$	$C_{14}H_{33}LiN_2OSSi$
M_r	1093.66	300.54	312.51
T [K]	173(2)	173(2)	173(2)
crystal size [mm]	0.5 x 0.4 x 0.3	0.3 x 0.3 x 0.2	0.3 x 0.2 x 0.2
space group	$Pa\bar{3}$	$P\bar{1}$	$P\bar{1}$
a [pm]	1909.5(2)	1000.46(2)	975.93(2)
b [pm]	1909.5(2)	1052.83(2)	1029.79(2)
c [pm]	1909.5(2)	1058.69(2)	1126.29(2)
α [°]	90	62.5120(10)	81.2780(10)
β [°]	90	73.1210(10)	73.4950(10)
γ [°]	90	66.7390(10)	61.9330(10)
V [nm^3], Z	6.9621(14), 4	0.90081(3), 2	0.95744(3), 2
ρ_{calcd} [Mgm^{-3}]	1.043	1.108	1.084
μ [mm^{-1}]	0.249	0.304	0.229
F(000)	2376	328	344
Θ range [°]	3.02 – 22.62	2.19 – 26.62	1.89 – 26.43
no. of refl. measd.	8934	14006	9786
no. of unique refl.	1539	3733	3914
R(int)	0.1613	0.0388	0.0193
data/restraints/ param.	1539 / 0 / 108	3733 / 0 / 170	3914 / 131 / 232
GooF on F^2	1.125	1.087	1.027
$R1$ [$I>2\sigma(I)$]	0.0508	0.0428	0.0419
$wR2$ (all data)	0.1383	0.1111	0.1138
$g1/g2$	0.06690 / 1.57280	0.06260 / 0.30730	0.07280 / 0.15990
largest diff. peak/hole [e nm^{-3}]	394 and −343	554 and -345	379 and -134

*Table 24: Crystal data and structure refinements for **5**, **6** and **7***

compound number	5	6	7
formula	$C_{18}H_{42}Cu_2N_4S_2$	$C_{24}H_{60}Li_4N_4O_2S_2Si_2$	$C_{32}H_{68}Li_4N_4O_2S_2$
M_r	505.76	584.82	632.78
T [K]	193(2)	173(2)	173(2)
crystal size [mm]	0.4 x 0.4 x 0.3	0.4 x 0.3 x 0.3	0.3 x 0.3 x 0.2
space group	$P2_1/c$	$C2/c$	$P2_1/n$
a [pm]	914.35(11)	2381.34(5)	1114.81(12)
b [pm]	1469.20(18)	992.41(2)	1608.21(17)
c [pm]	1016.38(12)	1741.51(4)	1200.07(13)
α [°]	90	90	90
β [°]	113.515(2)	111.306(2)	108.072(2)
γ [°]	90	90	90
V [nm^3], Z	1.25199(45), 2	3.83436(14), 8	2.04540(63), 4
ρ_{calcd} [Mgm^{-3}]	1.342	1.013	1.027
μ [mm^{-1}]	1.875	0.224	0.159
$F(000)$	536	1280	696
Θ range [°]	2.43 – 26.44	1.84 – 24.97	2.18 – 25.03
no. of refl. measd.	7075	21110	19882
no. of unique refl.	2577	3369	3616
R(int)	0.0243	0.0483	0.0293
data/restraints/ param.	2577 / 0 / 125	3369 / 232 / 302	3616 / 0 / 209
GooF on F^2	1.064	1.283	1.193
$R1$ [$I>2\sigma(I)$]	0.0312	0.0765	0.0610
$wR2$ (all data)	0.0793	0.1796	0.1520
$g1/g2$	0.04020 / 0.46340	0.07170 / 5.04360	0.06480 / 1.18460
largest diff. peak/hole [e nm^{-3}]	353 and –301	554 and -232	462 and -281

Table 25: Crystal data and structure refinements for 8, 9 and 10

compound number	8	9	10
formula	$C_{30}H_{56}Li_2N_6OS_2$	$C_{22}H_{39}LiN_4S_2$	$C_{35}H_{54}FeN_5S_4$
M_r	594.81	430.63	728.92
T [K]	100(2)	193(2)	100(2)
crystal size [mm]	0.35 x 0.35 x 0.25	0.35 x 0.3 x 0.2	0.4 x 0.4 x 0.3
space group	$P\bar{1}$	$Pna2_1$	$P\bar{1}$
a [pm]	985.31(8)	2521.08(18)	892.67(4)
b [pm]	1624.57(13)	1117.17(8)	1187.90(5)
c [pm]	2165.46(17)	1806.65(13)	1883.36(8)
α [°]	89.9240(10)	90	74.9800(10)
β [°]	88.744(2)	90	82.7660(10)
γ [°]	85.2960(10)	90	89.4980(10)
V [nm^3], Z	3.4538(5), 4	5.0884(6), 8	1.91294(14), 2
ρ_{calcd} [Mgm^{-3}]	1.144	1.124	1.265
μ [mm^{-1}]	0.185	0.224	0.643
$F(000)$	1296	1872	778
Θ range [°]	0.94 – 25.02	1.97 – 25.03	1.13 – 26.38
no. of refl. measd.	49882	53894	30550
no. of unique refl.	12183	8967	7774
R(int)	0.0719	0.0550	0.0255
data/restraints/param.	12183 / 125 / 813	8967 / 1 / 543	7774 / 0 / 420
GooF on F^2	1.038	1.099	1.056
$R1$ [$I>2\sigma(I)$]	0.0715	0.0582	0.0291
$wR2$ (all data)	0.1786	0.1474	0.0768
Flack x parameter[97]	–	0.43(7)	–
$g1/g2$	0.06000 / 5.90330	0.09270 / 2.67300	0.04090 / 0.72490
largest diff. peak/hole [e nm^{-3}]	698 and -662	949 and -433	424 and -188

*Table 26: Crystal data and structure refinements for **11**, **12** and **13***

compound number	11	12	13
formula	$C_{32}H_{46}Cu_2N_4S_4$	$C_{32}H_{70}Li_2N_8S_3$	$C_{28}H_{70}Li_2N_8S_3Si_4$
M_r	742.05	677.02	741.34
T [K]	173(2)	100(2)	193(2)
crystal size [mm]	0.3 x 0.3 x 0.2	0.4 x 0.4 x 0.3	0.4 x 0.3 x 0.2
space group	$P\bar{1}$	$P2_1/n$	$P2_12_12_1$
a [pm]	969.75(10)	1690.34(9)	977.95(7)
b [pm]	983.06(10)	976.88(5)	1526.89(11)
c [pm]	1869.19(19)	2632.89(13)	3175.9(2)
α [°]	87.163(2)	90	90
β [°]	88.847(2)	104.4130(10)	90
γ [°]	81.422(2)	90	90
V [nm^3], Z	1.7597(3), 2	4.2108(4), 4	4.7423(6), 4
ρ_{calcd} [Mgm^{-3}]	1.400	1.068	1.038
μ [mm^{-1}]	1.473	0.206	0.284
$F(000)$	776	1488	1616
Θ range [°]	2.10 – 26.43	1.60 – 25.03	1.28 – 25.03
no. of refl. measd.	27977	45293	38852
no. of unique refl.	7199	7442	8385
R(int)	0.0205	0.0268	0.0427
data/restraints/ param.	7199 / 1210 / 716	7442 / 378 / 544	8385 / 470 / 593
GooF on F^2	1.037	1.043	1.338
$R1$ [$I>2\sigma(I)$]	0.0401	0.0390	0.0616
$wR2$ (all data)	0.1092	0.1078	0.1385
Flack x parameter[97]	–	–	0.11(11)
$g1/g2$	0.06150 / 2.93020	0.05930 / 1.94790	0.05170 / 2.27720
largest diff. peak/hole [e nm^{-3}]	3058 and -512	484 and –507	370 and -307

*Table 27: Crystal data and structure refinements for **14**, **15** and **16***

compound number	**14**	**15**	**16**
formula	$C_{32}H_{70}Li_2N_8S_2Se$	$C_{18}H_{36}LiN_4S_2$	$C_{32}H_{56}Li_4N_4O_2S_4$
M_r	723.92	379.57	684.81
T [K]	173(2)	173(2)	100(2)
crystal size [mm]	0.4 x 0.3 x 0.2	0.3 x 0.3 x 0.2	0.3 x 0.2 x 0.2
space group	$P2_1/n$	$P2_1/n$	$P2_1/c$
a [pm]	1716.29(14)	931.29(12)	1394.75(6)
b [pm]	979.61(8)	1580.4(2)	1828.08(8)
c [pm]	2646.8(2)	1598.9(2)	1511.86(7)
α [°]	90	90	90
β [°]	103.2900(10)	96.310(2)	91.7140(10)
γ [°]	90	90	90
V [nm³], Z	4.3308(6), 4	2.3390(5), 4	3.8531(3), 4
ρ_{calcd} [Mgm⁻³]	1.110	1.078	1.181
μ [mm⁻¹]	0.993	0.235	0.279
$F(000)$	1560	828	1472
Θ range [°]	1.58 – 26.46	1.82 – 26.41	1.75 – 25.03
no. of refl. measd.	46516	24339	41531
no. of unique refl.	8883	4770	6796
R(int)	0.0323	0.0533	0.0635
data/restraints/ param.	8883 / 162 / 527	4770 / 0 / 236	6796 / 0 / 427
GooF on F^2	1.026	1.077	1.017
$R1$ [$I > 2\sigma(I)$]	0.0399	0.0528	0.0425
$wR2$ (all data)	0.1083	0.1455	0.1055
$g1/g2$	0.06210 / 1.39320	0.07780 / 1.56180	0.04830 / 2.75000
largest diff. peak/hole [e nm⁻³]	854 and -455	874 and -544	542 and -297

*Table 28: Crystal data and structure refinements for **17**, **18** and **19***

compound number	**17**	**18**	**19**
formula	$C_{25}H_{49}LiN_4O_2S$	$C_{22}H_{46}LiN_5S_2$	$C_{22}H_{46}LiN_5SSe$
M_r	476.68	451.70	498.60
T [K]	173(2)	173(2)	173(2)
crystal size [mm]	0.3 x 0.3 x 0.25	0.5 x 0.3 x 0.2	0.4 x 0.4 x 0.4
space group	$P2_1/n$	$P2_1/n$	$P2_1/n$
a [pm]	1012.92(9)	995.32(8)	997.01(9)
b [pm]	1601.06(14)	1591.64(13)	1606.39(15)
c [pm]	1796.99(16)	1779.67(14)	1773.06(17)
α [°]	90	90	90
β [°]	91.5070(10)	91.5970(10)	92.610(2)°.
γ [°]	90	90	90
V [nm^3], Z	2.9133(4), 4	2.8182(4), 4	2.8368(5), 4
ρ_{calcd} [Mgm^{-3}]	1.087	1.065	1.167
μ [mm^{-1}]	0.137	0.205	1.413
F(000)	1048	992	1064
Θ range [°]	1.70 – 25.07	1.72 – 25.03	1.71 – 26.40
no. of refl. measd.	26553	28618	30455
no. of unique refl.	5128	4973	5796
R(int)	0.0406	0.0309	0.0261
data/restraints/ param.	5128 / 0 / 308	4973 / 126 / 323	5796 / 0 / 284
GooF on F^2	1.335	1.221	1.046
R1 [$I>2\sigma(I)$]	0.0901	0.0627	0.0336
wR2 (all data)	0.1796	0.1468	0.0930
g1/g2	0.02640 / 5.243299	0.04410 / 2.91070	0.05270 / 1.14280
largest diff. peak/hole [e nm^{-3}]	418 and -301	365 and -327	427 and -266

*Table 29: Crystal data and structure refinements for **20**, **21a** and **21b***

compound number	**20**	**21a**	**21b**
formula	$C_{24}H_{54}Cu_2N_6O_2S_2$	$C_{40}H_{88}Li_2N_{10}S_3$	$C_{44}H_{88}Li_2N_6O_4S_3$
M_r	649.93	819.26	875.26
T [K]	100(2)	173(2)	173(2)
crystal size [mm]	0.2 x 0.2 x 0.15	0.3 x 0.2 x 0.2	0.3 x 0.2 x 0.2
space group	$P\bar{3}1c$	$P2_1/c$	$P2_1/c$
a [pm]	957.46(3)	1060.86(10)	1092.68(8)
b [pm]	957.46(3)	1787.60(16)	1269.00(14)
c [pm]	2041.53(11)	2727.6(3)	2755.8(2)
α [°]	90	90	90
β [°]	90	92.533(2)	94.869(2)
γ [°]	120	90	90
V [nm^3], Z	1.62079(11), 2	5.1676(8), 4	5307.6(7)
ρ_{calcd} [Mgm^{-3}]	1.332	1.053	1.095
μ [mm^{-1}]	1.470	0.179	0.182
$F(000)$	692	1808	1920
Θ range [°]	2.00 – 26.36	1.36 – 23.26	1.37 – 23.82
no. of refl. measd.	18357	49694	40135
no. of unique refl.	1110	7400	8147
R(int)	0.0220	0.1802	0.0711
data/restraints/ param.	1110 / 0 / 60	7400 / 396 / 641	8147 / 712 / 736
GooF on F^2	1.163	0.792	1.305
R1 [$I>2\sigma(I)$]	0.0383	0.0540	0.1225
wR2 (all data)	0.1026	0.1171	0.2619
g1/g2	0.05270 / 1.71360	0.04210 / 0.0	0.07650 / 16.55090
largest diff. peak/hole [e nm^{-3}]	1047 and -206	288 and -175	670 and -500

8   References

[1] F. A. Cotton, G. Wilkinson, *Advanced Inorganic Chemistry*; Wiley, New York, 1999.

[2] I. Langmuir, *J. Am. Chem. Soc.* **1919**, *41*, 868 and 1543.

[3] a) G. M. Aspinall, M. C. Copsey, A. P. Leedham, C. A. Russell, *Coord. Chem. Rev.* **2002**, *227*, 217. b) J. K. Brask, T. Chivers, *Angew. Chem.* **2001***, 113,* 4082*; Angew. Chem. Int. Ed. Eng.* **2001**.

[4] a) $B(NR)_3{}^{3-}$: U. Braun, T. Habereder, H. Noth, H. Piotrowski, M. Warchhold, *Eur. J. Inorg. Chem.* **2002**, *5*, 1132. b) $C(NR)_3{}^{2-}$: T. Chivers, M. Parvez, G. Schatte, *J. Organomet. Chem.* **1998**, *550*, 213. c) $Si(NR)_3{}^{2-}$: M. Veith, R. Lisowsky, *Angew. Chem.* **1988***, 102,* 1124*; Angew. Chem. Int. Ed. Engl.* **1988**, 27, 1087. d) $Si(NR)_4{}^{4-}$: J. K. Brask, T. Chivers, M. Parvez, *Inorg. Chem.* **2000**, *39*, 2505. e) $P(NR)_3{}^{3-}$: E. Niecke, M. Frost, M. Nieger, V. v. d. Gönna, A. Ruban, W. W. Schoeller, *Angew. Chem.* **1994***, 106,* 2170; *Angew. Chem. Int. Ed. Engl.* **1994**, *33*, 2111. f) $P(NR)_4{}^{3-}$: P. R. Raithby, C. A. Russell, A. Steiner, D. S. Wright, *Angew. Chem.* **1997***, 109,* 676; *Angew. Chem. Int. Ed. Engl.* **1997**, *36*, 649. g) $As(NR)_3{}^{3-}$: M. A. Beswick, S. J. Kidd, M. A. Paver, P. R. Raithby, A. Steiner, D. S. Wright, *Inorg. Chem. Comm.* **1999**, *2*, 612. h) L. T. Burke, J. C. Jeffery, A. P. Leedham, C. A. Russell, *J. Chem. Soc. Dalton Trans*. **2001**, 423. i) $Sb(NR)_3{}^{3-}$: A. J. Edwards, M. A. Paver, P. R. Raithby, M.-A. Rennie, C. A. Russell, D. S. Wright, *Angew. Chem.* **1994***, 106,* 1334; *Angew. Chem. Int. Ed. Engl.* **1994**, *33*, 1277. j) $S(NR)_3{}^{2-}$: R. Fleischer, S. Freitag, F. Pauer, D. Stalke, *Angew. Chem.* **1996***, 108,* 208; *Angew. Chem. Int. Ed. Engl.* **1996**, *35*, 204. k) $S(NR)_4{}^{2-}$: R. Fleischer, A. Rothenberger, D. Stalke, *Angew. Chem.* **1997***, 109,* 1140; *Angew. Chem. Int. Ed. Engl.* **1997**, *36*, 1105. l) $Se(NR)_3{}^{2-}$: T. Chivers, M. Parvez, G. Schatte, *Inorg. Chem.* **1996**, *35*, 4094. m) $Te(NR)_3{}^{2-}$: T. Chivers, X. Gao, M. Parvez, *Angew. Chem.* **1995***, 107,* 2756; *Angew. Chem. Int. Ed. Engl.* **1995**, *34*, 2549.

[5] a) F. Pauer, D. Stalke, *J. Organomet. Chem.* **1991**, *418*, 127. b) F. Pauer, J. Rocha, D. Stalke, *J. Chem. Soc. Chem. Commun.* **1991**, 1477. c) F. T. Edelmann, F. Knösel, F. Pauer, D. Stalke, W. Bauer, *J. Organomet. Chem.* **1992**, *438*, 1. d) S. Freitag, W. Kolodziejski, F. Pauer, D. Stalke, *J. Chem. Soc. Dalton Trans.* **1993**, 3479.

[6] a) B. Walfort, R. Bertermann, D. Stalke, *Chem. Eur. J.* **2001**, *7*, 1424. b) D. Hänssgen, H. Hupfer, M. Nieger, M. Pfendtner, R. Steffens, *Z. Anorg. Allg. Chem.* **2001**, *627*, 17.

[7] a) B. Walfort, D. Stalke, *Angew. Chem.* **2001**, *113*, 3965; *Angew. Chem. Int. Ed. Engl.* **2001**, *40*, 3846. b) D. Leusser, B. Walfort, D. Stalke, *Angew. Chem.* **2002**, *114*, 2183; *Angew. Chem. Int. Ed. Engl.* **2002**, *41*, *2079.*

[8] M. M. Labes, P. Love, L. F. Nichols, *Chem. Rev.* **1979**, *79*, 1.

[9] F. P. Burt, *J. Chem. Soc.* **1910**, 1171.

[10] M. Goehring, G. Weis, *Angew. Chem.* **1956**, *68*, 678.

[11] *Gmelin Handbook of Chemistry, Sulfur Nitrogen Compounds, 2*, Springer, Berlin 1985.

[12] a) R. Fleischer, D. Stalke, *Coord. Chem. Rev.* **1998**, *176*, 431. b) D. Stalke, *Proc. Indian Acad. Sci.* **2000**, *112*, 155.

[13] a) K. B. Sharpless, T. Hori, L. K. Truesdale, C. O. Dietrich, *J. Am. Chem. Soc.* **1976**, *98*, 269. b) K. B. Sharpless, T. Hori, *J. Org. Chem.* **1976**, *98*, 269. c) I. Dyong, H. Friege, T. zu Höhne, *Chem. Ber.* **1982**, *115*, 256. d) R. Bussas, G.. Kresze, H. Münsterer, A. Schwöbel, *Sulfur Rep.* **1983**, *2*, 215. e) G. Kresze, H. Münsterer, *J. Org. Chem.* **1983**, *48*, 3561.

[14] K. B. Sharpless, T. Hori, *J. Org. Chem.* **1976**, *41*, 176.

[15] a) G. Kresze, *Angew. Chem.* **1972**, *84*, 1154; *Angew. Chem. Int. Ed. Engl.* **1972**, *11*, 1106. b) N. Schönberger, G. Kresze, *Liebigs Ann. Chem.* **1975**, 1725. c) R. Bussas, G. Kresze, *Liebigs Ann. Chem.* **1980**, 629.

[16] a) H. W. Roesky, W. Schmieder, W. S. Sheldrick, *J. Chem. Soc. Chem. Commun.* **1981**, 1013. b) H. W. Roesky, W. Schmieder, W. Isenberg, W. S. Sheldrick, G. M. Sheldrick, *Chem. Ber.* **1982**, *115*, 2714.

[17] A. Gieren, P. Narayanan, *Acta Crystallogr.* **1975**, *A31*, 120.

[18] R. Fleischer, S. Freitag, D. Stalke, *J. Chem. Soc. Dalton Trans.* **1998**, 193.

[19] J. K. Brask, T. Chivers, B. McGarvey, G. Schatte, R. Sung, R. T. Boere, *Inorg. Chem.* **1998**, *37*, 4633.

[20] a) O. Glemser, J. Wegener, *Angew. Chem.* **1970**, *82*, 324; *Angew. Chem. Int. Ed. Engl.* **1970**, *9*, 309. b) O. Glemser, S. Pohl, F. M. Tesky, R. Mews, *Angew. Chem.* **1977**, *89*, 829*; Angew. Chem. Int. Ed. Engl.* **1977**, *16*, 789.

[21] W. Lidy, W. Sundermeyer, W. Z. Verbeek, *Z. Anorg. Allg. Chem.* **1974**, *406*, 228.

[22] a) R. Hoefer, O. Glemser, *Z. Naturforsch.* **1975**, *B30*, 460. b) F. M. Tesky, R. Mews, O. Glemser, *Z. Anorg. Allg. Chem.* **1979**, *452*, 103. c) F. M. Tesky, R. Mews, *Chem. Ber.* **1980**, *113*, 2188. d) F. M. Tesky, R. Mews, *J. Fluorine Chem.* **1988**, *38*, 399. e) R Mews, P. G. Watson, E. Lork, *Coord. Chem. Rev.* **1997**, 233.

[23] R. Fleischer, B. Walfort, A. Gburek, P. Scholz, W. Kiefer, D. Stalke, *Chem. Eur. J.* **1998**, *4*, 2266.

[24] R. Appel, J. Kohnke, *Chem. Ber.* **1971**, *104*, 3875.

[25] R. Appel, J. Kohnke, *Chem. Ber.* **1970**, *103*, 2125.

[26] B. Walfort, A. P. Leedham, C. A. Russel, D. Stalke, *Inorg. Chem.* **2001**, *40*, 5668.

[27] T. Chivers, *Can. J. Chem.* **2001**, *79*, 1841.

[28] N. Y. Derkach, G. G. Barashenkov, *Zh. Org. Khim.* **1976**, *12*, 2484.

[29] M. Herberhold, W. Z. Jellen, *Z. Naturforsch.* **1986**, *B 41*, 144.

[30] a) N. Y. Derkach, T. V. Lyapina, G. G. Barashenkov, *Zh. Org. Khim.* **1979**, *15*, 879. b) N. Y. Derkach, G. G. Barashenkov, E. I. Slyuusarenko, *Zh. Org. Khim.* **1982**, *18*, 70. c) N. Y. Derkach, G. G. Barashenkov, E. S. Levshenko, *Zh. Org. Khim.* **1983**, *19*, 1622.

[31] a) K. B. Sharpless, S. P. Singer, *J. Org. Chem.* **1976**, *41*, 2504. b) V. Bertini, F. Lucchesini, A. de Munno, *Synthesis* **1979**, 979. c) M. Bruncko, T.-A. V. Khuong, K. B. Sharpless, *Angew. Chem.* **1996**, *108*, 453; *Angew. Chem. Int. Ed. Engl.* **1996**, *35*, 454.

[32] M. Björgvinsson, H. W. Roesky, F. Pauer, G. M. Sheldrick, *Chem. Ber.* **1992**, *125*, 767.

[33] T. Chivers, X. Gao, M. Parvez, *J. Chem. Soc. Chem. Commun.* **1994**, 2149.

[34] N. J. Bremer, A. B. Cutcliffe, M. F. Farona, W. G. Kofron, *J. Chem. Soc. A* **1971**, 3264.

[35] J. Konu, A. Maaninen, K. Paananen, P. Ingmann, R. S. Laitinen, T. Chivers, J. Valkonen, *Inorg. Chem.* **2002**, *41*, 1430.

[36] F. Fache, B. Dunijic, P. Gamez, M. Lemaire, *Topics in Catalysis* **1997**, *4*, 201.

[37] a) T. Ohkuma, H. Ooka, S. Hashiguchi, T. Ikariya, R. Noyori, *J. Am. Chem. Soc.* **1995**, *117*, 2675 and 10417. b) T. Schareina, R. Kempe, *Angew. Chem.* **2002***, 114*, 1591; *Angew. Chem. Int. Ed. Engl.* **2002**, *41*, 1521.

[38] Houben-Weyl *Methoden der Organischen* Chemie, E11, parts 1 and 2, supplementary volume of the 4th ed., Thieme 1985.

[39] R. Fleischer, Thesis, Universität Würzburg **1997**.

[40] D. Ilge, Diplomarbeit, Universität Würzburg **1997**.

[41] a) F. T. Edelmann, F. Pauer, M. Wedler, D. Stalke, *Inorg. Chem.* **1992**, *31*, 4143. b) R. v. Bülow, H. Gornitzka, T. Kottke, D. Stalke, *J. Chem. Soc. Chem. Commun.* **1996**, 1639.

[42] E. Zintl, A. Harder, B. Dauth, *Z. Elektrochem.* **1934**, *40*, 588.

[43] H. Fleig, M. Becke-Goehring, *Z. Anorg. Allg. Chem.* **1970**, *375*, 8.

[44] M. W. Schmidt, M. S. Gordon, J. *Am. Chem. Soc.* **1985**, *107*, 1922.

[45] J. E. Huheey, *Inorganic Chemistry: Principles of Structure and Reactivity*, Harper and Row, New York, 1997.

[46] D. R. Kirklin, J. S. Chickso, J. F. Liebman, *Structural Chemistry* **1996**, 7, 355.

[47] M. Pfeiffer, Thesis, Universität Würzburg **2000**.

[48] J. Kuyper, K. Vrieze, *J. Chem. Soc. Chem. Comm.* **1976**, 64.

[49] L. Pauling: *Die Natur der chemischen Bindung*, Wiley, Weinheim **1973**[3].

[50] R. Fleischer, D. Stalke, *J. Organomet. Chem.* **1998**, *550*, 173.

[51] R. Fleischer, D. Stalke, *Organometallics* **1998**, *17*, 832.

[52] B. Walfort, T. Auth, B. Degel, H. Helten, D. Stalke, *Organometallics* **2002**, *21*, 2208.

[53] J. M. Guss, P. R. Harrowell, M. Murata, V. A. Norris, H. C. Freeman, *J. Mol. Biol.* **1986**, *192*, 361.

[54] S. Maier, W. Hiller, J. Strähle, C. Ergezinger, K. Dehnicke, *Z. Naturforsch.* **1988**, *B43*, 1628.

[55] a) A. Heine, D. Stalke, *Angew. Chem.* **1993**, *105*, 90; *Angew. Chem. Int. Ed. Engl.* **1993**, *32*, 121. b) P. Pyykkö, *Chem. Rev.* **1997**, *97*, 597.

[56] H. Ackermann, O. Bock, U. Müller, K. Dehnicke, *Z. Anorg. Allg. Chem.* **2000**, *626*, 1854.

[57] B. Walfort, Thesis, Universität Würzburg **2001**.

[58] a) Cambridge Structural Database, May **2002**. b) F. H. Allen, O. Kennard, Chem. Des. Automat. News **1993**, *8*, 131.

[59] a) U. Fessler, R. Hubener, J. Strähle, *Z. Anorg. Allg. Chem.* **1997**, *623*, 1367. b) E. Vermejo, A. Castineiras, R. Dominguez, R. Carballo, C. Maichle-Moessmer, J. Strähle, D.S. West, *Z. Anorg. Allg. Chem.* **1999**, *625*, 961.

[60] a) D. J. Chadwick, C. Willbe, *J. Chem. Soc. Perkin Trans. I* **1977**, 887. b) W. Bauer, J. Boersma, L. Brandsma, S. Harder, J. A. Kanters, R. Pi, P. v. R. Schleyer, H. Schöllhorn, U. Thewalt, *Organometallics* **1989**, *8*, 1688. c) B. J. Wakefield, *Organolithium Methods, Academic Press*, London, **1994**.

[61] D. J. Chadwick, I. A. Cliffe, *J. Chem. Soc. Perkin Trans. I* **1979**, 2845.

[62] N. Kurai, H. Takeuchi, S. Konaka, *J. Mol. Struct.* **1994**, *318*, 143.

[63] a) J. Erfkamp, A. Müller, *ChiuZ.* **1990**, *6*, 267. b) J. Kim, D. C. Rees, *Nature* **1992**, *360*, 553. c) M. M. Georgiadis, H. Komiya, P. Chakrabarti, D. Woo, J. J. Kornuc, D. C. Rees, *Science* **1992**, *257*, 1653. d) J. Kim, D. C. Rees, *Biochemistry* **1994**, *33*, 389.

[64] a) E. Hurt, G. Hanska, R. Malkin, *FEBS Lett.* **1981**, *134*, 1. b) J. R. Mason, R. Cammack, *Annu. Rev. Microbiol.* **1992**, *46*, 277. c) M. G. Golinelli, J. Gagnon, J. Meyer, *Biochemistry* **1997**, *36*, 11797.

[65] I. Bertini, S. Ciurli, C. Luchinat, *Structure and Bonding* **1995**, *83*, 1.

[66] B. Vendermiati, G. Prini, A. Meetsma, B. Hessen, J. H. Teuben, O. Traverso, *Eur. J. Inorg. Chem.* **2001**, 707.

[67] C. Diaz, J. Ribas, N. Sanz, X. Solans, M. Font-Bardia, *Inorg. Chim. Acta* **1999**, *286*, 169.

[68] M.-C. Chen, M. J. Eichberg, K. P. C. Vollhardt, R. Sercheli, I. M Wasser, G. D. Whitener, *Organometallics* **2002**, *21*, 749.

[69] R. Cordone, W. D. Barman, H. J. Taube, *J. Am. Chem. Soc.* **1989**, *111*, 5969.

[70] a) J. Chen, J. R. Angelici, *Organometallics* **1989**, *8*, 2277. b) R. B. Rauchfuss, A. E. Ogilvy, A. E. Skaugset, *Organometallics* **1989**, *8*, 2739.

[71] C. J. White, R. J. Angelici, M.-G. Choi, *Organometallics* **1995**, *14*, 332.

[72] A. F. Clifford, R. R. Olsen, *Analytical Chemistry* **1959**, *31*, 1860.

[73] a) R. A. Bonham, F. A. Momany, *J. Phys. Chem.* **1963**, *67*, 2474. b) W. R. Harshbarger, S. H. Bauer, *Acta Crystallogr.* **1970**, *B26*, 1010.

[74] P. A. Chaloner, S. R. Gunatunga, P. B. Hitchcock, *Acta Crystallogr.* **1994**, *C50*, 1941.

[75] A. T. Jeffries, K. C. Moore, D. M. Ondeyka, W. V. Morgantown, *J. Org. Chem.* **1981**, *46*, 2885.

[76] T. Chivers, X. Gao, M. Parvez, *Inorg. Chem.* **1996**, *35*, 4336.

[77] For general overview see: A. W. Johnson, *Ylid Chemistry*, Academic Press, New York, **1966**. Reviews: a) H. König, *Fortschr. Chem. Forsch.* **1968**, *9*, 487; b) L. Weber, *Angew. Chem.* **1983**, *22*, 516; *Angew. Chem. Int. Ed. Engl.* **1983**, *95*, 539.

[78] a) R. C. Laughlin, *Chem. Ztg.* **1968**, *92*, 383. b) R. C. Laughlin, *J. Am. Chem.Soc.* **1968**, *90*, 2651. c) D. Hänssgen, W. Roelle, *J. Organomet. Chem.* **1974**, *71*, 231.

[79] D. Leusser, Thesis, Universität Würzburg **2002**.

[80] J. K. Brask, T. Chivers, G. P. A. Yap, *Inorg. Chem.* **1999***, 38*, 5588.

[81] a) B. Nyberg, P. Kierkegaard, *Acta Chem. Scand.* **1968**, *22*, 581. b) A. F. Wells, *Structural Inorganic Chemistry*, Clarendon Press, Oxford, **1984**, p. 584.

[82] a) E. J. Corey, T. Durst, *J. Am. Chem. Soc.* **1966**, *88*, 5656; b) E. J. Corey, T. Durst, *J. Am. Chem. Soc.* **1968**, *90*, 5548.

[83] S. E. Kabir, M. Ruf, H. Vahrenkamp, *J. Organomet. Chem.* **1999**, 344.

[84] J. Roncali, *Chem. Rev.* **1992**, *92*, 711.

[85] O. J. Scherer, G. Wolmershäuser, R. Jotter, *Z. Naturforsch.* **1982**, *B87*, 432.

[86] F. Wudl, E. T. Zellers, D. Nalewajek, *J. Org. Chem.* **1980**, *45*, 3211.

[87] a) D. H. Clemens, A. J. Bell, L. O'Brien, *Tetrahedron Lett.* **1965**, 1487. b) O. J. Scherer, G. Wolmershäuser, *Z. Anorg. Allg. Chem.* **1977**, *432*, 173.

[88] a) U. Wannagat, H. Kuckertz, *Angew. Chem.* **1962**, *74*, 117. b) O. J. Scherer, R. Wies, *Z. Naturforsch.* **1970**, *B25*, 1486. c) C. P. Warrens, J. D. Woollins, *Inorg. Synth.* **1989**, *25*, 43.

[89] F. Pauer, Thesis, Universität Göttingen **1991**.

[90] I. Ruppert, V. Bastian, R, Appel, *Chem. Ber.* **1975**, *108*, 2329.

[91] D. Stalke, *Chem. Soc. Rev.* **1998**, *27*, 171.

[92] a) H. Hope, *Acta Crystallogr.* **1988**, *B 44*, 22. b) T. Kottke, R. J. Lagow, D. Stalke, *J. Appl. Crystallogr*. **1996**, *29*, 465. c) T. Kottke, D. Stalke, *J. Appl. Crystallogr*. **1993**, *26*, 615.

[93] Bruker AXS, Inc. Madison WI **2000**, *Program for data processing*.

[94] SADABS2: G. M. Sheldrick, Universität Göttingen **2000**, *Program for empirical absorption correction*.

[95] G. M. Sheldrick, *Acta Crystallogr.* **1990**, *A46*, 467.

[96] SHELXTL-NT V5.1: G. M. Sheldrick, Universität Göttingen **2000**, *Program for the refinement of crystal structures*.

[97] a) H. D. Flack, *Acta Crystallogr.* **1983**, *A39*, 876. b) G. Bernadinelli, H. D. Flack, *Acta Crystallogr.* **1985**, *A41*, 500.

Curriculum vitae

Persönliche Daten   Carola Selinka, geb. Hofmann

geboren am 12. Mai 1972 in Schweinfurt

Verheiratet seit Mai 2000

Schulbildung

09.1978 – 07.1982   Grundschule in Poppenhausen

09.1982 – 07.1991   Gymnasium mit Abitur in Schweinfurt

Berufsausbildung

09.1991 – 09.1992   Ausbildung zur Diplom-Kosmetikerin an der Berufs-
fachschule für Kosmetik und Fußpflege in Würzburg

Hochschulbildung

10.1992 – 06.1998   Studium des Lehramts an Gymnasien
Biologie/Chemie an der Julius-Maximilians-
Universität Würzburg

Abschluss: 1. Staatsexamen

03.1996 – 03.1997   Zulassungsarbeit im Arbeitskreis Prof. Dr. M. Christl
am Institut für Organische Chemie der Universität
Würzburg mit dem Thema: „Synthese neuer 1,4-
disubstituierter Cyclopenta[c]pyrane und deren
Folgeprodukte durch elektrophile aromatische
Substitution"

Promotion

09.1998 – heute   Arbeiten an der Dissertation im Arbeitskreis Prof. Dr.
D. Stalke am Institut für Anorganische Chemie der
Universität Würzburg im Arbeitskreis Stalke zum
Thema: „Synthetic Routes to Asymmetrical
Alkylenediimidosulfites and Novel Heteroarene-linked
Bis-diimidosulfinates and Bis-triimidosulfonates"

04.1999 – heute   Wissenschaftliche Angestellte am Institut für
Anorganische Chemie der Universität Würzburg

Publications

1. Christl, Manfred; Bien, Notker; Bodenschatz, Gabriele; Feineis, Erich; Hegmann, Joachim; Hofmann, Carola; Mertelmeyer, Stefan; Ostheimer, Joachim; Sammtleben, Frank; Wehner, Susanne; Peters, Eva-Maria; Peters, Karl; Pfeiffer, Matthias; Stalke, Dietmar; "Cyclopenta[*c*]pyrans form 6-oxo-6*H*-1,3,4-oxadiazines" *Chemical Communications* **1998**, 2387.

2. Holzapfel, Marco; Lambert, Christoph; Selinka, Carola; Stalke, Dietmar; "Organic mixed valence compounds with N,N-dihydrodimethylphenazine redox centres" *Journal of the Chemical Society, Perkin Transactions 2* **2002**, 1553.

3. Dunne, John P.; Tacke, Matthias; Selinka, Carola; Stalke, Dietmar; „A New Synthetic Route to Alkoxides and Aryloxides of Calcium" *Chemistry, Eur. J.* **2002,** submitted.

Poster

1. B. Walfort, C. Selinka, D. Stalke, Novel Dianionic Sulfur Ylides, Internationale Carbanionentagung ISCC-6, Marburg **2001**.

Erklärung

Hiermit erkläre ich an Eides statt, dass ich die Dissertation "Synthetic Routes to Asymmetrical Alkylenediimidosulfites and Novel Heteroarene-linked Bis-diimidosulfinates and Bis-triimidosulfonates" selbständig angefertigt und keine anderen als die von mir angegebenen Quellen oder Hilfsmittel benutzt habe.

Ich erkläre außerdem, dass diese Dissertation weder in gleicher oder anderer Form bereits in einem anderen Prüfungsverfahren vorgelegen hat.

Ich habe früher außer den mit dem Zulassungsgesuch urkundlich vorgelegten Graden keine weiteren akademischen Grade erworben oder zu erwerben versucht.

Würzburg, den 08.11.2002

_____

(Carola Selinka)